Coupling Nitrogen Transport and Transformation Model with Land Surface Scheme SABAE-HW and its Application on the Canadian Prairies

By

Alireza Hejazi

A Thesis submitted to the Faulty of Graduate Studies of
The University of Manitoba
in partial fulfilment of the requirements for the degree of

DOCTOR OF PHILOSOPHY

Department of Civil Engineering
University of Manitoba
Winnipeg, Manitoba

Abstract

The main goal of this research is to contribute to the understanding of nutrient transport and transformations in soil and its impact on groundwater on a large scale. This thesis specifically integrates the physical, chemical and biochemical nitrogen transport processes with a spatial and temporal Land Surface Scheme (LSS). Since the nitrogen biotransformation kinetics highly depends on soil moisture and soil temperature, a vertical soil nitrogen transport and transformations model was coupled with SABAE-HW. The model provides an improved interface for groundwater modeling to simulate soil moisture and soil temperature for a wide range of soil and vegetation. It is assumed that the main source of organic N is from animal manure. A-single-pool nitrogen transformation is designed to simulate nitrogen dynamics. Thus, the complete mathematical model (SABAE-HWS) is able to investigate the effects of nitrogen biochemical reactions in all seasons.

This thesis reports the first field comparison of SABAE-HW using an extensive ten-year data set from BOREAS/BERMS project located in Saskatchewan, Canada. The performance of SABAE-HWS is calibrated and verified using 3 years (2002-2004) data from Carberry site in Canada, Manitoba. The effects of three rates of hog manure application, 2500, 5000, and 7500 gal/acre, was investigated to study the distribution of soil ammonium and soil nitrate within the 120 cm of soil profile. The results clearly showed that there is a good agreement between observed and simulated soil ammonium and nitrate for all treatment at the first two years of study. However, it was found a significant difference

between observations and simulations at lower depths for 7500 gal/acre by the end of growing season of 2004. Also, 10 years climate data from OJP site was used to evaluate the effect of manure rates on the distribution of soil nitrate at Carberry site. The results indicated that to minimize the risk of nitrate leaching, the rate of manure application, accumulated soil nitrogen from earlier applications and the atmospheric conditions should be all taken into account at the same time. Comparing the results of SABAE-HWS and SHAW model also showed the importance of the crop growth model in simulating soil NH_4^+-N and NO_3^--N.

Acknowledgments

First and foremost, I would like to thank my advisor, Dr. Allan Woodbury, for having given to me such a wonderful opportunity to pursue this PhD study. I am thankful for your patience and critical advices during the course of my research. I am sincerely indebted to Dr. Youssef Loukili for his countless hours of support and inspirations given to me during the compilation of this thesis. I am very grateful to Dr. Wole Akinremi for generously sharing his time and knowledge and also providing me with a great data collection. I appreciate very much Dr. Tricia Stadnyk for her useful advices and recommendations during my PhD program. I would also like to thank Dr. Jonathan Sykes, my external PhD examiner, for his invaluable time to review my thesis and make suggestions and comments.

I want to thank all my friends, especially Pichak Group who made life in Winnipeg enjoyable for me. A special thanks to my best friend, Ehsan Azordegan, whose supports and encouragement have made this research possible. Wherever I go from here, you will never be forgotten.

Lastly, I am deeply thankful to my parents who gave me love, strength and support to achieve success in all stages of my life. I would not have been where I am now without your unconditional support. I would also like to thank my brother, Amin, for always being there.

Contents

List of Tables

List of Figures

List of Appendices

Chapter 1

Introduction

Freezing and thawing mechanisms play a critical role in chemical reactions, nutrient availability, and nitrogen transport in soils. Freeze/thaw cycles affect the rate of mineralization (ammonification and nitrification) of organic nitrogen. In addition, they increase the rate of ammonium (NH_4^+) and nitrate (NO_3^-) concentration. The reasons for these changes are related to the physical, chemical and biological processes which are dependent on soil characteristics, time and frequency of freezing, vegetation cover, soil moisture and, soil temperature (Freppaz et al., 2007). The movement of water through melting snow changes the stability and structure of snow and consequently results in the release of nutrients into the soil or surface water. According to Feng et al. (2001), the chemical composition of water generated from a melted snowpack is not the same as the average composition in the snowpack itself; rather, it varies during the melting process. The main reactions within the snowpack occur among the solid, liquid, and gas phases in the form

of oxidation/reduction reactions and dissolution of particles (Harrington and Bales, 1998).

Freeze and thaw cycles and their effects on solute transport, especially C and N, have been investigated by many researchers during the past years (Brooks et al., 1998; Boutin and Robitaille, 1995; Larsen et al., 2002; Henry 2007). Considerable attention has been paid to some important climate factors such as freeze length, intensity and frequency, and ecosystem factors (soil and vegetation cover). Taking the effect of such factors into account improves the modeling of the impact of freeze/thaw cycles on ecosystem water quality, atmospheric chemistry, nutrient cycling, and soil carbon storage function under different climatic conditions (Neilsen et al., 2001).

Since most of the results on this topic are based on laboratory treatments and short-duration field experiments, the effects of winter freeze and thaw on losses of N and C have not yet been studied thoroughly on a large scale. Of course, there are a few models that consider nutrient losses due to freezing and thawing. These models for simulating water flow, heat transfer, and solute transport in the unsaturated zone seem to be less applicable in areas with frozen soils. SHAW (Flerchinger and Saxton, 1989) and HYDRUS 1D/2D (Šimunek et al., 1998) are examples of well-known coupled models. In addition, there are some models specifically designed to simulate carbon and nitrogen dynamics in the soil such as COUP model (Jansson and Karlberg, 2001), RZWQM (Ahuja et al., 2000), DAISY (Hansen et al., 1991), and LEACHM (Hutson 2000). The Swedish model SOILN and its improved version, COUP model, were developed to simulate infiltration and runoff by implementing an option for water flow in frozen soil. In general, all of these models distribute organic matter, nitrogen, carbon, and mineral nitrogen over multiple

pools while allowing organic matter to be decomposed by microbial biomass population. They are able to consider important phenomena such as mineralization of crop residue and immobilization of soil mineral nitrogen, mineralization of soil organic nitrogen nitrification, denitrification, and volatilization loss of ammonia. All the models divide the soil column into layers to simulate the movement of nitrogen, carbon and water between those layers. Also, nitrogen transformation processes and plant nitrogen uptake are simulated within each layer at various rates. Moreover, these models simulate multiple components in an agricultural system with different objectives and degrees of complexity. Some of the modeling concepts are shared by all of them while others are unique to a particular model. These differences might be related to different types of kinetics in simulating the nutrient processes or different potential nutrient transport rates such as mineralization or nitrification rate coefficients (Shaffer and Hansen, 2001).

The advection-dispersion equation is usually used to model solute transport in the vadose zone. Since different mechanisms such as convection, dispersion, adsorption, and exchange between mobile and immobile water are involved in solute transport, two basic approaches have been proposed to simulate solute transport in the unsaturated zone. The first approach integrates all sources of dispersion into one coefficient which is called the dispersion coefficient. All the water is then assumed to be active in the transport process. In this approach, transport of adsorbed species (such as ammonium) is modeled with the local equilibrium assumption. The second approach assumes that solutes are available in three phases (solid, liquid, and gas) and the decay processes are different in each phase. It also assumes that water in the soil is partitioned into a mobile and an immobile part. Solute in the mobile water is transported by advection and dispersion while it is exchanged

with immobile water under the influence of concentration gradients. Solute in immobile water is transported only by diffusion. Interactions between the solid and liquid phases are described by nonlinear none-equilibrium equations. Note that SHAW model is based on the first modeling strategy to simulate solute transport while HYDRUS model follows the second approach.

More details on the mathematical equations and physical models will be discussed in Chapter 4. Although no specific physically-based model has been proposed to simulate nutrient transport in winter, many lab and field experiments have evaluated nutrient transport according to the aforementioned approaches. A summary of investigations on this topic is reviewed in the next Chapter.

1.1 Objectives

The main goal of this study is to contribute to the understanding of ammonium and nitrate transport and transformations in soil and its impact on groundwater, especially in fields subjected to cold regions hydrology. This work integrates the physical, chemical, and biochemical nitrogen transport processes with the spatial and temporal climate groundwater model (SABAE-HW) developed by Loukili et al. (2008). The technical objective of this thesis is to develop a vertical soil nitrogen transport and transformations model for a one dimensional soil column. As manure application is studied in this thesis, it is assumed that the main source of organic nitrogen is from animal manures (although the effects of nitrogen fertilizers are neglected here, it is obvious that there are still some other natural sources of nitrogen such as atmospheric rainfall which is always available).

Therefore, in contrast with COUP and RZWQM model, a single pool nitrogen transformation is used to describe the mineralization, nitrification and denitrification processes. Simple models assume that the mineralization process proceeds at a much slower rate than the nitrification process. Water percolating below the rooting depth contains the soluble chemicals and nutrients originated from manure. In fact, some of these nutrients find their way to groundwater. Since the NH_4^+ ion is strongly adsorbed by the soil particles, NH_4^+–N concentration in the percolating solution is generally very low. A majority of the leachate nitrogen is in the NO_3^- form. Generally, in laboratory reports, the amount of NH_4^+ and NO_3^- concentration are recorded as mineral concentrations and losses. Since the proposed model will solve two transport equations (ammonium and nitrate transport equations) separately, there is a potential to differentiate between NH_4^+ and NO_3^- concentrations.

In this study, it is assumed that ammonium is instantaneously converted into nitrate, despite the fact that it actually takes several weeks in the field. It is well known that nitrogen biotransformation kinetics depend on soil water and soil temperature. The fundamental problem on the quantification of these kinetics is the experimental determination of the potential kinetic rates which are soil texture dependent (%sand, %loam, % clay and %organic matter). These parameters can only be measured under optimal laboratory conditions such as constant soil water content and soil temperature. The real kinetic rates are derived from the potential ones by multiplying the real rate coefficient by environmental factors that rang between zero and one. Therefore, to properly model nitrogen dynamics, abiotic functions were used. These functions describe the effects of soil water and soil temperature on microorganisms.

Most of the nitrogen chemical and biological processes are often measured in the laboratory or in the field under controlled conditions. The strong interaction between physical factors, plant uptake, and nitrogen cycling processes causes a major difficulty in simulating the biological processes. For example, nitrogen mineralization is affected by the biological factors. However, nitrate leaching is more sensitive to initial and boundary conditions and hydraulic parameters (Garnier et al., 2001). The proposed mathematical model can be used to investigate the effects of nitrogen biochemical reactions in winter with the presence of vertical spatial heterogeneity. In addition, it is useful to understand the interaction between the transformation and the transport of nitrogen in the field. The ability to conduct sensitivity analysis is also an important application of coupled flow and transport models. The results of this study will help investigators to properly identify the model parameters and will also provide a significant guidance for laboratory and field experiments.

An upwind finite volume scheme is used to solve the solute transport and nitrogen transformations equations numerically. The finite volume method ensures continuous fluxes across boundary layers. The formulated nitrogen transport model will be coupled to SABAE-HW. A frozen soil is a complex physicochemical system containing three moisture phases, namely ice, vapor, and water. Since soil freezing conditions are provided by SABAE-HW soil layers, the model developed in this thesis will calculate the nitrogen concentrations using soil water and soil temperature in each time step. With these assumptions, it is believed that the proposed model (SABAE-HWS) has a strong potential to simulate the nitrogen transport and nitrogen transformations in winter time. Finally, SABAE-HWS will be tested and evaluated thorough field studies (Carberry site in ADA).

The Assiniboine Delta Aquifer is a large unconfined aquifer with a coarse textured soil located in the province of Manitoba, Canada. Since manure application is widely practiced in the ADA, the risk of nitrate contamination of the ADA has increased during the past years.

In summary, one of the main objectives of this thesis is to develop a model (SABAE-HWS) to simulate soil ammonium and soil nitrate within the soil profile. Since soil moisture and soil temperature play key roles in simulating NH_4^+-N and NO_3^--N, it is essential to find a model (SABAE-HW) to simulate the soil moisture and soil temperature in freezing and thawing soil. Depending on the soil, vegetation, and atmospheric condition, large differences might be obtained between simulated and observed water content. Thus, it is important to determine the accuracy of the SABAE-HW model in a broad range of soil and atmospheric conditions. SABAE-HW was applied to the Old Jack Pine (OJP) site to determine the snow depth, soil temperature and soil moisture. After validation of water flow and heat transfer, the model was coupled to a newly developed solute transport submodel. The coupled water balance and solute transport model was used and applied to Carberry site to estimate changes in soil ammonium and nitrate concentrations. Note that nitrate movement below the root zone occurs when there is a net drainage. When precipitation exceeds evapotranspiration and runoff, net drainage occurs. Because of annual variations in climate conditions, the potential for the nitrate loss will vary. Thus, it is essential to evaluate the performance of the model under different atmospheric conditions. Also, the effects of different rates of manure application, number of applications, and climate conditions on nitrate leaching were evaluated by using a long term climate record. Once the model is tested, it would be useful to assess a variety of Best Management Prac-

tices (BMPs) to minimize nitrate leaching to groundwater under actual atmospheric and field conditions. The results will also provide information on the level of risk of groundwater contamination associated with nitrogen transport and manure application.

1.2 Structure of the Thesis

In Chapter 2, the literature related to nitrogen transformations in winter and numerical solution of solute transport equations is studied. The effects of freezing and thawing on major nitrogen transformations such as mineralization, nitrification and denitrification will be reviewed. Also, some commercial solute transport and nitrogen dynamics models as well as models developed by individual developers including the solution techniques and their applications are reviewed in this Chapter.

Evaluation of the SABAE-HW model in the Canadian Land Surface Scheme (LSS) and a summary of model application regarding the actual field data from Old Jack Pine site will be discussed in Chapter 3. The comparison between SABAE-HW and SHAW (soil moisture, soil temperature and snow depth) and the field data will also presented in this Chapter.

Chapter 4 explains the theoretical equations of nutrient transport and nitrogen transformations including the advection-dispersion equation and first order equations. The modeling and coupling strategy to be employed in this thesis is described. In addition, the comparisons between analytical and numerical solutions of solute transport are presented in Chapter 4. This chapter also covers a brief description of the SABAE-HWS input data file.

In Chapter 5, a detailed description of Carberry site including the necessary input parameters to simulate soil ammonium and soil nitrate concentrations will be described. Statistical criteria to evaluate the performance of the SABAE-HWS model are also presented in detail.

A summary of SABAE-HWS results (NH_4^+-N and NO_3^- -N) and the model application will be presented in Chapter 6. This chapter includes the comparisons between the SABAE-HWS results, the SHAW model, and Carberry site data. The effects of different rates of manure application on nitrate leaching during the long climate record are also studied in this Chapter

The overall conclusions obtained from the results of the SABAE-HWS model and model applications as well as the future developments of the model are discussed in Chapter 7.

Chapter 2

Literature Review

In this Chapter, the role of key parameters such as soil moisture, soil temperature, and snow depth in measuring solute transport and nitrogen transformations will be reviewed. The effects of vegetation cover, soil type, and snow timing on nitrogen dynamics are also reviewed. This thesis emphasizes cold region hydrology with freeze and thaw activity. Most studies reviewed here are based on lab and field experiments. In addition, a brief review of some numerical models (not specifically at the presence of freezing and thawing), developed for simulating the solute transport and transformations, is presented.

2.1 Nitrogen Transformations

The main component of the nitrogen cycle starts with nitrogen gas in the air. Nitrogen is added to the soil through nitrogen fixation which is the process whereby N_2 is converted to ammonium (NH_4^+). Ammonium is usually incorporated into organic nitrogen either by

bacteria or other soil organisms (nitrogen uptake). When nitrogen is incorporated into organic matter, it is often converted back into inorganic nitrogen by a process called mineralization. If organisms die, bacteria consume the organic matter and lead to the process of decomposition. Ammonium is converted to nitrate by soil bacteria through the nitrification process. This process has some important consequences. Ammonium ions are positively charged and therefore are adsorbed to negatively charged clay particles and soil organic matter. The positive charge prevents ammonium nitrogen from being washed out of the soil or leached by rainfall. In contrast, the negatively charged nitrate ions are not held by soil particles and can be washed down the soil profile. This leads to decreased soil fertility and nitrate enrichment of downstream surface and groundwater. When nitrate is converted to gaseous form of nitrogen (N_2, N_2O, NO) by bacteria, denitrification occurs. In this section, a comprehensive review of nitrogen transport and transformation processes in cold weather is presented.

Most studies show the increased rate of C and N concentrations during the freeze and thaw period. Since frost affects the slow growing of microbial communities and also microbial biomass, the adaption of microbial community to lower temperature still need to be investigated carefully in future (Matzner and Borken, 2008). Nitrogen losses from a freeze–thaw cycle occur in the form of NH_4^+, NO_3^-, dissolved organic nitrogen (DON), or gaseous emissions (NO, N_2O, N_2). The net mineralization of N is a basic precondition for N losses. However, increased rate of N mineralization does not necessarily lead to additional N losses due to nitrogen uptake by roots and immobilization by microbes. Furthermore, it has been reported that the elevated N fluxes from deeper soils does not result in an increase of N net mineralization. Since the amount of nitrate uptake is reduced after

the soil frost, it could be a possible reason for the increased rate of nitrogen losses. Most investigators have reported an increase of N_2O emission during the thawing period in all ecosystems. The source of N_2O emission is mainly the fertilizer N in arable soils after thawing (Neilsen et al., 2001).

A series of laboratory experiments and field works have been accomplished to determine the effects of simulated freeze and thaw treatments on the transformation of nitrogen and nitrogen loss during the winter. Brooks et al. (1998) developed a model to show how snow cover controls subnivial (below snowpack) microbial process and N leachate from the snow-soil interface to surface waters. The model also showed the spatial and temporal differences in nitrate concentrations of surface waters in seasonally snow covered catchments. Subnivial processes are known as the major controls on the leaching loss of N from soil during snow melt. In fact, they contribute to insulation of soil from cold air. This allows heterotrophic microbial activity to immobilize N in the soil. In the proposed model by Brooks et al. (1998), solutes were released from the seasonal snowpack in the form of ionic pulse. The results showed that most of the inorganic N (80% NH_4^+ and lesser amount of NO_3^-) which is released from the snowpack moves to the underlying soils. In addition, depth and duration of the snowpack are the important parameters to control soil temperature and N cycling in high elevation catchments. Soil is able to extract inorganic N released from the seasonal snowpack. Note that, microbial activity has an effect on the source–sink relationships representing nitrogen during runoff. Since the production of nitrous oxide (N_2O) is based on microbial process, it can provide a non-destructive index of N cycling by biological processes. Moreover, disturbing the snow depth and duration show similar results in terms of the subnivial N_2O fluxes. Based on

the measurements of gaseous N fluxes from microbial processes, it can be deduced that the depth and timing of seasonal snow also affect the size of the microbial biomass N pool and the amount of N leached from the soil during the melting period. It is also a known fact that the climate change disturbs biogeochemical process by changing the snow cover and soil temperature regimes.

Deelstra et al. (2009) developed a catchment scale model to simulate runoff and nutrient losses in winter time. The main catchments of their study were located in Norway, Sweden, Finland, and Lithuania. A comprehensive analysis of field measurements showed that considerable amount of nutrient losses occurred during the winter time. A large variation of yearly N loss was observed for each catchment because of the different amounts of runoff in each area. N fertilizer application, agricultural practices, and hydrological flow could be the other reasons for this variation. Although there might be a positive relation between runoff and N losses in freezing period, a great discrepancy was observed for the yearly N losses. In addition, soil temperature and soil moisture are significant parameters that affect the available nitrogen before the beginning of the freezing period. The N loss did not change significantly due to the reduced amount of infiltration before the onset of the freezing period. However, during the thawing, the above–zero temperatures trigger runoff and infiltration processes which induce larger N losses.

There are four reasons for the increase of nitrogen fluxes in freezing and thawing periods: (1) increased rate of microbial transformation, (2) the amount of released N_2O from below frozen soils, (3) the quick growth of microbial transformation leading to freezing microbial mortality, and (4) disruption of soil aggregates leading to denitrification. Groffman et al. (2006) manipulated snow depth to elucidate fluxes of N_2O. It should be

mentioned that N_2O is an intermediate product of nitrogen transformation regarding the denitrification process. The results of field experiment confirmed the predicted increase in the amount of N_2O fluxes. The rate of NO_3^- leaching also increased due to the disrupted ecosystem caused by manipulation (shoveling the snow depth). A reduction in plant uptake was reported as the only reason for the increased rate of NO_3^- leaching. This field experiment also confirmed the hypothesis that C and N fluxes will not significantly increase due to rapid decomposition of fine roots after thawing period.

There have been some contradictory ideas regarding the biochemical nitrogen transformations in winter. The cumulative effects of lower temperature, soil frost, and consequent mineralization after thawing period clarify the overall net N mineralization (Matzner and Borken, 2008). Some investigators indicated that net N mineralization is not negligible in winter time, especially at the annual time scale (Miller et al., 2007). There have been conflicting reports regarding the effect of thawing on nitrogen mineralization. Some investigators have stated that nitrogen net mineralization increases after thawing period while there have been other studies indicating that there is no change in the N mineralization after soil frost (Freppaz et al., 2007; Hentschel et al., 2008). Even observations show different results for different vegetation covers and soil types (Neilsen et al., 2001).

More recently, a field experiment was done by Hentschel et al., (2009) to show the effects of soil frost on nitrogen net mineralization, solution chemistry, and seepage losses in temperate forest soil. The net mineralization of N was determined by collecting data directly from the field site without disturbing the soil. The N net ammonification and net nitrification did not show any differences in the spring and summer, neither in the frost

nor in the mineral soil. Although the quick response of the increase NO_3^- concentration was not observed after thawing, there was evidence to indicate that NO_3^- increased in forest vegetation at a 20-cm-soil depth. The results also revealed that frost and thawing did not cause significant changes in soil solution chemistry in winter time regarding the net effect of lower temperatures. It has been known that soil frost prevents the vertical water transport and consequently the removal of mineralized N with seepage. A small amount of NO_3^- appeared by growing heterotrophic microorganisms increased the net nitrification and NO_3^- concentration. Due to similar amount of NO and N_2O emission during the treatments time, there was no difference in denitrification rates when NO_3^- concentration increased. However, there was some evidence to show that less NO_3^- immobilization in snow removal is a cause of increasing NO_3^- in the late growing season. Measurements also indicated that those treatments (snow removal and soil frost) did not change NO_3^- fluxes in forest cover. Furthermore, the increase of NO_3^- concentration in the fall had a little effect on the leaching due to water flux. In addition, the net nitrification rate was more negatively influenced than the net ammonification with the temperature of -8 and -13 ºC and this suggested a higher sensitivity of nitrifiers to severe frost. Observations confirmed that respiration at -3 ºC was higher than the respiration in the non-frozen controls. A decrease of N mineralization was also reported after thawing period (Hentschel et al., 2008).

The cumulative effects of multiple freeze/thaw cycles must be known to estimate soil nitrogen losses over winter (Herrmann and Witter, 2002). Laboratory experiments indicated that the soil water content and soil temperature are the most important factors to control seasonal variations in the mineralization rate of soil organic nitrogen. The effects

of frost on N mineralization were highest in the first cycle and then decreased in later ones. However, emissions of N_2O from arable soil decreased in a repeated freeze-thaw cycle (Matzner and Borken,. 2008). There was evidence that frost decreased microbial biomass in arable soils at -5 ºC.

Freppaz et al. (2007) also evaluated the effects of a single and four sequential freeze-thaw cycles on the transformation processes of N and P. Four different soil types with different vegetation covers were chosen to test nitrogen transformations under two moisture contents (32 and 65 *KPa*). Although the results varied between the single freezing and thawing (SF) and 4SF, the significant increase was obvious in the net ammonification (NH_4^+ increase) in all soils. NO_3^- concentration was less affected for both experiments, only a little increase for those sites with forest vegetation cover. According to Freppaz et al. (2007), Cation Exchange Capacity (CEC) and pH have an influence on speciation of N and P through the combined effects on cation exchange (NH_4^+), sorption, N mineralization, and N nitrification (NO_3^-). One of the reasons of the increase in NH_4^+ levels might be the release of previously non-available NH_4^+ from organic collides by the disruptive action of the freeze/thaw cycles. It was also reported that the microbial biomass decreased under frost in alpine soils. The results of this study had been similarly shown by Hinman (1970). He had reported that several freeze/thaw cycles have more effects on the increase of NH_4^+ than single cycle but less effect on the increase of NO_3^-. The effects of freezing and thawing on microbial N concentration were also tested. Since multiple freeze/thaw cycles did not significantly increase nitrate concentration, it was found that single cycle is enough to cause serious disruption to the soil microbial population.

Neilsen et al. (2001) sampled soils from three different horizons (Oe, Oa, and A) to evaluate the effects of freezing on carbon and nitrogen cycling such as soil respiration, nitrogen mineralization, nitrification, and nitrous oxide (N_2O) production. After experimental treatments in the laboratory, the results showed that the rate of N and C cycling increased during the freezing period. However, the amount of increase varied with species, horizon and freeze treatment. For example, considerable amount of leachable NH_4^+ and NO_3^- was found during freezing treatments. There was also an increase in mineralization for maple cover when soils was subjected to severe soil freezing in the laboratory. On the other hand, there was no evidence to show nitrification by freezing treatments. In fact, NH_4^+ concentration increased while leachable NO_3^- decreased. This was an unexpected result because the increase in NH_4^+ concentration causes an increase in nitrification rate. As a consequence, it was possible that denitrification also increased when nitrification did increase. Although the amount of denitrification was not measured in this study, authors suggested that it is probable that denitrification increased because of an increase of N_2O during the freezing period.

Soil freezing also affects the disturbance of below ground environment and causes linkages between mineralization and uptake process which are important to nutrient conservation in forest vegetation area. The rate of decomposition and mineralization increased during freezing period because of the increase of fine root growth and also physical disruption of soil aggregates. This results in an increase of nitrogen concentration and N nutrient loss in soil solutions (Mitchell et al., 1996). Field and laboratory experiments were completed by disturbing the soil freezing to clarify the effects of soil freezing on soil solution N chemistry. A process-based model of catchment hydrology, BROOK90,

was used to simulate water flux and compare to the observations. This model was not able to measure soil temperature and soil freezing processes. The results showed that the rate of NO_3^- fluxes was accelerated by the manipulation of freezing soil. The total nitrogen leachate (NO_3^- + NH_4^+ + dissolved organic nitrogen) seemed to increase rapidly from the forest floor. This rate remained consistent with significant increases in extractable soil NO_3^- and net nitrification. They also compared the fluxes of dissolved inorganic N (NO_3^- +NH_4^+) entering and leaving the forest floor. The results indicated that most of the increase in Dissolved Inorganic Nitrogen (DIN) is not related to the reduced N plant uptake. It was reported that the hydrological N losses increased after freezing period because of enhanced supply of N occurred by physical disruption of soil. It was suggested that if soil freezing is repeated several times under warmer climate, the availability and loss of N might be changed. Although the effects of fine root mortality on increasing nutrient losses were noticeable, physical disruption of soil aggregates and reduced root uptake were reported as the main reasons of nitrogen losses (Fitzhugh et al., 2001).

Harrington and Bales (1998) developed a numerical model used by several investigators later. The model had the ability to simulate non-reactive solute from melting snow. It incorporated the effects of mass transfer between mobile and immobile liquid phase, advection, dispersion, and melting snow cover. It is important to mention that the amount of simulated solute concentrations of melt water was sensitive to discharge, dispersivity, mass transfer rate, residual water saturation, and the initial distribution of solute in the snowpack. They found that there are two considerable differences between snow and subsurface porous media: (1) the pore geometry changes quickly as the snow ages and causes changes in saturated hydraulic conductivity and the relation between capillary

pressure and snow wetness, and (2) several phenomena such as condensation, sublimation, freezing and thawing are able to transfer mass between three phases: liquid, solid and gas. The model was affected by three phases: solid ice, mobile liquid water and immobile liquid water. Five variables including solute concentrations, volume fractions, snow grain size, melt water, and snow temperature were defined in these phases. Because the melt water moves quickly to heterogeneous and three dimensional areas, the accuracy of melt water discharge (calculated by one dimensional proposed model) was reduced. Another limitation of the model was the inability to reproduce the melt water flow, especially in the presence of preferential and lateral flow. Therefore, the amount of solute concentration was not accurate. The model also reproduced the negative relationship between solute concentration and flow rate.

Natural and artificial tracers are used to measure the solute released from seasonal snowpack. Lee et al. (2008) applied rare earth elements as an artificial tracer to specify the snow layers. New snow, snowpack profiles, and snow melt were collected to measure the changes of $S0_4^{-2}$, Cl^- and NO_3^- concentrations. They reported that the maximum sulfate and nitrate concentration are five times higher in the melt water than in the new snow because snow metamorphism and then purification of snow grains leave the pore water with high solute concentration. They also found that the solute released by the snowpack is completely related to weather conditions; for example, there was a high concentration of natural tracers at the beginning of thawing periods. The results showed that natural solutes have a diurnal variation which is negatively correlated with diurnal melting cycle. The mobile–immobile solute transport model proposed by Harrington and Bales (1998) was used to prove their experiments. In this model, solutes in the mobile water were

transported by advection and dispersion while those in the immobile water were transported by exchange between immobile and mobile water. Since the result of the simulation was not satisfactory, they suggested that additional physical processes would be effective in solute transport in snow. Also, redistribution of solutes in snow was investigated in this study. The results showed that the NO_3^- and SO_4^- concentration have a strong correlation from fresh snow to snowpack profile and to the melt water. These observations confirmed that anion distributions in snow are modified by snow metamorphism and elution of snowmelt. Recrystalization is one example to show this fact. SO_4^- and NO_3^- will be removed by recrystallization from the ice and then both can be concentrated during cold days and finally mobilized in thawing periods.

A new version of the Mobile–Immobile water model (MIM) was also developed by Lee et al. (2008) to simulate the water flow and concentration–discharge relationships with rainfall and melt water under various chemical conditions. The numerical model was simplified by four assumptions: (1) one dimensional vertical flow equation was chosen to simulate the water flow ignoring the macroscopic preferential flow, (2) the snowpack was isothermal at melting point and it was assumed that density, porosity, and immobile water content did not change with time and depth in snowpack, (3) they ignored the effects of soil freezing on the snowpack during the experimental period, and (4) the value of intrinsic permeability was assumed to be constant through the snowpack. It was also assumed that the exchange rate coefficient between mobile and immobile is proportional to flow velocity. The result showed that the different values of soil moisture affect the amount of solute concentrations. In order to obtain good agreements between simulated and observed tracer concentrations, it was reported that water flow velocity should increase. The

snow depth was another factor that may affect the concentration discharge relationship in this study. With use of this model and changing the boundary conditions, they found that the solute distribution within the initial snowpack affects the solute transport.

In summary, the effects of freeze and thaw activities on nitrogen transport and transformation have been reviewed. Most of these studies were based on the lab experiments and field sites. Since these experiments are subjected to small and specific areas, numerical methods are extensively used to simulate solute transport and transformations at the big scales with the large period of time. In the next section, a brief summary of available solute transport and nitrogen dynamic models will be presented.

2.2 Selected Solute Transport Models

Solute transport is usually described by the Advection-Dispersion Equation (ADE) in the soil profile with extra terms accounting for adsorption and chemical reactions. The form of these terms can be linear or nonlinear adsorption or zero, first, and second order reactions. The amount of predicted leached solutes is sensitive to the dispersion parameter of the solute transport equation which lumps the effect of smaller scale transport velocity variation on solute spreading with chemical diffusion of solute (Vanderborght et al., 2006). Since analytical solutions are only reliable for simplified cases, numerical methods are widely used to solve the nonlinearity of soil properties. However, there are some difficulties associated with the numerical solutions of the solute transport equation which causes oscillations, especially in the case of advection dominance. During the past decade, numerous numerical models have been developed to simulate linear or nonlinear form of solute transport equation in porous media with varying degrees of complexity

and accuracy. Some examples of these models are: SWIFT (Reeves et al., 1986), TOUGH2 (Pruess 1991), CENTURY (Parton and Rasmussen, 1994), and FEFLOW (Diersch and Kolditz, 1998).

One of the simplified approaches describing solute transport assumes that the soil is homogenous and the interphase mass transfers are linear and instantaneous (local equilibrium assumption). Some other models consider that all soil water contributes to solute transport (physical non-equilibrium). In fact, dual porosity type formulation partitions the liquid phase into mobile and immobile regions. It is assumed that water flow is restricted to the mobile region and there is no water movement in the immobile domain. Thus, although the immobile domain can store water, it does not allow for the convective flow. However, solutes are able to be transferred from the mobile to the immobile region and vice versa (Kartha and Srivastava, 2008). "Dispersion" refers to the combination of mechanical and physical-chemical dispersion. Mechanical dispersion refers to a movement of flow through the porous medium. It increases with the fluid velocity. Physical-chemical dispersion refers to a molecular diffusion and increases with a rise in temperature. HYDRUS (Šimunek et al., 1998) is one of the well-known models developed based on concept of mobile and immobile liquid zones in the porous media.

The idea of coupled models with attention to the interaction between the saturated and unsaturated zones was introduced by Mehran et al. (1984). They presented a model capable of solving the flow and transport equations with respect to groundwater contamination. In their model, the flow region was divided into two areas: vadose zone and underlying saturated aquifer. In the vadose zone, dispersion-advection, plant uptake, ion exchange, and N transformations (nitrification, denitrification, mineralization and immobi-

lization) were all assumed to be effective. A one-dimensional solute transport equation, solved by finite difference method, was used in the vadose zone. On the other hand, advection-dispersion was the only process that is believed to change nitrate concentration in the saturated zone. Noorishad and Mehran (1982) proposed an upstream finite element method using two nodal point elements. Putti et al. (1990) developed a finite volume model with more focus on triangular control volumes for the convective and dispersive fluxes to eliminate oscillations. Ackerer et al. (1999) used the discontinuous finite element method to avoid numerical instabilities and create a very limited numerical dispersion. Lan and Chen (1996) also used the same methods to simulate solute transport in directional solidification. Rahnama and Barani (2004) developed a model using a control volume technique. Three dimensional solute transport equations were linearized and then the coefficient matrix was solved using three dimensional matrix algorithms.

Soraganvi and Kumar (2009) developed a new numerical scheme in which advection and dispersion parts of the equation were solved separately. The advection term was solved by finite volume methods while the dispersion term was solved by a fully implicit finite difference method. This scheme was used to reduce physical oscillations. Mazzia and Putti (2002) presented a model to simulate the transport of high brine concentration in groundwater. This model was based on two non-linear mass conservation equations; one for flow and the other one for the salt. The proposed numerical technique was based on the hybrid mixed finite element method for the discretization of diffusion and finite volume method for the convective term. Neumann et al. (2009) applied finite difference methods to solve the advection dispersion equation, either using backward, forward or central discretization. It was reported that the application of backward finite differences

resulted in significant numerical dispersion. However, the use of central scheme can cause numerical oscillation. All of these models were different due to different approximation methods such as finite difference, finite element, integral finite difference, different time discretization (semi-implicit and fully implicit), and different coupling processes (fully coupled, Picard linearization, Newton-Raphson linearization) (Younes et al., 1999).

Lafolie (1991) presented a model to simulate water flow, heat flow, and solute transport focusing on modeling plant water and plant nitrogen uptake. He used one dimensional water flow equation (Richard's equation) in the mass conservation form to avoid the discretization of first order derivatives. This equation was solved by a finite difference, fully implicit scheme, and a fixed point iterative technique. The solute transport was simulated using a local equilibrium assumption and the two-region physical non-equilibrium assumption. Garnier et al. (2001) developed a one dimensional mechanistic model for simulating water flow, heat flow and, solute transport. This model was linked to the proposed model by Lafolie (1991) with one of transformations of C and N. Soil organic matter was divided into 5 main organic pools with more attention to decomposition of humified organic matter. A physically based model with particular attention to non-point source pollution was suggested by Heng and Nikolaidis (1998), in order to simulate water and nutrient transport in a watershed. A two dimensional unconfined groundwater flow equation was used to simulate the movement of groundwater. This equation was solved by a strong implicit procedure. The chemical transport in the vadose zone and groundwater was modeled by one dimensional and two dimensional transport equations.

Simulating carbon and nitrogen dynamics also makes the models more complicated in terms of numerical solutions. In general, there are two basic groups of soil nitrogen dynamics models which are widely used for different applications in agriculture research:

1. European nitrogen dynamic models such as ANIMO (Berghuijs-vanDijk et al., 1985), DAISY (Hansen et al., 1991), and COUP (Jansson and Karlberg, 2001).

2. U.S. soil nitrogen dynamics model such as: RZWQM (Ma et al., 2001), LEACHM (Hutson 2000), and GLEAMS (Leonard et al., 1987).

These models are able to simulate soil carbon and nitrogen dynamics processes such as mineralization, nitrification, denitrification, and nitrogen uptake. Since organic carbon and nitrogen in the soil are heterogeneous, they are separated into the different carbon and nitrogen pools based on their physical, chemical, and biological characteristics. Depending on the model applications, the size and number of pools varies between models. Also, the organic matter decay rates and the other processes are calculated by different kinetic types or experimental functions (Shaffer and Hanson, 2001).

In addition, complex solute transport models such as SHAW (Flerchinger and Saxton, 1989) and HYDRUS (Šimunek et al., 1998) are available to simulate solute transport and transformations. Note that the SHAW and HYDRUS models are not able to simulate nitrogen dynamics through a soil column. A brief summary of the COUP, RZWQM, and SHAW models and their numerical schemes will be presented in the next section. These models have been extensively verified through laboratory and field experiments. These models can be set up to consider the effect of various parameters on nutrient transformations. COUP is able to simulate freeze and thaw effects on the soil, and consequently on nutrient transformations. This model can be utilized effectively to study nitrogen dy-

namics in agriculture farms. Although RZWQM does not consider freeze and thaw events, its various applications in agricultural systems make it one of the well-known models for simulating nutrient dynamics. SHAW considers solute transport in the soil column but it is not able to simulate nitrogen transfer and dynamics.

2.2.1 COUP Model

The COUP (COUPled heat and mass transfer) model is a soil water and heat transport model integrated with a SOIL Nitrogen dynamics model (SOILN). It is a one dimensional vertical structure model including two coupled partial differential equations of water and heat transport. The soil water and heat model provides variables for the soil nitrogen model such as soil moisture, soil temperature, surface runoff and infiltration. SOILN (Johnsson et al., 1987) includes all major transformations and transport processes of C and N in the soil. The full Coup-Model has been presented in detail by Jansson and Karlberg (2001).

The COUP model has been largely used to study nitrogen dynamic processes in arable soils under various vegetation covers and fertilizers types. This model considers the main soil nitrogen dynamics processes such as mineralization, immobilization between organic and inorganic forms, nitrification, denitrification, and nitrogen uptake by plants. All soil nitrogen transformations are dependent on soil water content, especially denitrification which is very dependent on the lack of oxygen in the soil atmosphere. Therefore, denitrification increases quickly with rising soil wetness. All transformations are also temperature dependent in terms of soil nitrogen dynamics; hence soil heat process becomes very important in the simulation of nitrogen transformations. COUP is a linked

soil water and heat transfer model with a sophisticated treatment of the heat processes including the effects of snow cover. In terms of temperature response, the COUP model uses a *Q10* expression (the temperature response function) which is a common function for chemical reaction.

The general soil water response for all processes except denitrification is based on the assumption that activity decreases on either side of an optimal range of soil water content. Mineralization and immobilization are controlled by carbon processes in organic matter. In fact, organic matter is divided into several pools, mainly fast and slow cycling pools. Important nitrogen dynamics processes are from fast cycling to slow cycling pool (mineralization from each organic pool to ammonium or the reverse processes such as immobilization). The COUP model considers a first order rate process for the nitrification of ammonium to nitrate. The rate constant may also be multiplied by a function of e_{ph} for pH. It is noted that the first order rate process was driven by the excess of ammonium. The general form of first order kinetics is:

$$\frac{dN}{dt} = -k_1 N \qquad 2\text{-}1$$

where N (mg/kg) is the ammonium or nitrate concentration in soil and k_1 (1/day) is the first-order rate constant.

Denitrification is described by a macro-scale response function that incorporates the effects of processes at the microscale level. Denitrification is calculated as a zero order rate process from potential denitrification rate which accounts for the effects of different soil and different cropping systems. Also, the effect of soil aeration, soil nitrate concentration and soil temperature are considered through a response function. The general form of zero-order kinetics is expressed as:

$$\frac{dN}{dt} = -k_0 \qquad 2\text{-}2$$

where k_0 (1/day) is the zero-order rate constant.

The actual growth of plant is calculated as the potential growth reduced by non-optimal temperature, leaf nitrogen concentration and transpiration. In fact, the nitrogen demand is proportional to the daily growth. Also, the actual uptake is the smaller than nitrogen demand and the available soil nitrogen.

2.2.2 RZWQM Model

The RZWQM (Root Zone Water Quality Model) is a fully functional system model. RZWQM is basically a process level model for the simulation of soil water, soil temperature, plant growth, and C and N soil dynamics. The major feature of this model is its ability to simulate various agricultural management practices and their effects on water quality and crop production. This model has five organic C and N pools. Two surface residues pools and three soil organic matter pools. Differences between pools include C:N ratio and decomposition rate constants.

In RZWQM, mineralization and immobilization are determined by the decay of organic pools and the growth of microbes. Organic matter decay in each pool is simulated by a first order reaction. First order rate coefficients are then modified for effects of soil temperature, oxygen, aerobic condition and ionic strength. In terms of simulation of nitrification, three types of kinetics (zero order, first order and Monod) models are used to describe the nitrification processes. Note that RZWQM initially used first order kinetics for NH_4^+ concentrations greater than 3 millimoles N per liter of pore water. The new version of this model considers a simple zero order function because the first order assumption

has little effect on C and N soil dynamics. The zero order rate coefficient is a function of soil temperature, oxygen concentration, pH, and population of the autotrophs.

The simulation of denitrification process is empirically-based because of the spatial and temporal variability of anaerobic conditions in the soil. Soil anaerobic conditions can be determined by soil oxygen or soil water content. The mathematical simulation of denitrification is also zero or first order or Michaelis-Menten kinetics. RZWQM uses first order kinetics to simulate denitrification which is affected by soil anaerobic conditions, soil temperature, pH, soil carbon substrate and population of the denitrifiers. RZWQM also considers urea hydrolysis and ammonia volatilization. For both processes, first order kinetics is used. The rate coefficient of urea hydrolysis is a function of soil temperature and soil aerobic conditions. Air temperature and wind speed are the most important components affecting the rate coefficient of ammonia volatilization. Since microbial population and soil water content do not affect urea activity, they are not considered in the model for urea hydrolysis (Shaffer and Hansen, 2001).

Plant nitrogen uptake is driven by plant nitrogen demand which can be estimated from a logistic curve or by interaction with a plant growth model. RZWQM includes a plant growth submodel to determine N demand at various growth stages. In this model, all inorganics forms of N in a soil layer are plant available nitrogen. Nitrogen uptake from each soil layer is first determined from transpiration water stream. If total N uptake from all the soil layers is less than N demand, an active uptake mechanism in the form of Michaelis Menten kinetics is involved, in order to meet the demand until all the plant available N is finished (Ma et al., 2000). The general form of Michaelis-Menten kinetics is defined as:

$$\frac{dN}{dt} = -k_m \frac{N}{N+k_c} \quad 2\text{-}3$$

where k_m is the maximum rate constant (1/day) and k_c is the saturation coefficient.

2.2.3 SHAW Model

The Simultaneous Heat and Water (SHAW) model has been developed to simulate soil freezing and thawing, heat, water, and solute transport within a one-dimensional profile. The model also simulates transpiration through a multispecies plant canopy. The unique feature of this model is the prediction of heat, water and, chemical transfer in the presence of soil freezing and thawing. Heat and water fluxes are modeled by daily or hourly weather conditions of air temperature, wind speed, humidity, solar radiation, and precipitation. Soil moisture, soil temperature and solute fluxes are computed between nodes for each time step. A fully implicit finite difference approximation is used to solve the mass balance equations for each node. The SHAW model considers solute adsorption in the soil profile. In terms of solute transfer, the model considers molecular diffusion, convection, and hydrodynamic dispersion. Diffusion of solutes through the soil is affected by moisture content. Solute convection is only in the direction of moisture flow and is proportional to moisture flux and solute concentration. Since uniform velocity is assumed in all pores, solutes are transported by convection at the mean velocity of moisture flow. However, they are dispersed about the mean velocity due to differences in velocity between and within soil pores. A detail description of SHAW including all equations and functions is given by Flerchinger et al. (2000).

In contrast with the COUP and RZWQM model, the SHAW model is not able to simulate nitrogen dynamics such as mineralization, nitrification, and denitrification. Howev-

er, there are solute sink terms to simulate the amount of solutes that are lost from the soil by degradation or extraction by roots. Solute degradation is assumed to follow an exponential decay. Half-life of solute in the soil environment plays a key role in calculating solute degradation. Solute extraction by the plant roots is assumed non-selective and equal to the concentration of solutes within the soil solution extracted by the roots. Also, a linear adsorption equation is used to simulate solute concentrations which are adsorbed to the soil. In this case, a partitioning coefficient is specified between the soil and the soil solution. Depending on the solute and soil type, the value of partitioning coefficient is varied between 0 and 60: Zero is for a completely mobile solute such as chloride which is not adsorbed by the soil and 60 is assigned to potassium which is tightly bound to soil particles.

Since SHAW is able to simulate soil moisture, soil temperature, and solute transport within snow, the results of the SABAE-HWS model was compared with results of the SHAW model. SHAW is appropriate for this study as it can simulate heat, water, and solute transfer for freezing and thawing conditions. This model has been tested in a variety of studies evaluating the coupled heat, water flow, and solute transport in the unsaturated zone (Nassar and Horton, 1999; Nassar et al., 2000).

2.3 Summary

In summary, any model of solute transport and soil nitrogen dynamics is dependent on soil water content, water flux, and soil temperature. In order to simulate soil nitrogen dynamics, accurate description of these parameters is necessary in cold regions hydrology. Therefore, the first step before calculating solute transport is to properly model soil mois-

ture, soil temperature, and water movement. In the next Chapter, a detailed description of the land surface scheme SABAE-HW capable of simulating snow depth, soil temperature, and soil moisture with high accuracy will be discussed. Depending on the model application, a single soil organic nitrogen pool was adopted to simulate nitrogen dynamic processes. The coupled nitrogen transport, water flow, and heat transfer model (SABAE-HWS) will then be used to simulate soil ammonium and soil nitrate nitrogen originated from manure in Carberry site. Also, the effects of manure treatments on nitrate leaching will be investigated using long term weather records.

Chapter 3

Land Surface Scheme Improvements and Field Comparisons

This Chapter covers the general methodology of the Canadian Land Surface Scheme SABAE-HW. Also, the results of field comparisons (OJP site) under freezing and thawing soil conditions will be discussed in detail. Soil moisture, soil temperature, and snow depth which are extremely important in simulating solute transport and transformations are modeled and compared to the observations.

3.1 Introduction

In considering drought, a tightly coupled Land Surface Scheme (LSS) and groundwater model needs to be developed. The methodology necessary for developing these models has only been recently explored. Jyrkama et al. (2002) found that use of a simple hydrologic model to produce spatially varied groundwater recharge patterns, significantly im-

proved groundwater simulations. In this study, an attempt was made to build on this approach by using a detailed LSS in place of a simple hydrology. This is justified since LSSs have been designed as components of Global Climate Models (GCMs) and are better equipped to deal with increased variability and shifts in mean conditions that are expected under climate change scenarios including drought. Tight coupling of these models will be required to simulate the impact of simultaneous irrigation/recharge on surface energy/water conditions and on groundwater potentiometeric surfaces. Developments with respect to an improved lower boundary in a soil column are crucial to allow land surface schemes to be tied to groundwater models.

Of critical importance in these schemes is the accuracy by which fluxes to the atmosphere are simulated; this includes latent and sensible energy fluxes. Also, understanding and predicting soil moisture and soil temperature in porous media is of importance in the environment sciences and engineering, especially in studying cold regions hydrology. The effects are many and include physical, chemical, and biological processes such as soil respiration, evapotranspiration, nitrification, and denitrification. Soil moisture and soil temperature are the most crucial variables to control the variation of CO_2 flux from the surface and soil respiration within the soil. Strong correlation has also been reported between these variables and soil respiration (Fang and Moncrieff, 1999; Tang et al., 2006). Note that because of their effects on microbial activity, soil water and temperature are important factors that control seasonal variations in mineralization of soil organic matter. In addition, the relative importance of the physical, chemical and biological processes highly depends on soil moisture and snow depth. Thus, changes in soil moisture and soil temperature can affect the rate of ammonium and nitrate concentration below the

surface (Freppaz et al., 2007). At this point in time, many soil-water-plant models such as SABAE-HW (Loukili et al., 2008), CLASS (Verseghy 1991; Verseghy et al., 1993), COUP (Jansson and Karlberg, 2001), HYDRUS 1D/2D (Šimunek et al., 1998; Šimunek et al., 2008), and SHAW (Flerchinger and Saxton, 1989) have been developed to simulate water content and heat transfer under special conditions such as freezing and thawing, varied vegetation and solute transport. Each of these models has unique features and simplifications to solve for fluid, flow, heat transport, and so on, depending on their applications. However, these codes are sometimes difficult to verify, at least in field environments and practical applications, due to the many input parameters required. Thus, evaluating the conceptual models implicit in each code under field conditions is a major and complex research challenge. For example, SABAE-HW is a multilayered version of the Canadian Land Surface Scheme (CLASS 2.6). It is a one dimensional, physically-based model that was developed to simulate soil moisture, soil temperature, and snow depth for a wide range of soil and vegetation types. The model also considers the effects of soil freezing and thawing on soil water dynamics.

In recent years, several models have been evaluated with the BOREAS project data. Levine and Knox (1997) developed a frozen soil temperature code (FroST) to simulate soil moisture and heat flux. The model was applied to Old Jack Pine (OJP) and Black Spruce (BS) field data at the BOREAS northern and southern studies area. The predicted snow depth results showed a qualitatively good fit with measured data, whereas predicted soil temperature results were underestimated compared to measured data. Moreover, there were large differences between the simulated results and observed data when snow was present. Differences of about 50 percent were observed between simulated (snow

depth and soil temperature) and measured data in winter. Two different versions of CLASS, the Canadian Land Surface Scheme (2.7 and 3.1), were also tested and verified by the OJP site data (Bartlett et al., 2006). Although Class (3.1) has been modified and updated in terms of canopy resistance, mixed precipitation, snow density, and snow interception, it still underestimated snow depth and soil temperature values but not as much as CLASS (2.7). Furthermore, the 1998-2003 data for the BOREAS/BERMS project was used to calibrate a forest hydrology model (ForHyM) which was able to simulate all major water and heat fluxes in a forest ecosystem. By entering daily weather and soil parameters as the input file, the code calculated soil moisture, soil temperature, and frost depth at any depth. The code was designed to consider canopy closure, ground cover, and forest floor depth. In spite of the satisfactory agreement between observed and calculated values in terms of snow depth, the simulated soil water content was not in a good agreement with measured data. Soil moisture was underestimated in winter and overestimated in summer. Simulated soil temperature results were also reported in a good fit during summer but there were some differences with observed data in winter (Balland et al., 2006).

In addition to these model verification efforts, a few statistical studies were also carried out to show the relationships between landscape mean snow depth and fixed point snow depth in the BERMS field sites. As has been reported, single, fixed-point measures of snow did not adequately represent the average snow depth at this site. Once empirical relationships were found between the fixed point depth and snow surveys for the accumulation season, scaling factors were recommended to improve the interpretation of the fixed point measurements in order to model snow depth. These factors should be employed to increase confidence in the use of snow measurements at OJP site for modeling

and climate variability changes. High correlation coefficient value (0.98) was found when a simple linear relationship was applied between fixed point and landscape mean depths at OJP site (Neumann et al., 2006).

The purpose of this chapter is to evaluate the performance of SABAE-HW model by comparing predicted variables such as soil moisture, temperature and so on from the BOREAS (Boreal Ecosystem Atmosphere Study) and BERMS (Boreal Ecosystem Research and Monitoring Sites) field sites. Measured meteorological data over an extensive 10-year period is used to evaluate the model. SABAE-HW is also inter-compared and tested with the results of the SHAW model which is a vertical, one dimensional code with a detailed energy balance-based scheme. Although it was reported that SHAW generally overestimated evaporation and underestimated water storage and drainage, this code was selected for the comparison because it is a well-known model and includes snow accumulation and evapotranspiration from multispecies plant canopy (Loukili et al.,2008). SHAW's application has been extensively verified (Flerchinger et al.,1996; Xiao et al., 2006a; Xiao et al., 2006b). Calibration will be minimal, as most parameters are taken from default code values and publications. It is believed that the SABAE-HW code has now been verified and can be used for the simulation of fundamental variables of soil physics under different vegetation and freeze and thaw events. SABAE-HW has been also coupled with nutrient transport equations to control nitrate transport at the field scale (Chapter 4). The model can be further used to assess a variety of BMPs (Best Management Practice) aimed at minimizing nitrate leaching to ground water under actual atmospheric and field conditions (Chapter 6).

3.2 Methodology

A large number of models for simulating water flow and heat transport in the saturated and unsaturated zone have been developed for a wide range of applications in research and management. Modeling approaches range from analytical (simple or semi analytical) to complex numerical solutions. Analytical solutions can only be useful for simplified transport systems including linearized governing equations, homogenous soils, and constant or highly simplified initial boundary conditions. However, numerical models are able to solve the highly nonlinear nature of problems even in heterogeneous soils. Generally, since numerical methods are able to solve practical problems such as complicated geometries and realistic initial and boundary conditions, they are superior to analytical methods. It should be noted that the stable numerical solutions require fine discretization of time and space resulting in high simulation time.

All of these models are usually based on two basic equations: water flow and heat movement:

$$\frac{\partial\theta(\Psi)}{\partial t} = \frac{\partial}{\partial z}\left[K(\Psi)(\frac{\partial\Psi}{\partial z} + 1)\right] - W \qquad 3\text{-}1$$

$$\frac{\partial G(\theta)T}{\partial t} = \frac{\partial}{\partial z}\left[\lambda(\theta)\left(\frac{\partial T}{\partial z}\right) - G_w q T\right] \qquad 3\text{-}2$$

In Eq. 3-1, z is the vertical coordinate positive downwards, t is time, Ψ is pressure head, θ is soil moisture, W is a sink term representing root water uptake, $K(\Psi)$ is the unsaturated hydraulic conductivity function. In Eq. 3-2, T is temperature, λ is thermal conductivity, and G and G_w are the volumetric heat capacities of the soil and the liquid phase, respectively.

In this model, the flow rates are expressed by the Darcian equation for 1D flow:

$$q(z) = K(z)\left(\frac{d\Psi}{dz} + 1\right) \quad 3\text{-}3$$

where *K(z)* represents the hydraulic conductivity and *Ψ(z)* is the soil water suction. These parameters are defined by (Clapp and Hornberger, 1978):

$$K(z) = K_{sat}\left[\frac{\theta_{l(z)}}{\theta_p}\right]^{2b+3} \quad 3\text{-}4$$

$$\Psi(z) = \Psi_{sat}\left[\frac{\theta_{l(z)}}{\theta_p}\right]^{-b} \quad 3\text{-}5$$

where K_{sat} and Ψ_{sat} are the saturated hydraulic conductivity and the effective saturated soil water suction, respectively. θ_p is the pore volume fraction, and *a* and *b* are soil texture parameters. It is noted that *q(0)* is related to rainfall and evaporation rates.

The heat flux is also determined as:

$$F(z) = -\lambda(z)\frac{dT}{dz} \quad 3\text{-}6$$

where *λ(z)* represents the thermal conductivity interpolated between its dry and saturated values according to the relative moisture content.

The snowpack is also modeled in SABAE-HW. The heat capacity of snow is calculated from the heat capacity of ice and the densities of snow and ice:

$$c_s = \frac{c_a \rho_s}{\rho_1} \quad 3\text{-}7$$

where c_s and c_a are the heat capacities of snow and ice and ρ_s and ρ_1 are the densities of snow and ice respectively. Snow density is assumed to be constant with depth due to the need for a multilayer snowpack but the magnitude of ρ_s increases exponentially with time starting from a fresh snow value of 100 kg m^{-3}. Similar to snow density, snow albedo also depends on grain size. The magnitude of snow albedo is assumed to decrease exponentially with time from a fresh snow value of 0.84. Snowpack melting is also considered in the model.

3.2.1 Conceptual Model Description

As mentioned, SABAE-HW (Soil Atmosphere Boundary, Accurate Evaluations of Heat and Water) is a soil multilayer version of the Canadian Land Surface Scheme (CLASS2.6). SABAE-HW is also physically-based model that used the same methodologies imbedded in CLASS (2.6). It was designed to provide an improved interface for groundwater modeling to calculate soil, heat, and moisture transfer with a refined mesh. The general minimal residual (GMRES) iterative algorithm was implemented to solve soil heat flux terms.

SABAE-HW requires three extensive input files: atmospheric, vegetation, and soil characteristic files. Half-hourly atmospheric inputs are: short wave radiation, long wave radiation, precipitation, surface temperature, wind speed, air pressure, and specific humidity. Precipitation is considered as the snow precipitation when the air temperature is less than zero. The code has been designed for four different vegetation types: needleaf, broadleaf, crops, and grass. Two lower boundary conditions are applied: a water table and unit gradient boundary conditions. The first condition determines the water surface in groundwater and the second one represents a free drainage at the bottom of soil column. Atmospheric conditions above the upper boundary condition and soil condition at the lower boundary define heat and water fluxes in to the system. Subsequently, SABAE-HW calculates daily and half-hourly soil moisture (frozen and unfrozen), soil temperature, snowpack depth, evaporation, surface energy balance (sensible and latent heat flux), and net radiation.

3.2.2 Site Description

The performance of SABAE-HW was evaluated using a 10 year (1997-2006) measurement stream from one of the Southern study areas of the BOREAS/BERM project, namely, the Old Jack Pine site (OJP). This site is a mature forest with jack pine trees ranging in height from 12-15 m located in Saskatchewan (53.916 N, -104.692W; Elev. 579) (Figure 3-1). The mean annual precipitation is 467.2 mm and the mean annual air temperature is 0.4 ºC (1971-2000 Waskesiu normal). The soil type is sand with a well-drained soil texture. The vegetation ground cover is mostly mature jack pine with a sparse green alder (Alnus crispa), predominantly lichen ground cover (Bernier et al., 2006). This ground cover type provides thermal insulation to the soil and since it is permeated by snow, it essentially becomes a part of snowpack in winter.

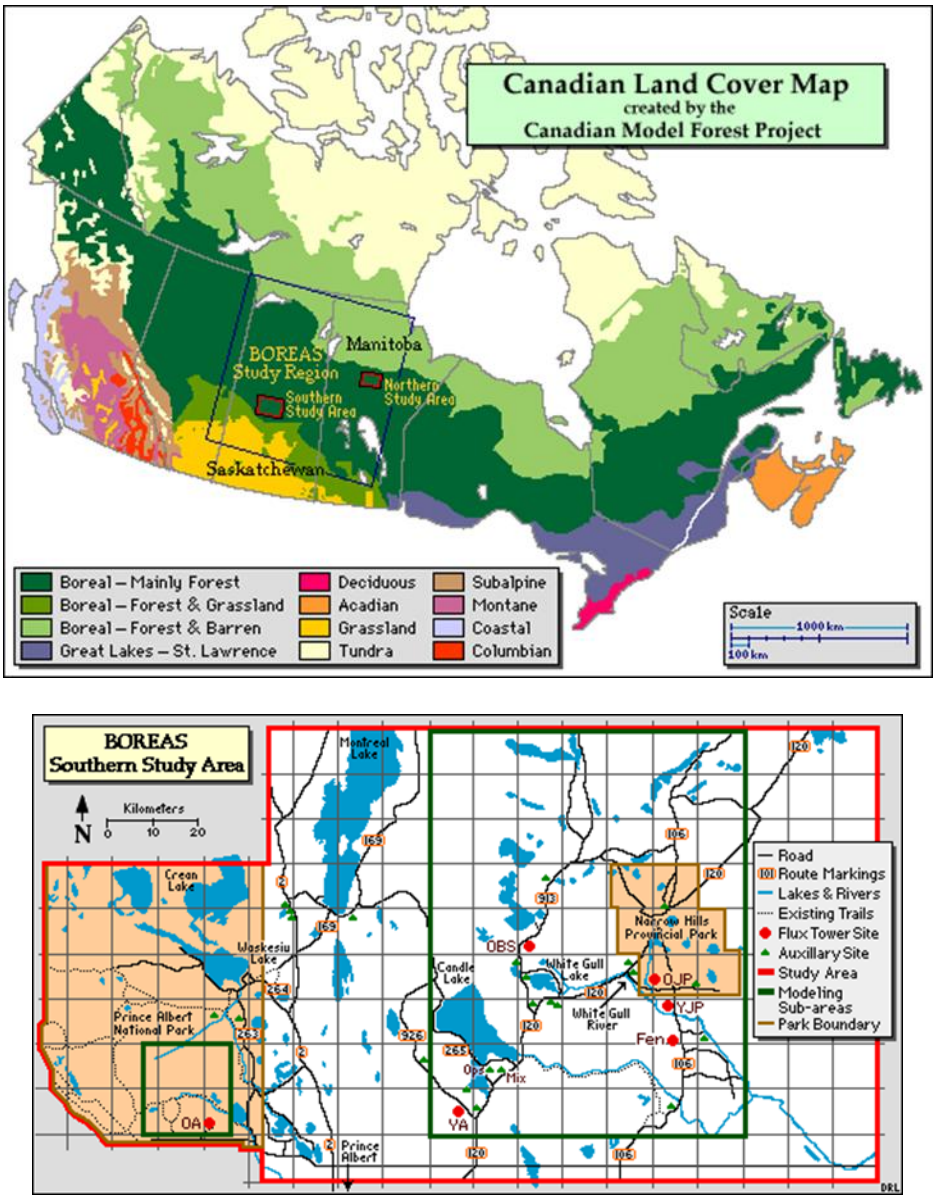

Figure 3-1: The location of Old Jack Pine site, the BOREAS/BERMS Southern Study Area, Saskatchewan, Canada

3.2.3 Instruments

The snow depth at OJP is measured using a SR50 sensor from Campbell Scientific. There are two of these sensors at OJP; one located in a clearing canopy and another located un-

der the forest canopy. A Canadian snow sampler was also used to measure accumulative snow depth and provided data on integrated snow density and snow water equivalent (Forrest and Knapp, 2000). Soil moisture data were measured using CS615 probes from Campbell Scientific. At the OJP, the first two probes (0-15 and 15-30 cm) were installed at a 45 degree angle (for higher resolution). The probes give a layer moisture average for each 15 cm and the CS615 probes are 30 cm long. Therefore when measuring a 15cm layer, higher resolution will be obtained than when measuring a 30 cm layer. The deeper probes are installed at 30cm intervals and also give a layer average (30-60 and 90-120 cm). The measurements were recorded 6 times in a day at those described ranges. Soil temperatures were also measured by use of a Cu-Co thermocouple sensor made by Queens University (BOREAS/BERMS reports). It is basically a rod that is inserted in to the soil with thermocouples mounted at known intervals (2, 5, 10, 20, 50, and 100 cm). Soil temperature, like atmospheric data, was monitored every 30 minutes (Keshta et al., 2010).

3.3 Model Evaluation

SABAE-HW was compared against measured data at the OJP site over the period 1997 to 2006. Since the code has been developed for Δt=30 min, a great source of data to assess the performance of SABAE-HW was required. The code requires three input files: atmospheric, vegetation, and soil type. Half-hourly atmospheric inputs include short wave radiation, long wave radiation, precipitation, surface temperature, wind speed, air pressure, and specific humidity. Since the vegetation type was dominated by jack pine, they

were classified as a needleaf in the model. To determine the soil moisture characteristics, SABAE used the formulas suggested by Clapp and Hornberger (1978):

$$\psi(\theta) = \psi_s \left(\frac{\theta}{\theta_s}\right)^{-b} \quad 3\text{-}8$$

$$K(\theta) = K_s \left(\frac{\theta}{\theta_s}\right)^{2b+3} \quad 3\text{-}9$$

where ψ_s is the soil water suction at $\theta=\theta_s$, K_s is the saturated hydraulic conductivity, θ is the soil moisture, θ_s is the soil moisture at saturation point (pore volume fraction) and b is an empirical constant.

Soil parameters such as saturated hydraulic conductivity and pore volume fraction were specified from observation data. Unfortunately, there were no Clapp and Hornberger soil moisture constants available for the OJP site. Thus, the parameters b and ψ_s were determined by finding the best match between Clapp and Hornberger and van Genuchten soil characteristic curves as all soil parameters in van Genuchten formula had previously been reported for OJP site (Kuchment et al., 2006a). All the model parameters used for SABAE-HW and SHAW model are listed in Table 3-1.

Table 3-1: A summary of SABAE-HW soil and vegetation inputs

parameters	values
% sand	95-99
%clay	1-5
Sand index	15
Clay index	1.4
Pore volume fraction (m^3/m^3)	0.4
Saturated soil water suction (m)	0.22
Saturated hydraulic conductivity (m/s)	$16.8e^{-6}$
b	2.30
Canopy height (m)	14
Leaf area index (m^2/m^2)	1.9
Visible albedo	0.04
Near-infrared albedo	0.19
Root depth(m)	1

Sand index = min ((%sand-17)/5, 15) Clay index = min ((%clay+2)/5, 12)

Two approaches were adopted for imposing the boundary condition at the bottom of the domain. The first approach was to apply unit gradient boundary to the bottom of the grid. Thus, the total depth of soil column was 3 meters (11 layers). In the second approach, since the actual water table is near a depth of 7 meters, the soil column was extended to 7 meters (19 layers) to fix the water table boundary condition at the bottom of soil column. In both cases, the first two layers have a thickness of 15 cm, with 30 cm and 40 cm for the rest of layers (Figure 3-2). Furthermore, based on the observed data (soil

moisture and soil temperature), the fixed point (Dirichlet condition) was used for upper boundary condition. The exact value of observed soil moisture and soil temperature data at t=0 (first time step) was applied for initial conditions at the middle of each layer. In the case of a water table boundary condition, initial soil moisture was set to a value of porosity at the bottom of the soil profile. Leaf area indices, visible albedo, near infrared albedo, vegetation rooting depth, and canopy mass used in simulating hydrological processes of the site were based on various publications (Bartlett et al., 2006; Kuchment et al., 2006b).

It is noted that soil temperature and soil moisture are both calculated at the midpoint of each layer. To obtain a reasonable result of calculated parameters in winter time, the model was initialized to observed values on August 1, 1997. It is important to mention that the same scheme was adopted for SHAW model regarding the number of layers and boundary conditions.

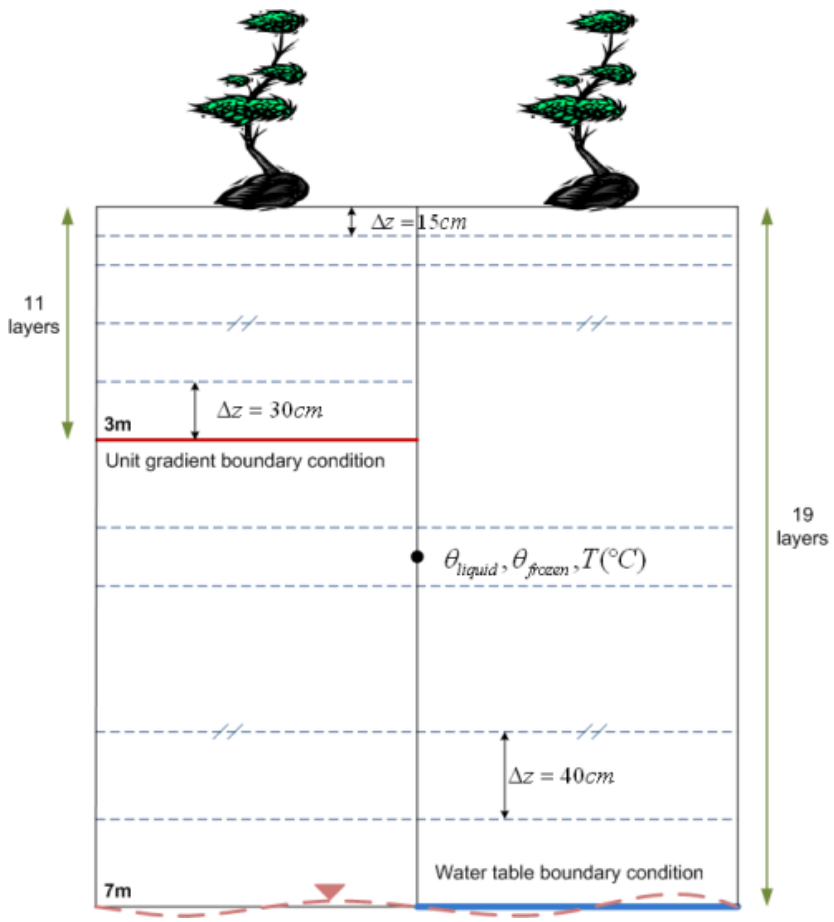

Figure 3-2: Overview of the lower boundary conditions in SABAE-HW applied for the OJP site

The Average Error (AE), the Root Mean Square Error (RMSE), and correlation coefficient (r) are computed to compare simulated variables to the field data (Bruijn et al., 2009). The average error demonstrates how well the simulated data approximates the field data, either being above or below measured values, whereas the root mean square error is a measurement for the variation between datasets. The closer the calculated values are to zero, the better approximation of simulated to the field data. However, the best approximation is achieved when correlation coefficients are close to one. These performance measures, used for comparing model predictions to observations, are calculated as:

$$\mathrm{AE} = \frac{(\sum_{i=1}^{n} S_i - O_i)}{n} \quad 3\text{-}10$$

$$R\mathrm{MSE} = \sqrt{\frac{(\sum_{i=1}^{n} S_i - O_i)^2}{n}} \quad 3\text{-}11$$

$$\mathrm{r} = \frac{(\sum_{i=1}^{n} O_i - \bar{O})(\sum_{i=1}^{n} S_i - \bar{S})}{\sqrt{(\sum_{i=1}^{n} O_i - \bar{O})^2 (\sum_{i=1}^{n} S_i - \bar{S})^2}} \quad 3\text{-}12$$

where S_i is the simulated value, O_i is the observed value, $\bar{S}$ and $\bar{O}$ are the mean of simulated and observed values, and n is the number of data point.

3.4 Results and Discussion

3.4.1 Snowpack

The result of simulated and measured snow depth over 10 years study at OJP site is given in Figure 3-3. Comparing the distribution of measured and SABAE snow depth shows a satisfactory agreement, especially during the period 2003-2006. Although SABAE simulated snow depths slightly lower than observed data (maximum 35% difference in winter 2002), there is a good correlation between SABAE and observed data. The correlation coefficient value of 0.96 was found for the SABAE model. However, the SHAW model shows a different pattern when the snowpack is formed. In fact, snow depth increases drastically and then drops gradually sooner than SABAE compared to measured data. Figure 3-4 shows the plots of average error and root mean square error versus time for the SABAE and SHAW model with regard to the field data. Both SABAE plots show the closer values to zero. Furthermore, as detailed in Table 3-2, SABAE simulated the snow

depths with higher correlation value than SHAW which is a good indication of SABAE in terms of simulation of snow depths.

Table 3-2: Average Error, Root Mean Square Error and Correlation values for simulated and measured snow depth within Old Jack Pine site from Sep. 1997 to Dec. 2006

Measured data versus SABAE			Measured data versus SHAW		
Average err	RMSE	Correlation	Average err	RMSE	Correlation
-0.007	0.04	0.96	-0.02	0.06	0.90

Figure 3-4 also confirmed the results of snow depths modeled by CLASS (2.7 and 3.1) and ForHyM model (Bartlett et al., 2006). Note that all three models underestimate the values of snow depth. However, FroST (Levine and Knox, 1997) overestimated snow depth results in winter 1994 at the OJP site. A 50% difference between measured and predicted snow depth has been observed in winter time. Variation in snow density over time and snow reflectance which was constant in the model has been reported as the main reason for these differences. In fact, the model assumed that snow density increases only if air temperatures are above zero while the density of actual snow varies as snow ages and compacts over time.

According to Neumann at al. (2006) at many of the BERMS research sites, fixed point snow depth measurements cannot approximate the average landscape depth taken by snow surveys. They strongly recommended that adjustment factors should be employed for the snow fall to obtain a reasonable result in terms of hydrological and surface processes. In order to produce the best overall fit between simulated and measured snow depth, a maximum correction factor of 1.4 was applied to the precipitation data in winter of 98 to 2000. Correction factors were reduced to 1.1 for the remaining years.

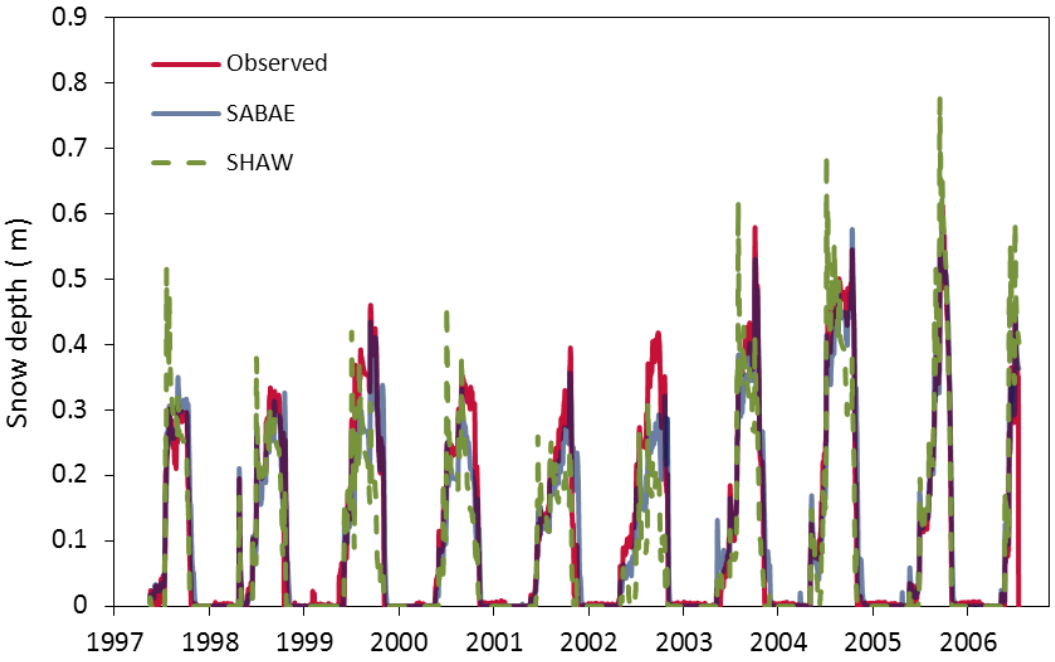

Figure 3-3: Simulated and measured snow depths Sep. 1997 to Dec. 2006

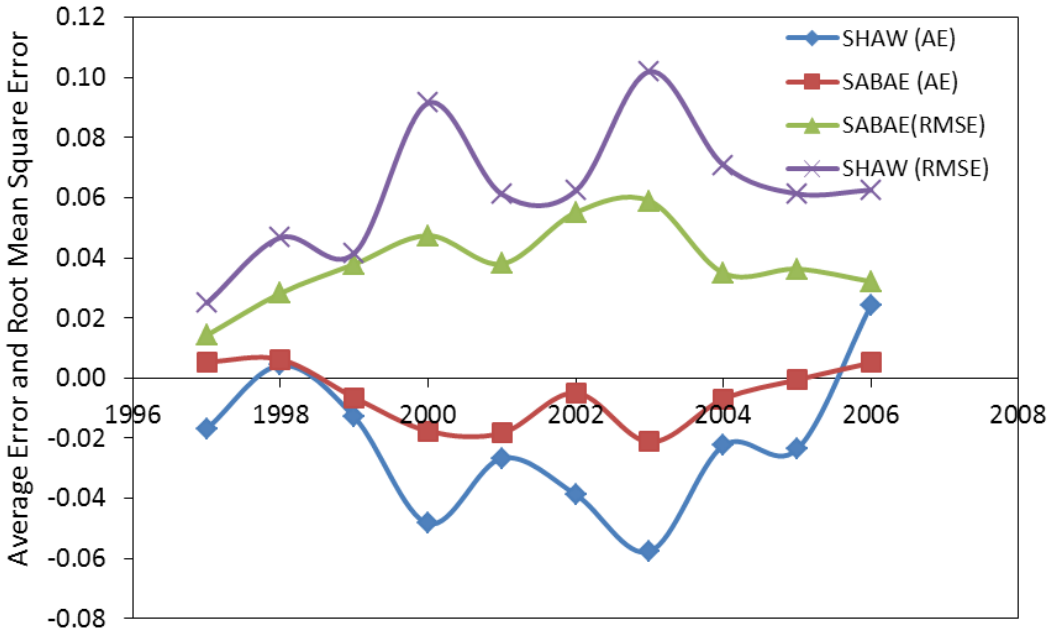

Figure 3-4: Average Error and Root Mean Square Error for SABAE and SHAW simulated snow depth from Sep. 1997 to Dec. 2006

Figure 3-5 and Figure 3-6 show the simulated and measured Snow Water Equivalent (SWE) and snow density at OJP site from Nov 2002 to March 2003. It is noticed that the variations of snowpack density is dependent on the meteorological conditions. In addition, the snow that falls at colder temperatures is less dense than the wet snow falling at temperatures greater than zero. Since rain falling on a snowpack freezes at the density of ice, mixed precipitation results in a less dense snowpack. Snow density affects both the snow's specific heat and thermal conductivity. Differences between the observed and modelled density can be used to explain differences between the observed and modelled snowpack depth. Since the snow on the canopy is considered as a source of sublimation by SABAE-HW, the simulated SWE was lower than the observed SWE. In general, underestimation by the simulated SWE and overestimation by the simulated snow density for the OJP site resulted in an underestimation of snow depth. Therefore, a less dense snowpack increased the snow depth. As a result, the insulating effect of the snowpack on soil surface temperature profile also increased. Note that the results reported here are only for the year 2002 to 2003. This study does not compare simulated SWE and snow density to the observed data for the entire 10-year study period due to the field data limitation.

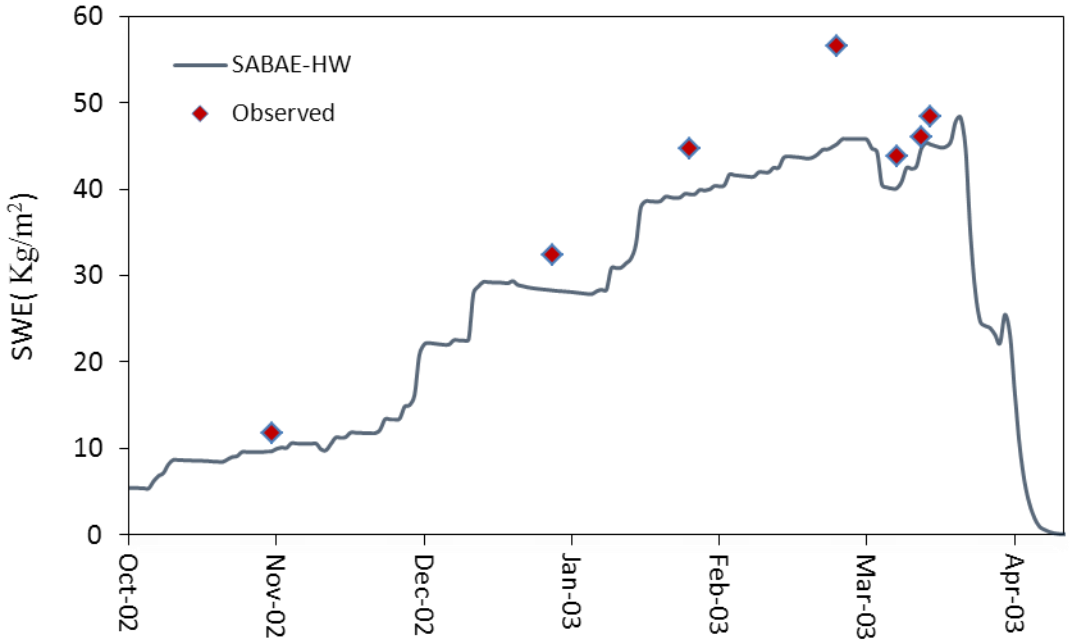

Figure 3-5: Simulated and observed SWE in the OJP for year 2002/2003

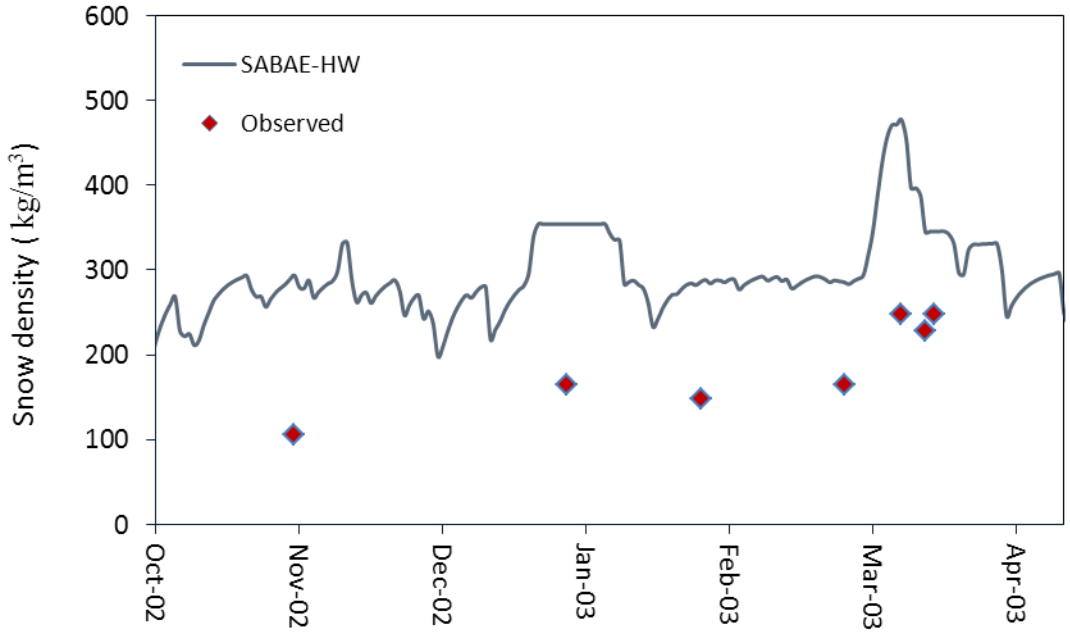

Figure 3-6: Simulated and observed snow density in the OJP site for the year 2002/2003

3.4.2 Soil Temperature

Figure 3-7 shows the simulated and measured soil temperatures at four depths with the water boundary condition at the bottom of the soil profile at the OJP site. In general, there is a strong correlation between simulated soil temperatures (SABAE and SHAW) and measured data. However, there are differences during those times when a snowpack is present. Table 3-3 shows that the agreement between the simulations and observations was satisfactory during the summer of 2003 (June to September). High correlation coefficient values (0.92 to 0.98) were found for simulated soil temperatures, but as the air temperature drops after November, both models underestimated soil temperatures in winter. The negative average error represents model's underestimation of the field data. As shown in Table 3-4, the average errors reported for both models were negative. However, the SABAE error values were relatively close to zero, indicating SABAE was accurate in estimating soil temperatures in winter. Similar results were found during 10 years of study on OJP site.

Although both SABAE and SHAW take into account the soil insulation, there are discrepancies between measured and modeled soil temperatures in winter. In fact, the insulating effect of the snow does not allow for colder temperatures to penetrate the soil. Moreover, the vegetation cover which is permeated by snow enhances thermal insulation to the soil below. Thus, in comparing to the predicted soil temperature, a significant rise in actual soil temperature is expected. As shown in Figure 3-7, the effects of soil insulation on simulated soil temperature decreases at a depth of 105cm. Decreasing the snow depth reduces the degree of insulation and results in colder soil temperatures. In addition, analysis indicates that each SABAE grid appears cooler than those simulated by SHAW

and field observations and generates an ice content much sooner in winter. This might be related to a fixed minimum liquid soil moisture content from the parent model CLASS (2.6) that limits liquid soil moisture to 4%. Since soil layers are permitted to go lower by SHAW, some additional energy loss may be consumed by the latent heat of fusion rather than cooling temperatures below the freezing temperature. Table 3-5 shows that although both SABAE and SHAW models have approximately the same correlation coefficient (0.98), SABAE average error and root mean square error are closer to zero at lower depths than errors computed by SHAW. In spite of the fact that a strong correlation was found for both models at the deeper depths (105 cm), SHAW showed a smaller average error than SABAE.

Table 3-3: Average Error, Root Mean Square Error and Correlation values for simulated and measured soil temperatures at various soil depths within Old Jack Pine site from Jun. 2003 to Sep. 2003 (Water boundary condition)

	Measured Data Versus SABAE			Measured Data Versus SHAW		
depth	Average err	RMSE	Correlation	Average err	RMSE	Correlation
7.5	0.60	1.88	0.92	-1.24	1.89	0.94
22.5	0.25	1.46	0.92	-1.38	1.75	0.94
50	-0.14	1.13	0.92	-1.51	1.71	0.95
100	-2.10	2.24	0.97	-2.65	2.70	0.98

Table 3-4: Average Error, Root Mean Square Error and Correlation values for simulated and measured soil temperatures at various soil depths within Old Jack Pine site from Nov. 2002 to Apr. 2003 (Water boundary condition)

	Measured data versus SABAE			Measured data versus SHAW		
depth	Average err	RMSE	Correlation	Average err	RMSE	Correlation
7.5	-1.69	2.29	0.93	-2.27	3.22	0.90
22.5	-1.75	2.24	0.92	-2.01	2.55	0.93
50	-1.99	2.40	0.91	-1.96	2.23	0.94
100	-1.37	1.54	0.97	-0.80	0.95	0.97

Table 3-5: Average Error, Root Mean Square Error and Correlation values for simulated and measured soil temperatures at various soil depths within Old Jack Pine site from Aug. 1997 to Dec. 2006 (Water boundary condition)

depth	Measured Data Versus SABAE			Measured Data Versus SHAW		
	Average err	RMSE	Correlation	Average err	RMSE	Correlation
7.5	-0.70	2.06	0.98	-1.06	1.97	0.97
22.5	-0.80	1.84	0.98	-1.03	1.67	0.97
50	-1.01	1.83	0.98	-1.00	1.49	0.98
100	-1.18	1.30	0.97	-0.85	1.34	0.98

A comparison of simulated and measured values of soil temperature with the unit gradient boundary condition for the same period of 1997 to 2006 is given in Figure 3-8. Although the coefficients of correlation did not change for SHAW and SABAE model, both models showed larger errors with regards to the unit gradient boundary condition at the bottom of soil profile. In point of fact, soil temperatures are underestimated compared to predicted soil temperatures with a water table boundary condition. The saturated lower boundary condition probably did not underestimate soil temperature as much because the increased water content raised the heat capacity and heat content of the soil layers, and with more water, there is more heat released when each layer freezes. Interestingly, as it is shown by Table 3-6, average errors and root mean square errors calculated for SHAW model are smaller than SABAE.

Table 3-6: Average Error, Root Mean Square Error and Correlation values for simulated and measured soil temperatures at various soil depths within Old Jack Pine site from Aug. 1997 to Dec. 2006 (Unit gradient boundary condition)

	Measured Data Versus SABAE			Measured Data Versus SHAW		
depth	Average err	RMSE	Correlation	Average err	RMSE	Correlation
7.5	-1.36	2.92	0.97	-1.30	2.24	0.97
22.5	-1.51	2.69	0.97	-1.20	1.90	0.98
50	-1.68	2.65	0.97	-1.19	1.68	0.98
100	-1.86	2.45	0.95	-0.96	1.49	0.98

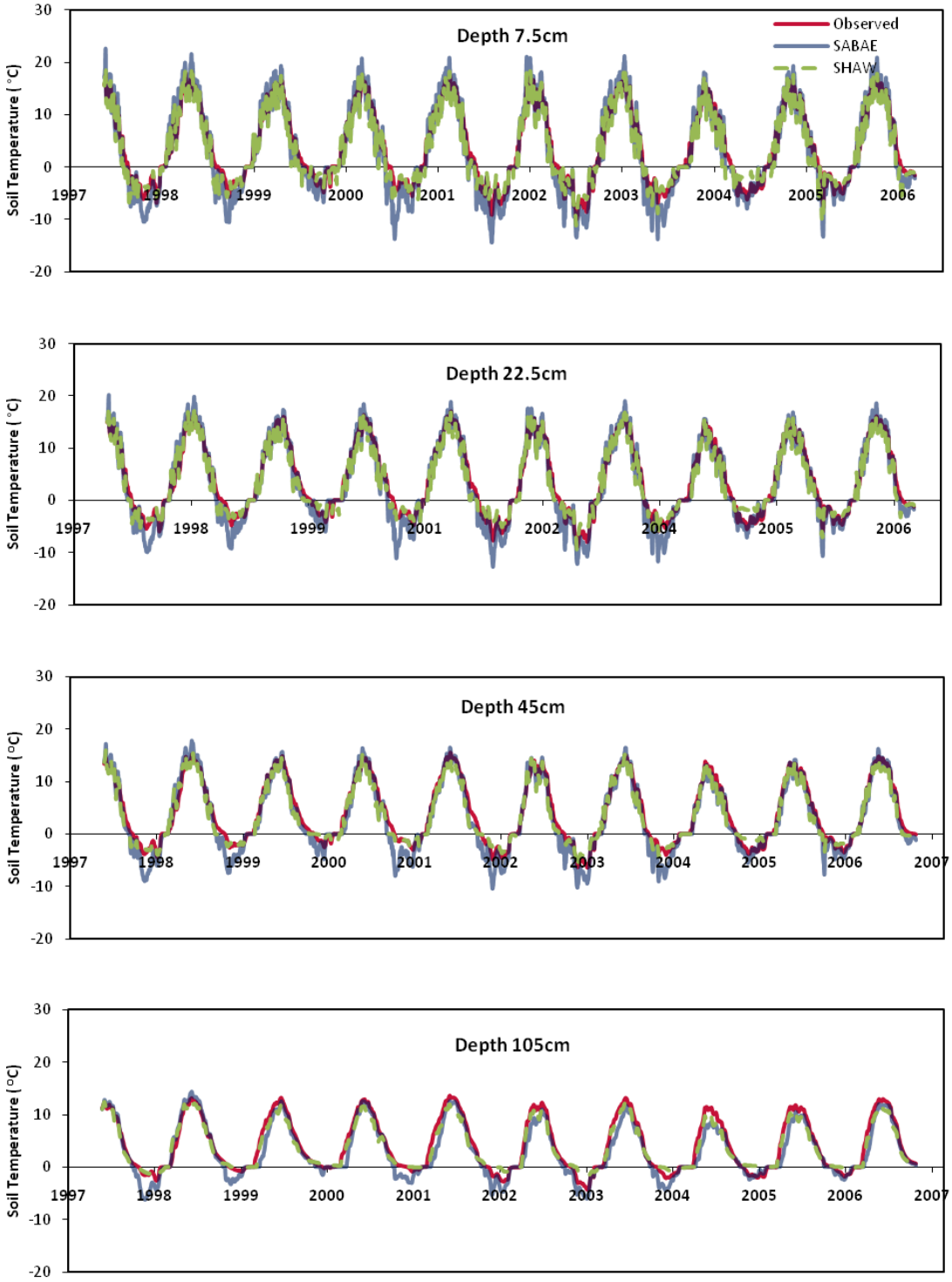

Figure 3-7: Simulated and measured soil temperatures 7.5, 22.5, 45 and 100 cm below the soil surface from Aug.1997 to Dec.2006 (Water boundary condition)

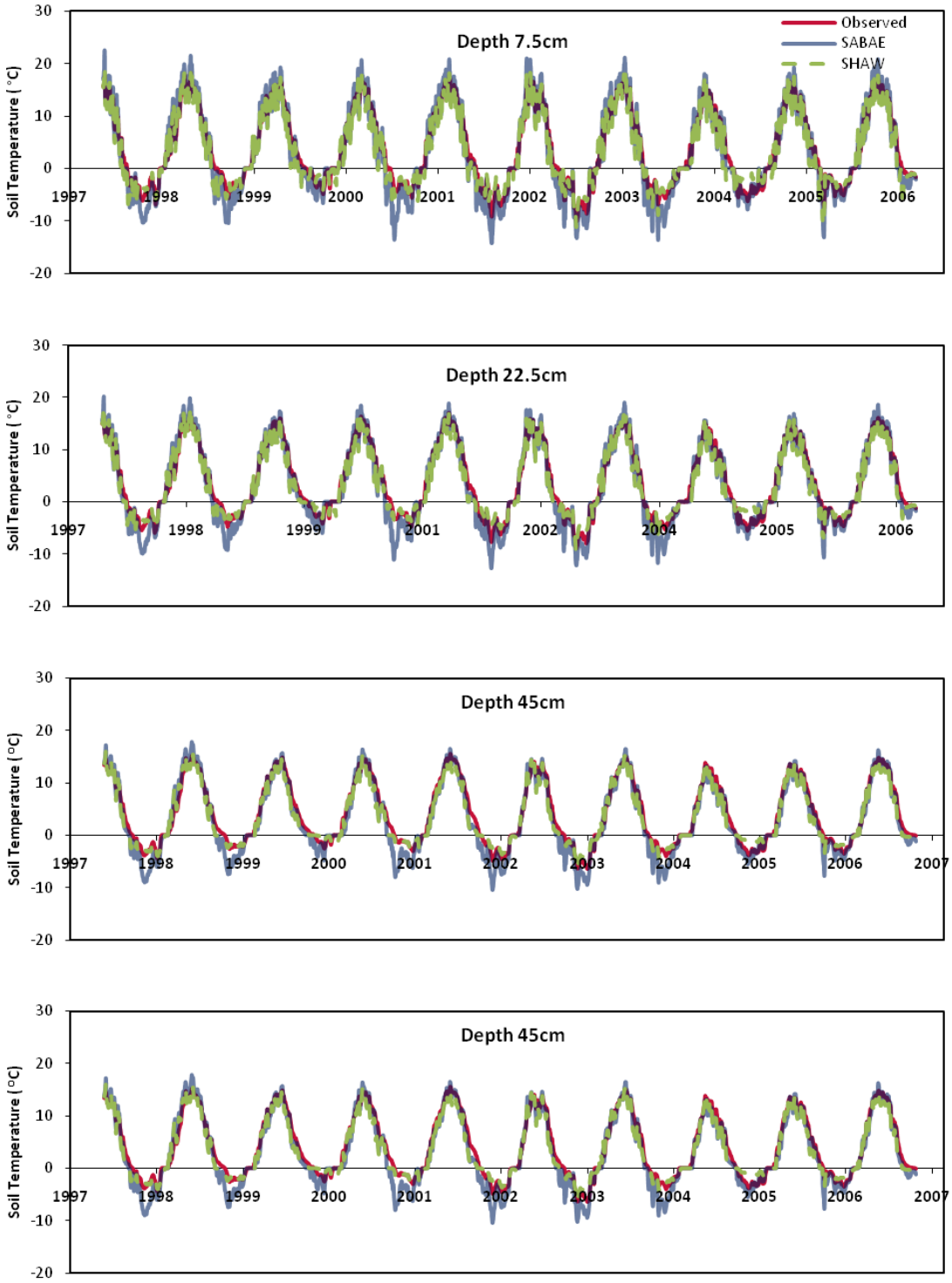

Figure 3-8: Simulated and measured soil temperatures 7.5, 22.5, 45 and 100 cm below the soil surface from Aug.1997 to Dec.2006 (Unit gradient boundary condition)

3.4.3 Soil Moisture

Figure 3-9 compares the distribution of the simulated and measured unfrozen water content in the soil profile at OJP site with a water table boundary condition. As apparent from these figures, soil moisture correlations are not as good as snow depth and soil temperature distribution, especially in lower soil layers. The positive values of average error indicate that soil moisture is overestimated by both SABAE and SHAW (Table 3-7). As indicated by relatively small AE values (Table 3-7), model bias in predicting soil moisture was generally small. Over the simulated period, the average of AE values was 0.03 and 0.05 in SABAE and SHAW, respectively. However, the main disagreement between models and measurements is at greater depths, when both models gave a correlation of less than 0.25 for the depth of 90-120 cm. In addition, SABAE and SHAW did not present the similar correlation coefficient between simulated and measured for the top 90cm of the soil profile. An average value of 0.55 was found for SABAE while SHAW presented a small value (less than 0.30) in terms of correlation, which indicates a better fit between simulated and field data by SABAE.

Table 3-7: Average Error, Root Mean Square Error and Correlation values for simulated and measured soil moisture at various soil depths within Old Jack Pine site from Aug. 1997 to Dec. 2006 (Water boundary condition)

	Measured data versus SABAE			Measured data versus SHAW		
depth	Average err	RMSE	Correlation	Average err	RMSE	Correlation
0-15	0.007	0.04	0.53	0.06	0.10	0.13
15-30	0.02	0.04	0.62	0.05	0.08	0.35
30-60	0.01	0.05	0.42	0.03	0.05	0.32
60-90	0.02	0.05	0.57	0.03	0.05	0.25
90-120	0.01	0.05	0.26	0.03	0.04	0.30
120-150	0.03	0.06	0.12	0.04	0.05	0.23

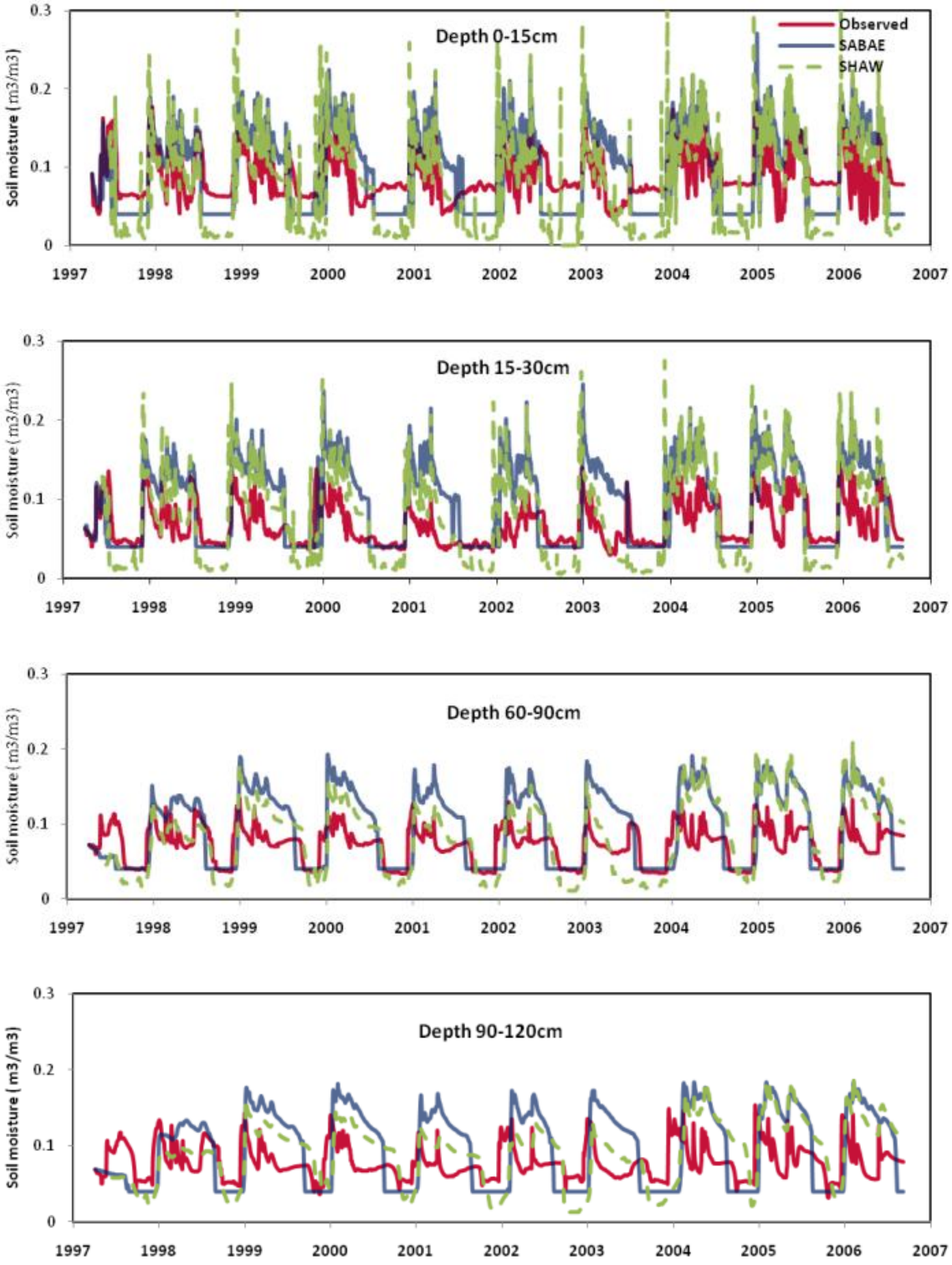

Figure 3-9: Simulated and measured soil moistures 7.5, 22.5, 45 and 105 cm below the soil surface from Aug. 1997 to Dec. 2006 (Water boundary condition)

As it was shown in Figure 3-9, although both models underestimated unfrozen soil moisture in winter, small differences between simulated and observed soil moisture were found. Compared to observed soil moisture in winter, it was found a difference of 0.01 and 0.04m^3m^{-3} for SABAE and SHAW models, respectively, which demonstrates the ability of SABAE to simulate unfrozen soil moisture in winter. However, relatively large differences (about 0.08m^3m^{-3}) were obtained in summer for both models, especially at deeper soil layers. These discrepancies might correspond to the points where the data were chosen. Since SABAE and SHAW computes the value of soil moisture at the middle of each layer, the results of simulated and observed data were compared at the depths of 7.5, 22.5, 75, and 105 cm. Unfortunately, the exact value of observed data at these points had not been reported. In fact, each soil moisture observation is an average of 2 or more samples taken at 30cm intervals. Thus, the simulated soil moistures by SABAE and SHAW were calculated specifically for one point at the middle of each layer while the measured soil moistures are corresponding to the average of soil moisture in each layer. Also, the amount of underestimation of liquid water in the soil in winter is probably a result of the minimum possible value for liquid water, a model parameter. The actual soil moisture reading depends on the soil organic matter, soil texture, and soil bulk density close to each sensor. Because of the coarse nature of the soil at the OJP site, water contents are always very low. It has been reported that even if two soil moisture probes are located at the same depth but different locations, it is unlikely to obtain the same soil moisture values (Balland et al., 2006). Moreover, there has been an attempt to improve calculations of soil moisture by decreasing the depths of soil layers. However, no significant improvement of the simulated results was obtained.

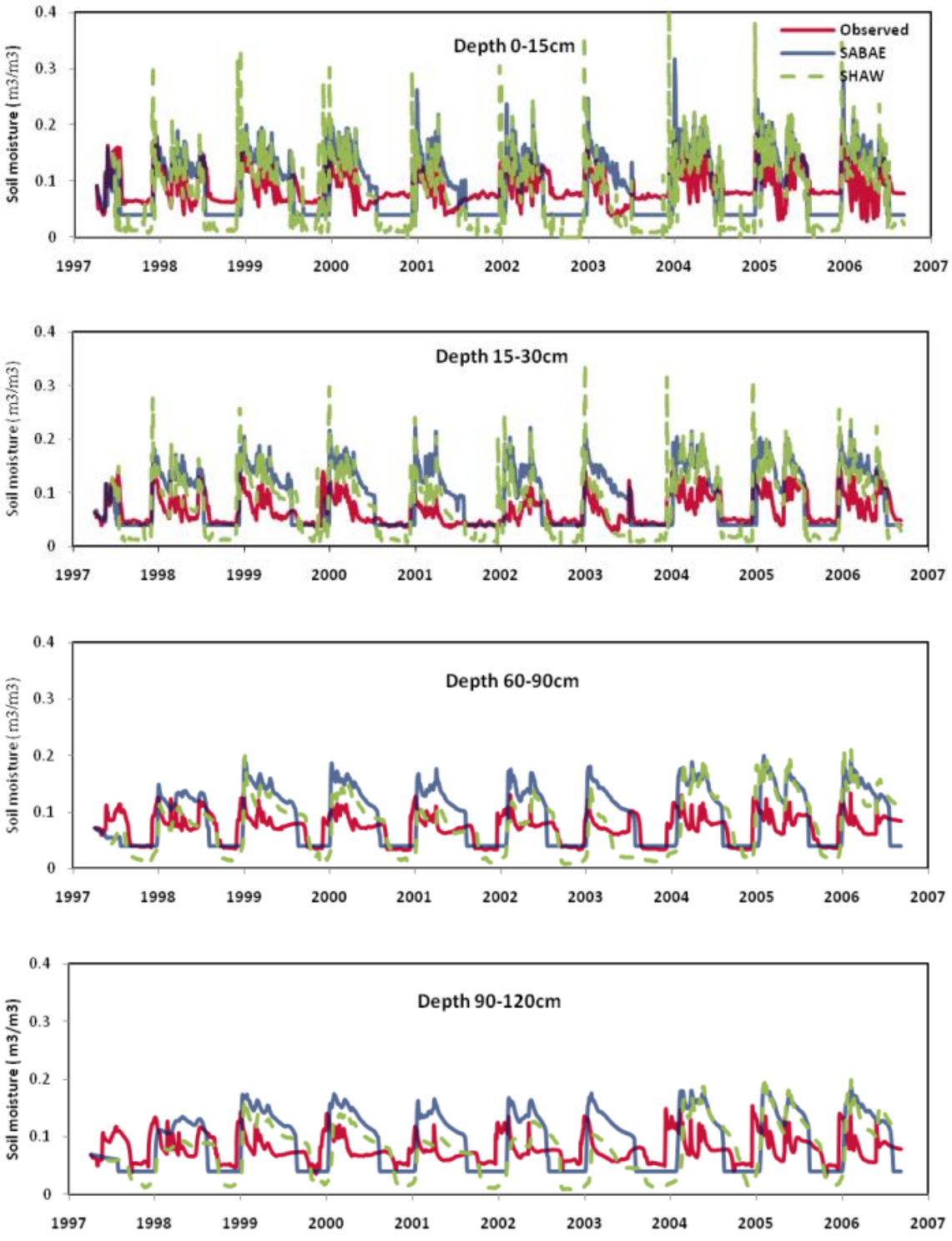

Figure 3-10: Simulated and measured soil moistures 7.5, 22.5, 45 and 105 cm below the soil surface from Aug. 1997 to Dec. 2006 (Unit gradient boundary condition)

Both codes calculate volumetric water content based on the initial soil moisture, and characteristics of soil texture including the percent of sand, silt, clay, and organic matter. There are implicit default values such as soil saturation point, porosity, permanent wilting point, and soil permeability, all which affect soil moisture. Furthermore, SABAE-HW did not account for the amount of runoff, although this is likely to be very small. Figure 3-10 also compares calculated and measured soil temperatures with the unit gradient boundary condition. For the whole period of study, the unit gradient boundary does not influence the moisture of soil layers. Although the coefficient of correlation is slightly smaller than the case presented using the water boundary condition, the average error and root mean square error are still the same (Table 3-8).

Table 3-8: Average Error, Root Mean Square Error and Correlation values for simulated and measured soil moisture at various soil depths within Old Jack Pine site from Aug. 1997 to Dec. 2006 (Unit gradient boundary condition)

	Measured data versus SABAE			Measured data versus SHAW		
depth	Average err	RMSE	Correlation	Average err	RMSE	Correlation
0-15	0.005	0.04	0.51	0.06	0.10	0.13
15-30	0.02	0.04	0.59	0.05	0.07	0.40
30-60	0.01	0.05	0.37	0.03	0.05	0.36
60-90	0.02	0.04	0.51	0.02	0.05	0.30
90-120	0.01	0.05	0.21	0.01	0.04	0.20
120-150	0.02	0.05	0.09	0.01	0.04	0.20

Direct comparison of soil moisture between models and measurements can be very challenging. Besides measurement and representative errors reported in this study, there are many factors that determine the storage of unsaturated moisture in the subsurface. To make a proper assessment of change in storage, evapotranspiration needs to be taken into account. Figure 3-11 shows a good match between the cumulative observed evapotranspi-

ration and the cumulative simulated evapotranspiration at the OJP site using a data from year 2001. The cumulative observed evapotranspiration using the eddy covariance technique was 301 mm and simulated evapotranspiration was 294 mm. However, simulated evapotranspiration by the SHAW model was 399 mm. Note that it has been reported that SHAW generally overestimates evaporation and underestimates water storage and drainage.

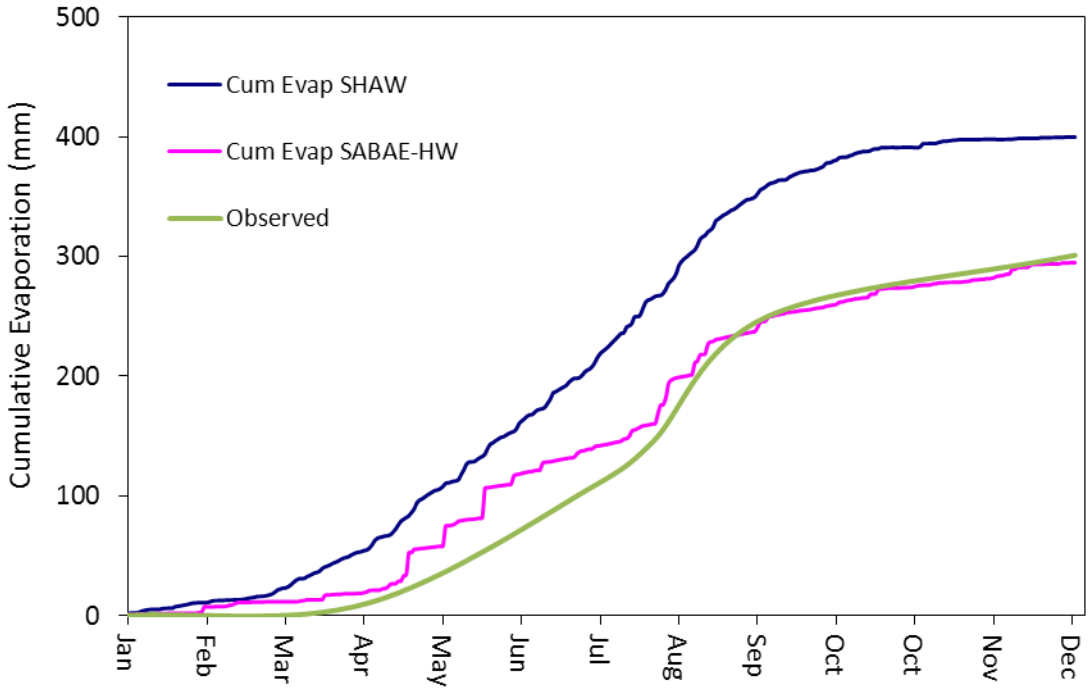

Figure 3-11: Observed and modeled cumulative evapotranspiration (mm) in the OJP site (2001)

3.5 Summary

In summary, the results of the simulations were in satisfactory agreement with the observations in terms of snow depth, soil temperature, and soil water content. Comparison of simulated results between SABAE-HW and SHAW also indicated the potential of SA-

BAE-HW as a Canadian Land Surface Scheme (LSS) coupled with a solute transport model. In order to investigate the distribution of soil ammonium and soil nitrate nitrogen through the soil profile, the model will be coupled with a nitrogen transport model. Next Chapter will focus on the development of SABAE-HW which includes coupling with solute transport and nitrogen transformations model (SABAE-HWS).

Chapter 4

Nitrogen Transport and Transformations

This Chapter starts with the basic concept of the mathematical description of solute transport. The theoretical equations of the nutrient transport and transformations of the SABAE-HWS model are presented in detail. The mineralization of organic nitrogen to ammonium, nitrification to nitrate, and then nitrogen uptake are important processes which control nitrogen balance and nitrogen losses in this study. Numerical and analytical solutions of advection-dispersion equation and the comparison between their results are also discussed. Finally, a quantitative description of the integrated water flow and solute transport model to simulate soil moisture, soil temperature, soil ammonium, and soil nitrate nitrogen is introduced.

4.1 Introduction

There are many solute transport models which differ greatly in degrees of complexity and utility, ranging from simple state models which do not consider chemical reactions, to complex dynamic models which consider all major soil solution reactions. The usefulness of solute transport models in making predictions of field conditions is limited by inadequacy of water flow models in describing the spatial and temporal distribution of water flow and heat transport. The partial differential equation for water flow has been solved by many authors using different techniques with, or without, considering the sink-source term (Lafolie, 1991; Mirbagheri, 2004; Heinen, 2006; Lee et al., 2006; Darban et al., 2008).

Generally, the basic equation of solute transport is expressed as:

$$\frac{\partial \theta C}{\partial t} + \frac{\partial \rho S}{\partial t} = \frac{\partial}{\partial z}\left(\theta D \frac{\partial C}{\partial z} - qC\right) + R \qquad 4\text{-}1$$

where C (mg/kg) and S (mg/kg) are solute and adsorbed concentration, respectively. θ (m^3/m^3) is the soil water content, ρ (g/cm^3) is the dry bulk density, D (m^2/day) is the dispersion coefficient, q (m/day) is the volumetric fluid flux, and R is a sink-source term that accounts for first order reactions. In this study, nitrogen transformations such as mineralization, nitrification, and denitrification are simulated by first order rate processes.

4.2 Nitrogen Transport Equations

Transport of ammonium and nitrate in saturated and unsaturated soil is described by the advection-dispersion equation. Since the adsorption of ammonium on the bulk soil is critical to take into account, the transport equation of ammonium can be expressed as:

$$\frac{\partial \theta C_4}{\partial t} + \frac{\partial \rho S}{\partial t} = \frac{\partial}{\partial z}\left(\theta D \frac{\partial C_4}{\partial z}\right) - \frac{\partial}{\partial z}(qC_4) + R_4(C_1, C_3, C_4) \quad 4\text{-}2$$

where C_4 (mg/kg) is the ammonium solute concentration, C_1 (mg/kg) and C_3 (mg/kg) are the nitrogen content and nitrate concentration, respectively. S (mg/kg) is the adsorbed concentration on soil particles, ρ (g/cm^3) is soil bulk density, and q (m/day) is Darcy flux in the z direction. In the above equation, D (m^2/day) is the component of the dispersion coefficient tensor which combines the diffusion of nitrogen in the soil and the hydrodynamic dispersion resulting from the variation of darcy velocity:

$$D = D_0 + \xi\,|v| \quad 4\text{-}3$$

where D_0 (m^2/day) is the coefficient of effective molecular diffusion, ξ (m) is dispersivity, and v (m/day) is the pore water velocity which is $v=q/\theta$. *R4* (kg m^{-2} day^{-1}) is the sink and source term of ammonium transport equation:

$$R_4(C_1, C_3, C_4) = R_{m4}(C_4) + R_n(C_4) + R_{p4}(C_4) \quad 4\text{-}4$$

where R_{m4} (kg m^{-2} day^{-1}) is the net mineralization of ammonium, R_n (kg m^{-2} day^{-1}) is the nitrification rate, and R_{p4} (kg m^{-2} day^{-1}) is root uptake rate of ammonium

The ion exchange process governing NH_4^+ adsorption-desorption is assumed to be the linear Freundlich form (Saâdi and Maslouhi, 2003, Yang et al., 2008):

$$S = k_d C_4 \quad 4\text{-}5$$

where k_d (m^3/kg) is distribution coefficient representing the ratio between NH_4^+ adsorbed and NH_4^+ in the soil solution.

Substituting Eq.4-5 into Eq.4-2 and considering the conservation equation of water leads to:

$$\frac{\partial}{\partial z}\left(\theta D \frac{\partial C_4}{\partial z}\right) - q\frac{\partial C_4}{\partial z} - (\theta + k_d \rho)\frac{\partial C_4}{\partial t} = -SC_4 - R_4(C_1, C_3, C_4) \quad 4\text{-}6$$

The advection-dispersion equation (Eq. 4-2) is converted to nitrate transport equation by disregarding the adsorption of nitrate on the bulk soil:

$$\frac{\partial \theta C_3}{\partial t} = \frac{\partial}{\partial z}\left(\theta D \frac{\partial C_3}{\partial z}\right) - \frac{\partial}{\partial z}(qC_3) + R_3(C_1, C_3, C_4) \quad 4\text{-}7$$

where R_3 is the source and the sink term of nitrate transport:

$$R_3(C_1, C_3, C_4) = R_{m3}(C_1, C_3, C_4) + R_n(C_4) + R_{dn}(C_3) + R_{p3}(C_3) \quad 4\text{-}8$$

To solve Eq.4-6 and Eq.4-7, two boundary conditions at the soil surface and the bottom of soil column are required. A solute flux type boundary condition (third type) is used at the upper boundary:

$$\theta D \frac{\partial C_i}{\partial z} - v\theta C_i = Q(t) \qquad at \quad z = 0 \quad 4\text{-}9$$

where the chemical species *i* are nitrate and ammonium concentrations and *Q(t)* is the flux of solute applied at surface. This boundary enables a more accurate interpolation of velocities at the top of the soil profile. At the lower boundary condition, either no flux condition or free drainage may be used. :

$$\frac{\partial C_i}{\partial z} = 0 \qquad at \quad z = L \quad 4\text{-}10$$

The initial condition at *t=0* is also defined as:

$$C_i(z, 0) = C_0^i(z) \quad 4\text{-}11$$

4.3 Soil nitrogen transformations

Although nitrogen is as essential nutrient for crop production, it is also one of the major pollutants in ground water and surface water. Nitrogen is first added to the soil by animal manure, chemical fertilizers, and atmosphere deposition. Nitrogen in soils generally is classified as organic or inorganic nitrogen. Ammonia, nitrate, and nitrite are some exam-

ples of inorganic nitrogen in the soil. It has been reported that 95% of N in surface soils are in organic forms. However, inorganic form of N is important to investigate because of its direct impact on plant growth and the environment (Alvarez-Benedi and Munoz-Carpena, 2005). Ammonium and nitrate which are the main concerns of this study are major inorganic forms of N in the soil. They are not only readily taken up by plants but leach into groundwater or even surface water. As mentioned in the literature review, mineralization of plant organic matter and atmospheric deposition are the main sources of nitrogen in forest ecosystems. Mineralization yields ammonium (NH_4^+) which can be volatilized to ammonia, or nitrified to nitrate (NO_3^-). Volatilization of NH_4^+ is rare in winter, based on the lab and field experiments reviewed in Chapter 2. When nitrogen demand is smaller than the available NH_4^+, nitrification occurs. Nitrate leaching is first found at the lower soil profile and then moves to surface and ground water. Nitrate is a mobile anion easily transported with water (Piatek et al., 2005). The main nitrogen transformations in this study can be summarized as shown in Figure 4-1.

Generally, nitrification is a dual-step process conducted by two groups of autotrophic bacteria. First, nitrosomonas bacteria convert NH_4^+ to nitrite NO_2^- and then nitrobacter organisms convert the NO_2^- to NO_3^-. There is no accumulation of NO_2^- in the soil column as the second reaction occurs very quickly. Therefore when nitrification is presented mathematically, it is accounted as a single step process (Scott, 2006).

According to Piatek et al. (2005), the largest amount of NO_3^- leaching occurred when there is a large runoff area, especially during early spring snowmelt. At this time, vegetation and microbial uptake of inorganic nitrogen is considerably low. Possible sources of

NO_3^- in groundwater are atmospheric NO_3^- from snow, mineralization in soils under the snowpack, and nitrification (McHale et al., 2002; Schleppi et al., 2003).

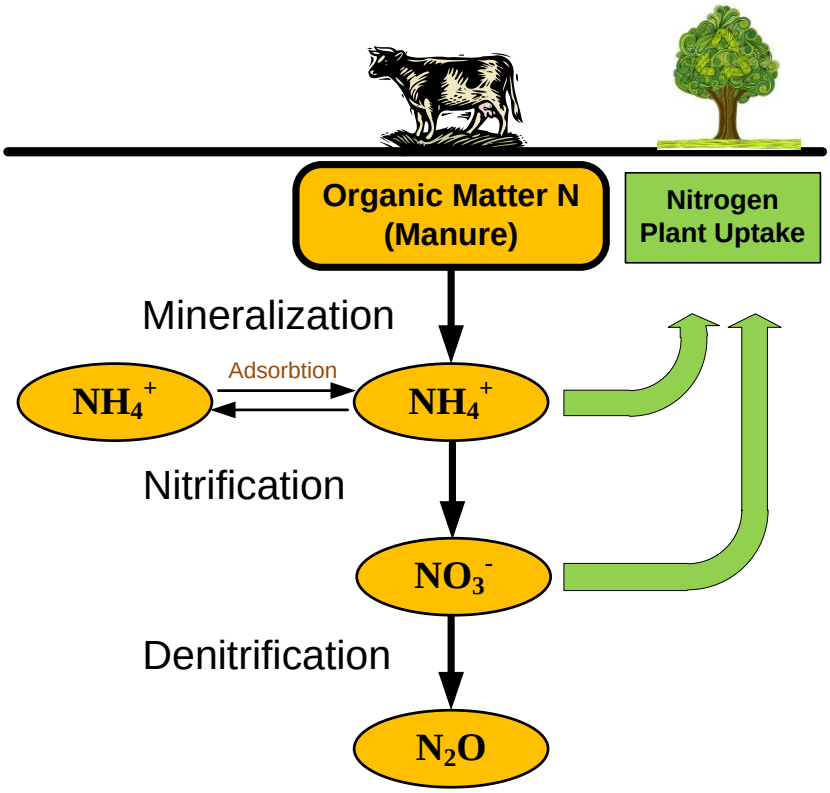

Figure 4-1: A simplified scheme for the nitrogen cycle

According to the literature review, the aforementioned processes play an important role in terms of nitrogen transformations during the winter time. The changing rates of these processes are still an ongoing research topic during the freeze and thaw period. Mineralization, nitrification and, denitrification are modeled by using first order kinetics. Studies on nitrogen transformation associated with first order kinetics can be found in Chowdary et al. (2004), Saâdi and Maslouhi, (2003), and Heinen, (2006). The general equation for a first order rate process is presented as:

$$\frac{dC}{dt} = -kC \qquad 4\text{-}12$$

where *k* (1/day) is the transformation rate coefficient.

Models have become sophisticated in terms of the type and complexity of solute transport processes. These processes include simple chemical reactions (first order decay or linear sorption) and nonlinear sorption, exchange process, and physical and chemical non-equilibrium transport (Šimunek et al., 1998; Šimunek and Van Genuchten, 2008). To simulate carbon and nitrogen transformations some options are added to solute transport models, in order to simulate the amount of distributed organic matter.

Depending on environmental conditions, various N transformation processes will take place below the ground with different intensities in winter. It is assumed that all reactions (mineralization, nitrification and denitrification) obey the first order kinetics and this assumption is valid under most field conditions with unlimited substrate concentration. The mathematical model describing nitrogen transformations are:

$$\frac{d[NH_4^+]}{dt} = -k_{nit}[NH_4^+] + k_{min}[N_{org}] \quad 4\text{-}13$$

$$\frac{d[NO_3^-]}{dt} = -k_{det}[NO_3^-] + k_{nit}[NH_4^+] \quad 4\text{-}14$$

$$\frac{d[N_{org}]}{dt} = -k_{min}[N_{org}] \quad 4\text{-}15$$

Eq. 4-13 to Eq. 4-15 are considered as the sink and source for Eq. 4-6 and Eq. 4-7.

4.3.1 Abiotic Functions

The mineralization, nitrification and denitrification rates are influenced by abiotic factors such as soil moisture, soil temperature, and soil PH. The combined effects of these factors produce an optimal value which is multiplied by abiotic functions to consider the sensitivity of such transformations to environmental factors such as soil temperature and soil moisture. The response functions are usually classified as temperature and soil water

response. Although the abiotic functions are generally the same for all nitrogen dynamic processes but they differ between the various models.

Temperature response function usually affects the processes such as decomposition and nitrification rate. In this study, the soil temperature function is calculated based on a Q_{10} expression which is a commonly used function for some nitrogen dynamic models such as the COUP model:

$$f(T) = \begin{cases} Q_{10}^{\frac{T-T_b}{10}} & (T \geq T_{th}) \\ \frac{T}{T_{th}} Q_{10}^{\frac{T-T_b}{10}} & (T < T_{th}) \end{cases} \qquad 4\text{-}16$$

where Q_{10} is the response to a 10 ºC soil temperature change, T is the soil temperature (ºC), T_b is the base temperature at which $f(T)$=1 and T_{th} is a threshold temperature (ºC).

The effect of soil water content differs between the processes. The common function for all processes except denitrification can be expressed as:

$$f(\theta) = \begin{cases} \frac{\frac{1}{\theta} - \frac{1}{\theta_{RSW}}}{\frac{1}{\theta_{WP}} - \frac{1}{\theta_{RSW}}} & \theta < \theta_{WP} \\ 1 & \theta_{WP} \leq \theta \leq \theta_{fc} \\ e_s + (1 - e_s) \frac{\frac{1}{\theta_S} - \frac{1}{\theta}}{\frac{1}{\theta_S} - \frac{1}{\theta_{fc}}} & \theta > \theta_{fc} \end{cases} \qquad 4\text{-}17$$

where θ is the soil moisture content, θ_{RSW} is the residual soil water content, θ_{WP} is the soil water content at wilting point, θ_{fc} is the soil moisture at field capacity, θ_s is the saturated water content, and e_s is the relative effect at saturation.

The soil moisture response function has different dependence on soil water content for denitrification (Lafolie et al., 1997):

$$f(\theta) = \begin{cases} \frac{\theta - \theta_{th}}{\theta_s - \theta_{th}} & \theta \leq \theta_{th} \\ 0 & \theta > \theta_{th} \end{cases} \qquad 4\text{-}18$$

where θ_{th} is the threshold water content for denitrification.

In this study, nitrogen cycle is modeled in a very simple way. Only one pool is considered for organic matter (carbon and microbial dynamics are not modeled). Mineralization of organic matter, nitrification of ammonium and denitrification are modeled as first order processes which is the common process in most of the models. In fact, a first order process is a chemical process where the rate of solute concentration out of the pool is directly proportional to the solute concentrations.

4.3.2 Mineralization

Mineralization is nitrogen transformation that is controlled by carbon processes in organic matter. Organic matter is usually divided into two pools, mainly fast cycling pools and slow cycling pools. Since it is assumed that the only source of organic N is manure, a single pool is considered to represent the mineralization of the available manure organic nitrogen (Scott, 2006). The first order kinetic reaction for mineralization is defined as (Saâdi and Maslouhi, 2003):

$$\frac{dN_{org}}{dt} = -k_{min}\rho(N_{org} - N_{\infty}) \qquad 4\text{-}19$$

where N_{org} is the amount of mineralizable organic N (kg/m^2), k_{min} is the mineralization rate coefficient (1/day), and ρ is the soil density(kg/m^3).

$$N_{org}(t) = N_{\infty} + \left(N_{org}(0) - N_{\infty}\right)exp^{(-k_{min}t)} \qquad 4\text{-}20$$

where N_{∞} in the organic nitrogen applied at the soil surface (kg/ m^2), supposed to be instantaneously present in the top soil.

4.3.3 Nitrification

Nitrification plays a significant role in the attenuation of NH_4^+ in the unsaturated zone. This process is sensitive to environmental conditions and the presence of inhibitors. It is also a viable process taking place in a range of soil water contents. It has been observed that the rate of nitrification decreases at high soil moistures in unsaturated zone (Buss et al., 2004). Nitrification is a two-stage process in which ammonium can be oxidized by some bacteria to generate energy.

$$NH_4^+ + 1.5O_2 \rightarrow NO_2^- + H_2O + 2H^+ \quad 4\text{-}21$$

$$NO_2^- + 0.5O_2 \rightarrow NO_3^- \quad 4\text{-}22$$

The Nitrification of ammonium to nitrate is considered to be a first order rate process in an assumed equilibrium ammonium. A first order kinetics reaction is used to describe nitrification:

$$\frac{dC_3}{dt} = k_{nit}C_4 \quad 4\text{-}23$$

$$\frac{dC_4}{dt} = -k_{nit}C_4 \quad 4\text{-}24$$

where k_{nit} is the first order rate conditional constant(day^{-1}).

4.3.4 Denitrification

Denitrification is an anaerobic biological process. In this process, nitrate nitrogen is converted into the nitrogen gas. All of the simple models are usually based on potential denitrification rate. Since it is accepted that environmental soil conditions affect the denitrification process, abiotic functions are used to calculate the rate of denitrification. According to Heinen (2006), since denitrification is determined by the non-availability of oxy-

gen, most investigators agree that oxygen dynamics in the soil is not easy to measure. Thus, water content is used as a complementary variable instead of oxygen diffusion. The higher the water content results in the less oxygen. It is also important to take into account that soil temperature, soil nitrate, and soil acidity affects the rate of denitrification. Other factors that influence denitrification are soil temperature and soil acidity (pH).

The general mathematical function to describe the actual denitrification is presented as (Johnsson et al., 1987; Heinen, 2006; Oehler et al., 2005):

$$R_{dn} = \propto . f(T). f(\theta). f(N). f(pH) \qquad 4\text{-}25$$

where α is a parameter depending on the exact formulation and *f(pH)* is a dimensionless reduction function for soil *pH*. *f(N)* is also a nitrate dimensionless function which is described as:

$$f(N) = \frac{N_{NO3^-}}{N_{NO3^-} + H} \qquad 4\text{-}26$$

where N_{NO3}^- is the actual nitrate soil content and *H* is half saturation constant.

The parameter α refers to the type of denitrification. There are two types of parameter α to simulate denitrification:

1) α represents the potential denitrification rate (D_p)
2) α represents a first order denitrification coefficient (k_d)

Sixty-five percent of the available models used the first order decay to calculate denitrification. It has been reported that zero order process is used at high nitrate concentrations which nitrate is not limiting while first order process is applied at low nitrate concentrations. In this case, nitrate becomes limiting and α represents potential denitrification rate (D_p). This parameter can be measured in situ or on soil samples with high nitrate

contents. Thirty-five percent of all models used this method to describe denitrification (Heinen 2006).

Some models consider the second approach (first order decay process) to simulate denitrification ($\alpha = k_d$), where k_d is a first order denitrification coefficient and measures as a parameter from experimental data. As stated before, actual denitrification will be influenced by environmental conditions such as the abiotic functions for soil moisture and soil temperature. In this approach, function *f(N)* is not a dimensionless reduction factor and is dependent upon the nitrate content of the soil: *f(N)=N*

Since the nitrate concentration is not high during the winter time, the second approach is considered in the SABAE-HWS model. In addition, since the soil moisture is not high in this study, the amount of predicted denitrification is expected to be low. However, it is also possible to switch from the first order process to zero order process in the model to properly simulate the denitrification rate in deep soil layers.

4.3.5 Plant Nitrogen Uptake

Since the actual plant N uptake is dependent on plant growth, root distribution, water movement, nitrogen transport, and C and N dynamics, it is considered as one of the most important processes in solute transport models. Any errors in simulating the above processes results in missing the accuracy of the model in predicting the plant N uptake. The basic parameters to simulate nitrogen uptake are plant available total nitrogen (NH_4^+ and NO_3^-) and N concentration at the root surface. The nitrogen uptake function is defined as (Saâdi and Maslouhi, A. 2003):

$$Q_{UP}^N(z,t) = \frac{x_i}{\Delta z_i} J_O^N(t) \qquad 4\text{-}27$$

where $J^N_O(t)$ is the actual nitrogen uptake rate by the dry matter of the plant ($kgm^{-2}day^{-1}$) and x_i is the nitrogen fraction of available nitrogen taken up by roots in layer Δz_i:

$$J_O^N(t) = \frac{dN}{dt} = \begin{cases} A \,.\, t.\,(G - t) & for\ t < G \\ 0 \end{cases} \quad 4\text{-}28$$

where *G* is the time at which plant stops to uptake nitrogen (harvest date) and *t* is the emergence date. *A* is parameter assuring that nitrogen uptake is maximal at the harvesting date (kg $m^{-2}day^{-1}$): $A=6N_{max}/G^3$ if $t=G$ and $N=N_{max}$, where N_{max} is the cumulative nitrogen mass in the crop at harvest (kg/m^2) and N is the actual cumulative nitrogen mass at time t in the dry matter of the crop (kg/m^2).

Nitrogen fraction of available nitrogen is defined as (Scott, 2006):

$$x_i = f(\theta)\frac{R_{r_i} C_{i_j} \Delta z_i}{\sum_{i=1}^{n_{EZD}} R_{r_i}(C_{i_{NO_3^-}} + C_{i_{NH_4^+}})\Delta z_i} \quad 4\text{-}29$$

where j denotes to the NH_4^+ and NO_3^- substance, $f(\theta)$ is the soil moisture response function, n_{EZD} is the number of layers in the evaporative zone and R_{ri} is the root density factor for the i^{th} layer (cm root/cm^3 soil):

$$R_{r_i} = 0.173[R_d - (d_i - 0.5\Delta z_i)] \quad 4\text{-}30$$

where d_i is the depth to the bottom of sections *i* and R_d is the maximum rooting depth:

$$R_d = \frac{EZD}{1 + e^{(6-12r)}} \quad 4\text{-}31$$

where *EZD* is the evaporative zone depth and r is the full root growth time: $r=t/80$. 80 days refers to a fully grown root system for most of the crops after planting.

It should be noted that there are several approaches to simulate nitrogen root uptake. Since all of these approaches increase the input data, it is recommended to use those functions with less input data.

4.4 Nitrogen Balance

Mineralization, nitrification and nitrogen uptake are assumed to be the most important nitrogen transformation processes in this study. Note that, although denitrification has been accounted for the model, it is ignored ($k_{den}=0$) as the amount of denitrification is approximately zero in sandy soils. Figure 4-2 shows nitrogen balance for the simulation period of this study considering manure as the source of ammonium and nitrate in the soil.

Here are the explicit terms for the sinks and sources of NH_4^+-N and NO_3^- -N transport equations due to mineralization and nitrification processes in the soil:

For the NH_4^+-N transport equation (Eq. 4-6):

$$R_4 = \frac{\mathrm{d}N_{org}}{\mathrm{dt}} - \frac{\mathrm{d}C_4}{\mathrm{dt}} + Q_{uptake}^{NH4} \qquad 4\text{-}32$$

Substituting Eq. 4-19, Eq. 4-24, and Eq.4-27 into Eq. 4-32 results in:

$$R_4 = \frac{k_{min}N_{org}}{\Delta \mathrm{z}} - k_{nit}\theta C_4 + Q_{uptake}^{NH4} \qquad 4\text{-}33$$

And for NO_3^- -N transport equation (Eq. 4-7):

$$R_3 = \frac{\mathrm{d}C_3}{\mathrm{dt}} + Q_{uptake}^{NO3} \qquad 4\text{-}34$$

Substituting Eq. 4-23 and Eq. 4-32 into Eq. 4-34 results in:

$$R_3 = k_{nit}\theta C_4 + Q_{uptake}^{NO3} \qquad 4\text{-}35$$

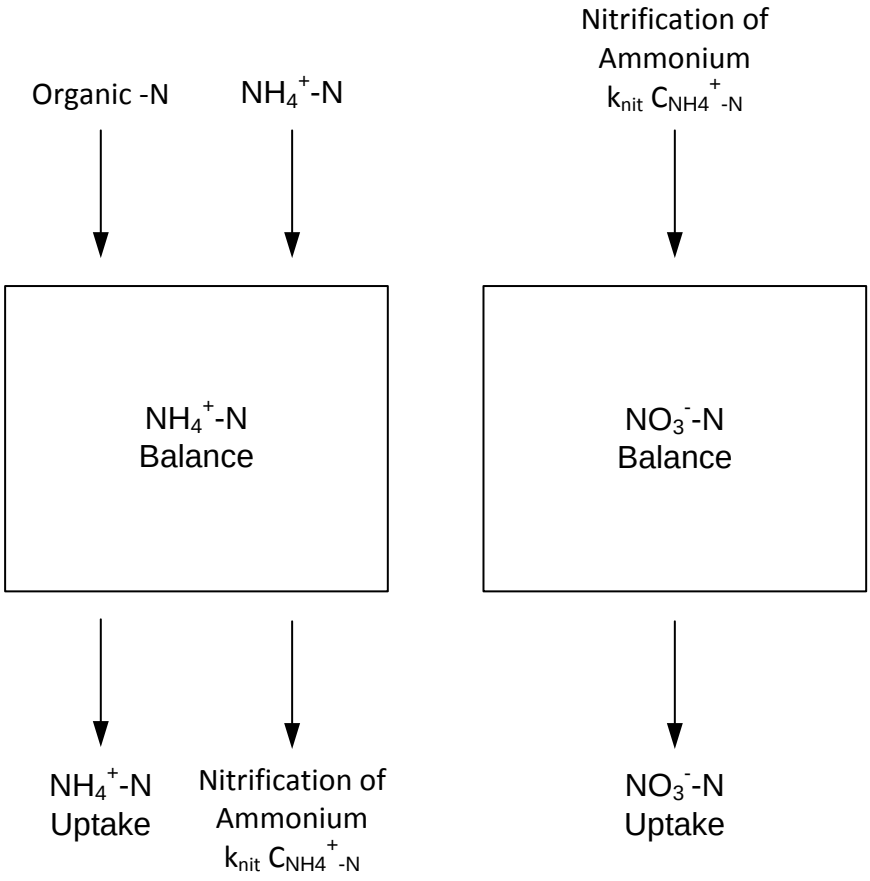

Figure 4-2: Nitrogen balance of soil profile regarding the manure application

4.5 Numerical Solution

An upwind finite volume approximation is used to solve the nitrogen transport equations subject to their initial and boundary conditions. The finite volume method insures continuous fluxes across the boundary layers. In addition, similar to SABAE-HW, the time increment remains constant through the simulation which is 30 minutes. It is noted that although the parental code (CLASS) had been developed for the hourly time increments, 30 minutes time interval was selected for SABAE-HW to increase the accuracy of the model

in simulating soil moisture and soil temperature. Using Figure 4-3 for the nodes and segments, the general discrete form of solute transport Eq. 4-1 is given by:

$$\theta_i \frac{C_i - \bar{C}_i}{\Delta t} \Delta z_i + D_{i-1,i} \frac{C_i - C_{i-1}}{\Delta z_{i-1/2}} - D_{i,i+1} \frac{C_{i+1} - C_i}{\Delta z_{i+1/2}} + q_{i-1,i,i+1} \Delta z_i C_i = R_i \quad 4\text{-}36$$

where $\Delta z_{i+1/2} = (\Delta z_i + \Delta z_{i+1})/2$.

The following characteristic equation is used in the expression of the water flux:

$$q_{i-1,i,i+1} = \begin{cases} q_{i-1,i} & if\ (q_{i-1,i} + q_{i,i+1})/2 \geq 0 \\ q_{i,i+1} & if\ (q_{i-1,i} + q_{i,i+1})/2 < 0 \end{cases} \quad 4\text{-}37$$

In fact, Eq. 4-37 shows the direction of flux movement. The negative values of water flux determine the upward direction of flux caused by evaporation or root suction and the positive values determine the downward direction of flux. At each time step, darcy fluxes are calculated at the interlayers while soil moisture and soil temperature are computed at middle of each layer. Thus, the upstream darcy fluxes are used in the nitrogen transport finite volume discretization. Once soil temperatures, soil moistures, and water fluxes are provided by SABAE-HW, the N transport portion of the code calculates the distribution of soluble nitrogen regarding the nitrogen transformations of nitrogen. Figure 4-3 shows the schematic diagram of the structure of the integrated model.

The discretization of ammonium equation is detailed below. It is noted that the discretization of nitrate equation also follows the same pattern as ammonium equation. The first term in Eq. 4-2 is a diffusion and dispersion term:

$$\int_{v_i} \frac{\partial}{\partial z}\left(\theta D^4 \frac{\partial C_4}{\partial z}\right) dz = \int_{v_i} \left(\theta D^4 \frac{\partial C_4}{\partial z}\right) ds = \left[\theta D^4 \frac{\partial C_4}{\partial z}\right]_{i-1,i}^{i,i+1} \quad 4\text{-}38$$

$$= \left[D_{i,i+1} \frac{C_{i+1}^4 - C_i^4}{(\Delta z_i + \Delta z_{i+1})/2}\right] - \left[D_{i-1,i} \frac{C_i^4 - C_{i-1}^4}{(\Delta z_{i-1} + \Delta z_i)/2}\right] \quad 4\text{-}39$$

where

$$D_{i,i+1} = \lambda_{i,i+1} |q_{i,i+1}| + \theta_{i,i+1} |D_{0\ i,i+1}| \quad 4\text{-}40$$

$$D_{i-1,i} = \lambda_{i-1,i}\left|q_{i-1,i}\right| + \theta_{i-1,i}\left|D_{0\ i-1,i}\right| \quad 4\text{-}41$$

The convection term in Eq. 4-2 is differenced as:

$$\int_{v_i} \frac{\partial}{\partial z}(qC^4)dz = \int_{v_i} qC^4\, ds = [qC^4]_{i-1.i}^{i,i+1} = \left[q_{i,i+1}C_{i,i+1}^4\right] - \left[q_{i-1,i}C_{i-1,i}^4\right] \quad 4\text{-}42$$

where

$$q_{i,i+1}C_{i,i+1}^4 = \begin{Bmatrix} q_{i,i+1}\, C_i^4 & if & q_{i,i+1} > 0 \\ q_{i,i+1}\, C_{i+1}^4 & if & q_{i,i+1} < 0 \end{Bmatrix} \quad 4\text{-}43$$

$$q_{i-1,i}C_{i-1,i}^4 = \begin{Bmatrix} q_{i-1,i}\, C_{i-1}^4 & if & q_{i,i+1} > 0 \\ q_{i-1,i}\, C_i^4 & if & q_{i,i+1} < 0 \end{Bmatrix} \quad 4\text{-}44$$

Multiplying and collecting the unknown *C* terms on the left side and the known *C* terms on the right hand side, the general form of equation is:

$$A_{i,i-1}(C_{i-1}^4) + A_{i,i}(C_i^4) + A_{i,i+1}(C_{i+1}^4) = F_i \quad 4\text{-}45$$

where

$$A_{i,i-1} = -\max\left(0, q_{i-1,i}\right) - \frac{D_{i-1,i}}{(\Delta z_{i-1}+\Delta z_i)/2} \quad 4\text{-}46$$

$$A_{i,i} = \max\left(0, q_{i,i+1}\right) - min\left(0, q_{i-1,i}\right) + \frac{D_{i,i+1}}{(\Delta z_i+\Delta z_{i+1})/2} + \frac{D_{i-1,i}}{(\Delta z_{i-1}+\Delta z_i)/2} - k_{nit} \quad 4\text{-}47$$

$$A_{i,i+1} = \min\left(0, q_{i,i+1}\right) - \frac{D_{i,i+1}}{(\Delta z_i+\Delta z_{i+1})/2} \quad 4\text{-}48$$

$$F_i = (R_{m4})_i + R_{p4}\left(\overline{C_i^3}, (C_i^4)^p\right) + (\theta_i + \rho_i k_d)\frac{\overline{C^4}}{\Delta t} \quad 4\text{-}49$$

The finite volume discretization is also written similarly for the nitrate equation for each node from 2 to *i-1* node in the profile. This set of equations is solved for defined boundary conditions using the Thomas Tridiagonal matrix algorithm.

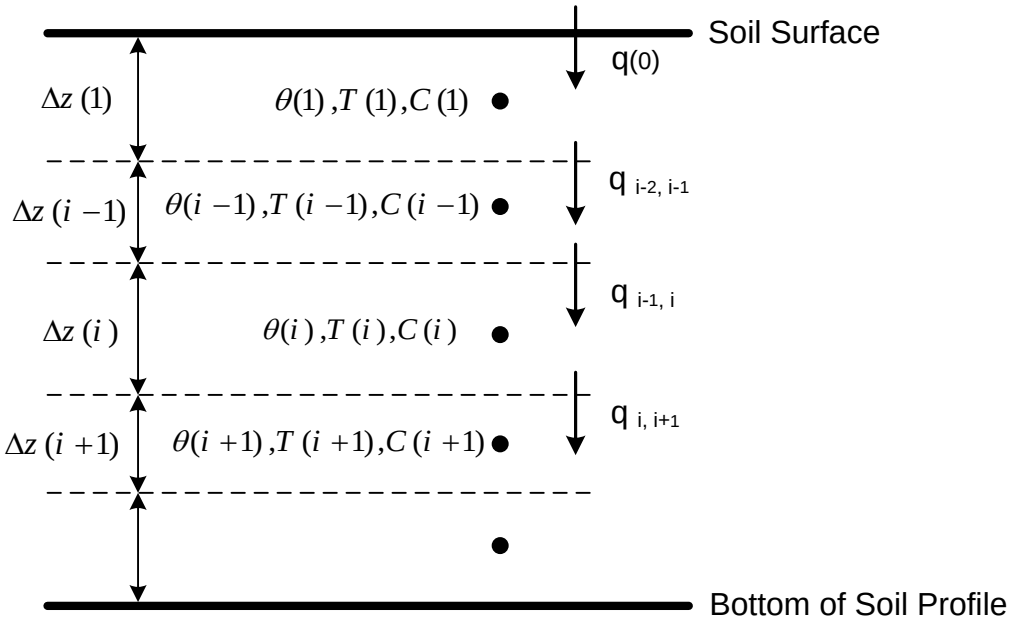

Figure 4-3: Schematic diagram of scheme solutions in soil profile

4.6 Coupling Water Balance and Nitrogen Transport

The water balance and the solute transport equations are numerically solved, using the same spatial and temporal discretization. Both systems operate on a 30 minute time step and its spatial discretization is chosen according to the soil information available and the number of layers required for simulation. First, water flow and heat transfer systems (SABAE-H and SABAE-W) are solved to simulate soil moisture (θ), water flux (q), and soil temperature (T) at each layer. The variables θ and T are then used to calculate the abiotic functions. Soil moisture and interval fluxes are set into the systems of equation describing mass transport of NH_4^+-N and NO_3^--N (SABAE-S). The amount of minerali-

zation and nitrification is also calculated for the NH_4^+-N system. First the system of NH_4^+-N transport is solved for the ammonium concentrations, and then the system of NO_3^--N transport for the nitrate concentration. Regarding the discretization, the coupling of nitrogen transport to the SABAE-HW model is achieved at the time step level (Figure 4-4). For the spatial discretization, the coupling is also ensured through the direct incorporation of calculated soil temperature, moisture and water fluxes into the solute transport discretized equations.

The computer code is written in visual FORTRAN and has been compiled under Intel FORTRAN. The input data files are classified as *sabaeatmo.dat*, *sabaesite.dat*, *sabaesoil.dat*, and *sabaenitr.dat* (See Appendix A). The atmospheric data are stored in the *sabaeatmo.dat* file. Domain and the number of layers in the soil profile are designed in *sabaesoil.dat* file. This file also allows users to select either water boundary condition or unit gradient boundary condition at the bottom of soil profile. The soil hydraulic characteristics database as well as initial layers' soil temperature and soil moisture are detected in *sabaesoil.dat* file. There are four vegetation types investigated in the model: needleaf, broadleaf, crop, and grass. All the input data related to each of these vegetation types are supplied in the *sabaesite.dat* file. *Sabaenitr.dot* file includes the input data of crop growth model and dispersive parameters of the site. The initial soil ammonium and soil nitrate of each layer is also determined in this file. The daily output variables are categorized as: energy and water balance terms, soil water and soil moisture in layers, meteorological terms, and soil ammonium and soil nitrate in layers.

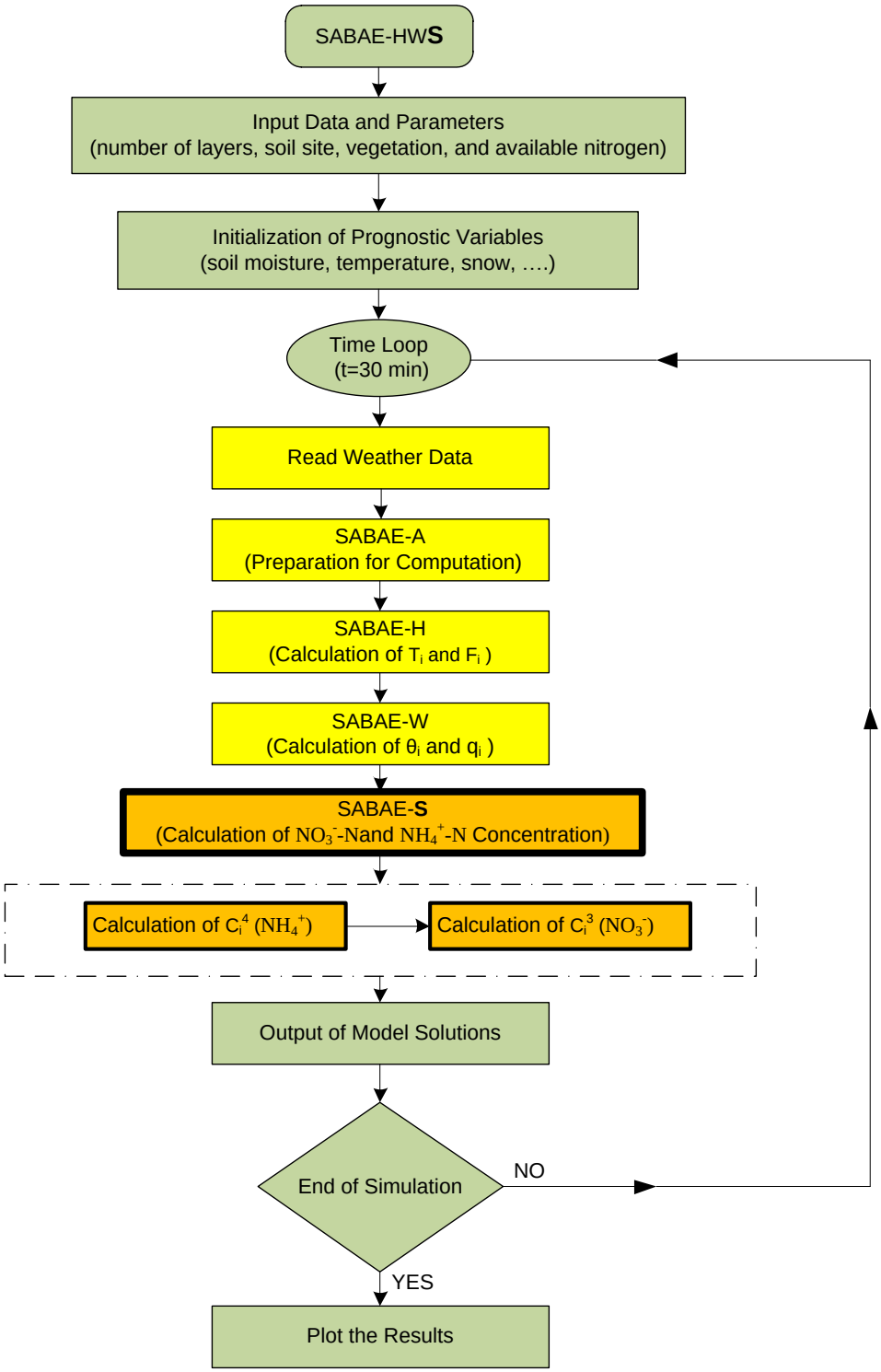

Figure 4-4: Descriptive Algorithm for SABAE-HWS model

4.7 Analytical Solution in Uniform Flow

Analytical solutions have an important role for validating numerical approaches. They also sometimes offer fundamental insight about governing physical processes. Many analytical solutions for transient infiltration have been developed for transport in groundwater under different boundary conditions. A large number of these solutions solve one dimensional unsteady uniform flow through a homogenous domain (Shan and Javandel, 1997; Jaiswal et al., 2009; Yadav et al., 2010). One of the well-known solutions given by Kumar et al. (2009) considers a longitudinal finite domain. The solute dispersion parameter is considered temporally dependent and flow velocity is assumed uniform. The linear advection-dispersion equation in one dimension maybe written as:

$$\frac{\partial C}{\partial t} = \frac{\partial}{\partial t}\left(D(z,t)\frac{\partial C}{\partial t} - u(z,t)C\right) \qquad 4\text{-}50$$

where C represents the solute concentration, D is the solute dispersion and u is the flow velocity.

Two different types of boundary conditions were considered: constant concentration and solute flux boundary condition. In the first approach, domain is assumed initially solute free. Dirichlet boundary condition and a second type boundary condition are considered at the top and bottom of the domain, respectively. The initial and boundary conditions for Eq. 4-50 are as follows:

$$C(z,t) = 0 \qquad 0 \le z \le L, t = 0 \qquad 4\text{-}51$$

$$C(z,t) = C_0 \qquad z = 0 \qquad 4\text{-}52$$

$$\frac{\partial C(z,t)}{\partial z} = 0 \qquad z = L \qquad 4\text{-}53$$

In the second approach, the source of input condition may not be uniform. It may increase with time due to human and other responsible activities. This type of condition is described by a mixed type or third type condition:

$$-D(z,t)\frac{\partial C}{\partial z} + u(z,t)C = u_0 C_0 \qquad z = 0 \qquad 4\text{-}54$$

The initial and lower boundary condition still remained as the same as uniform continuous input.

To demonstrate that the numerical approach yields the correct results, the finite volume solute transport code was compared to the analytical solution of Kumar et al. (2009). It is considered that dispersion is proportional to the linearly interpolated velocity. The concentration values are evaluated for uniform input and varying input in a finite domain $0 \leq z \leq 1$ (km) at times t (years) = 0.1, 0.4, and 1. Temporal dependent solute dispersion along uniform flow of continuous input and increasing natures is as follows:

$$D = D_0 \exp(-mt) \qquad 4\text{-}55$$

where m=0.1 (1/day)

The other input values are C_0=1.0, u_0=0.11 (km/year) and D_0=0.21 (km^2/year). u_0 and D_0 are defined as uniform flow velocity and initial dispersion coefficient, respectively.

Figure 4-5 and Figure 4-6 represent the comparison of the results obtained using the code and analytical solution with different boundary conditions. In Figure 4-5, the uniform input concentration value is 1.0 at all times while the concentration value increases at z=0 with time in Figure 4-6. A complete agreement between the numerical and analytical solutions were found in case of uniform input at t= 0.1, 0.4, and 1 year as shown in Figure 4-5. Although the increasing inputs did not make a substantial difference between numerical and analytical solutions at t= 0.1 year, there were small difference between the

concentration values near the origin at t= 0.4 and 1 year. The analytically simulated values are slightly higher than the numerical values near the source of pollutant but the trend reverses beyond the origin.

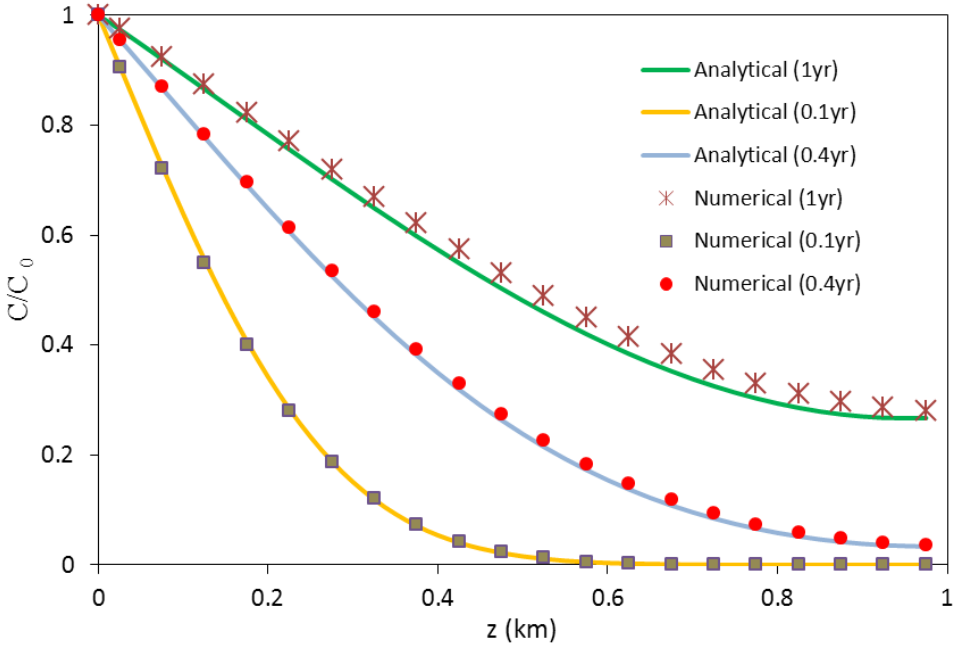

Figure 4-5: Comparison of analytical and simulated temporal dependent solute concentration along uniform flow of uniform input

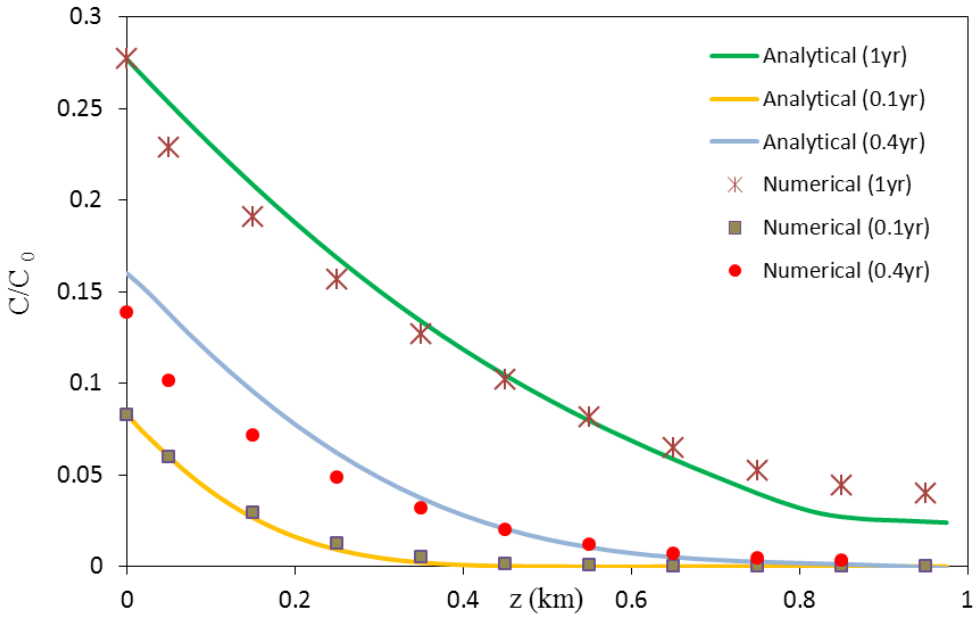

Figure 4-6: Comparison of analytical and simulated temporal dependent solute concentration along uniform flow of increasing nature

4.8 Summary

SABAE-HWS, a coupled water flow, heat transfer, and solute transport model, is useful to simulate soil moisture, soil temperature, soil ammonium, and soil nitrate nitrogen within the soil profile. It is a model which integrates water movement, heat transfer, solute transport, and nitrogen transformation to predict the movement of soil nitrogen with soil water. Water flow in the soil profile is simulated by a numerical solution of Richard's equation. Solute transport is also simulated by a numerical solution of the advection-dispersion equation. The results of SABAE-HWS will be validated using a 3 year data from Carberry site located in Manitoba. The physical and chemical properties of the soil site and experimental design of field study are explained in the next Chapter. The results of the integrated model were also compared with the results of the SHAW model. Comparison of simulated results by SABAE-HWS to the observed data and SHAW will be covered in Chapter 6.

Chapter 5

Study Site and Data Analysis

A detailed description of the Carberry site including the necessary input parameters for the SABAE-HWS model is presented in this Chapter. Atmospheric conditions, physical and chemical properties of the soil have a strong impact on nitrogen dynamics in the climate-groundwater-nutrient transport model. This chapter reviews the experimental design of the field study which mainly focuses on manure application. Finally, statistical performance measures used for comparing simulated variables and observed data are described. Correlation, root mean square error, coefficient of residual mass, and graphical comparisons are used to evaluate the performance of the model.

5.1 Site description and Experimental Design

The field study is located at 10 km northwest of the town of Carberry, Manitoba (latitude 49.90 °N and longitude 99.35 °W). Carberry is located within the Assiniboine Delta Aquifer (ADA) which is an unconfined aquifer and widely used as a source of water for irrigated potatoes. The soil type is mainly classified as a loamy sand soil. The upper 75 to 90 cm is loamy sand with the underlying material of sandy loam to loam. The depth to water

table was 5-6 m. This site has been cropped to buckwheat, barely and canola three years before starting the experiment (Enn, 2004). The soil characteristics of the site and also the chemical properties of the soil are given in Table 5-1.

Table 5-1: Physical and chemical properties of the Carberry site soil

Depth (cm)	Sand (%)	Silt (%)	Clay (%)	pH	EC dS/m	BD gr/cm^3	FC (%)	NO_3-N mg/kg	NH_4-N mg/kg
0-10	77.9	10.2	11.8	6.37	0.32	1.31	28	5.70	4.45
10-20	72.8	13.5	13.7	6.61	0.30	1.42	28	5.99	3.73
20-30	69.8	17.9	12.3	7.01	0.28	1.45	26	5.76	3.14
30-60	74.0	13.3	12.7	7.71	0.31	1.51	23	1.88	3.44
60-90	65.6	20.2	14.7	8.29	0.33	1.49	25	1.14	3.60
90-120	48.6	31.6	19.8	8.33	0.34	1.50	34	1.17	3.65

Intensive livestock production leads to the production of considerable amount of manure. Animal manures are primarily applied on the cropland in Manitoba. The combination of an unconfined aquifer (ADA) underlying coarse textured soil increases the potential for aquifer contamination. Moreover, Manitoba hog manure has increased over the past 40 years and now Manitoba is the third largest hog-producing province in Canada (Burton and Ryan, 2000). Since manure is rich in organic nitrogen and ammonium-nitrogen, the application of manure at the maximum allowable rate of application is the favour of the farmers. Note that manure also contains a small amount of nitrate as well. Ammonium-nitrogen is an inorganic form of nitrogen in manure. As ammonium N in

manure is immediately available for crop uptake, the quantity of NH_4^+-N in manure is important. Organic nitrogen of manure is calculated as the difference between total nitrogen and ammonium nitrogen. The organic nitrogen is mineralized to inorganic nitrogen to be utilized by the plant.

According to Manitoba Agriculture‘s website (http://www.gov.mb.ca/agriculture/), the rate of manure application highly depends on the soil moisture and land use and should not exceed the nitrogen requirement of the crop. Also, soil and weather conditions are of particular importance because they influence the availability of the manure nitrogen to plants. To evaluate the manure application, Carberry site has been chosen for this study. The field experiment was conducted in 2002 for three growing seasons with 6 treatments and four replicates for a total of 24 experimental units. Each plot is measured as a 10 by 10 m unit. Treatments include three different rates of hog manure: 2500, 5000, and 7500 gal/acre (23400, 46800, 70200 L/ha) applied at the soil surface in the spring. Nitrogen, phosphorus fertilizers, and also bromide are applied for the rest of the plots (Figure 5-1).

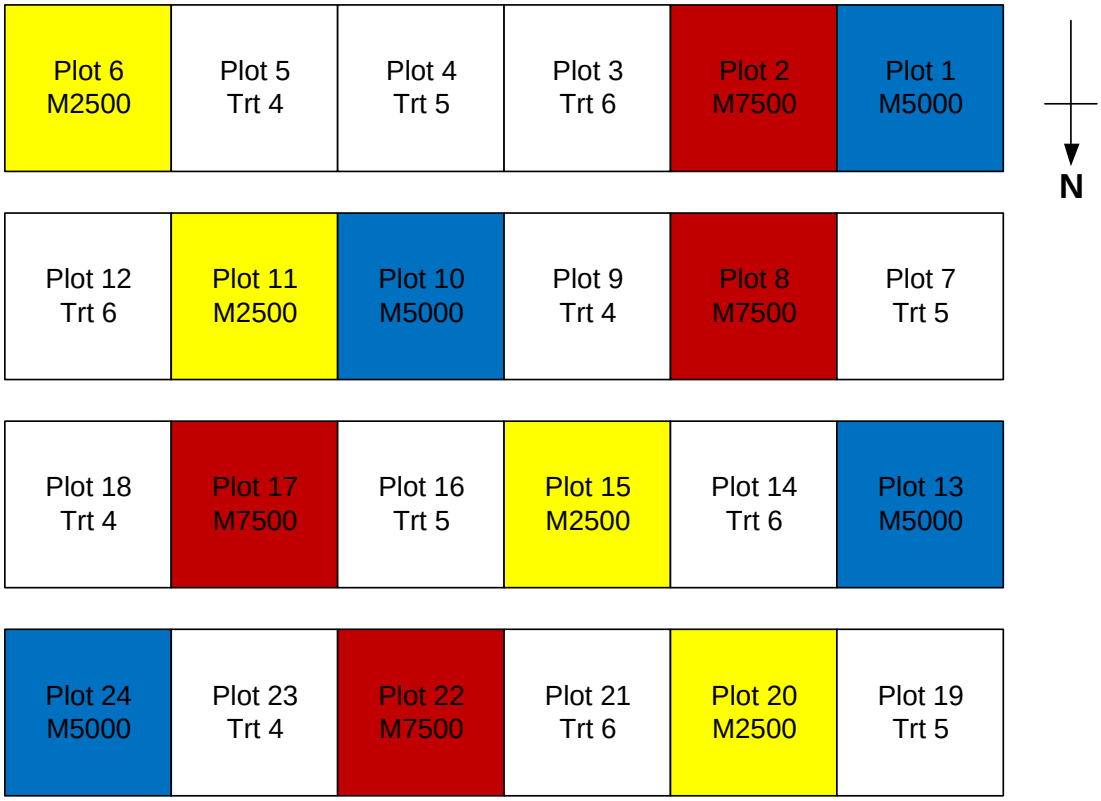

Figure 5-1: Plot design for the Carberry field site with three rates of manure application (Yellow: 2500 gal/acre, Blue: 5000 gal/acre, Red: 7500 gal/acre)

The liquid manure is applied to a depth of approximately 6 cm using the Aerway system. The spiked wheels of the Aerway system disturbed the soil surface and then manure performed on the surface. The liquid hog manure contained 10.5 kg total N/1000 gallons. The inorganic form of nitrogen in manure is found as ammonium nitrogen (NH_4^+-N). Note that lab tests will normally test for total N and ammonium nitrogen. Approximate organic N can be determined by subtracting ammonium-nitrogen (NH_4^+-N) from total N. Table 5-2 lists the applied manure organic-N and NH_4^+-N for different rates of manure applications. It is usually recommended that manure should be sampled before the actual application. Sampling at the time of application resulted in the changes of nutrient con-

centrations due to nitrogen transformations and atmospheric losses. The details of field operations and the dates are given in Table 5-3.

Table 5-2: Organic nitrogen and ammonium field rates for the year of 2003 and 2004

	Organic-N Rate(kg/ha)			NH^+_4-N Rate(kg/ha)		
Liquid Hog Manure(gal/acre)	2500	5000	7500	2500	5000	7500
2003	13.7	27.4	41.1	54.7	109.4	164.1
2004	15.6	31.2	46.8	83.8	167.6	251.4

Table 5-3: Field operation during the year 2002, 2003 and 2004

Field Operation	2002	2003	2004
Cultivation	May 15	May 17	May 6
Manure application	May 18	May 18	May 27
Seeding	May 28	May 20	May 28
Harvest	September 6	August 19	September 18

5.2 Data collection

The simulations were conducted using a data set from Carberry site. The data set includes three field plots with different rates of hog manure from year 2002 to 2004. Hourly meteorological inputs, provided from the atmospheric station at the middle of the field experiment, were recorded from September 2002 to December 2004. Precipitation, wind speed, short wave radiation, relative humidity, and air temperature were collected hourly. Fig-

ure 5-2 shows measured daily rainfall and estimated monthly evapotranspiration for the study period. In contrast to the first two years, the 2004 growing season was wet with annual precipitation of 530 mm. The total precipitation of year 2003 and 2004 was 349 and 379 mm, respectively. It has been reported that the normal annual precipitation of the area was 481 mm (Akinremi, 2005).

The available monthly soil moistures and daily soil temperatures, from depths of 0-10, 10-20, 20-30, 30-60, 60-90 and 90-120 cm, were used to validate the simulated soil moistures and soil temperatures. Soil water contents were measured gravimetric and daily by TDR probes. Five soil sampling exercises were carried out in 2002 and 2003, but only 3 in 2004 to measure ammonium and nitrate concentrations. Nitrate and ammonium concentrations were monitored at different depths by soil extraction with 2N KCl (Potassium chloride) at a soil to solution of 1:5.

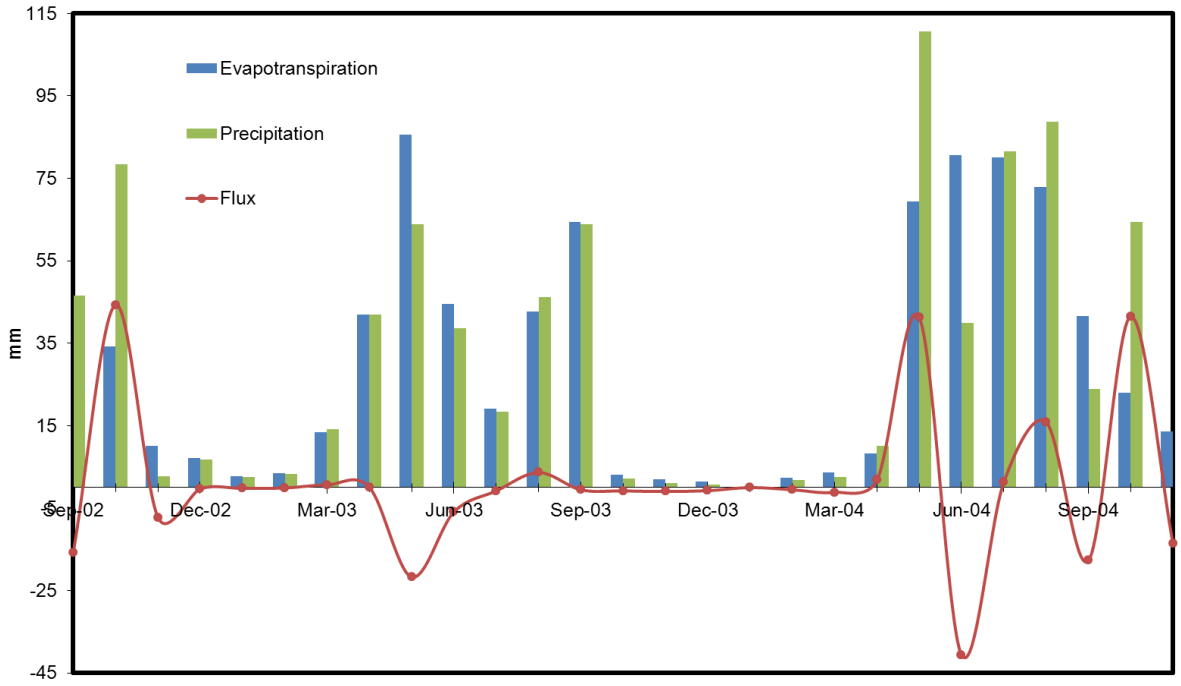

Figure 5-2: Monthly precipitation, evapotranspiration, and water flux at the soil surface of Carberry site

5.3 Model Evaluation

The performance of the integrated land surface scheme SABAE-HWS was evaluated using a 3-year data set from Carberry. Since hydrologic processes and also soil temperature play a major role in simulating nitrogen transport and transformations, SABAE-HW performance is expected to have a direct impact on the performance of SABAE-HWS. Soil temperatures are also necessary to accurately simulate nitrogen dynamics under cold conditions (Youssef et al., 2006).

Therefore, the model first was manually calibrated by statistically comparing observed and simulated soil moisture and soil temperature. Correlation (r), Root Mean Square Error (RMSE) and Coefficient of Residual Mass (CRM) were used to show the statistical performance of the SABAE-HWS for the Carberry site.

Modeling ammonium and nitrate concentration for the Carberry site is a challenging task due to different rates of manure application. To verify the accuracy of the model, SABAE-HWS is also tested with the results of the SHAW model during 2003. The SHAW model accounts for solute absorption by the soil profile and includes the processes of solute transfer: molecular diffusion, convection, and hydrodynamic dispersion.

As discussed in Chapter 3, a lower water boundary condition is considered safer and more accurate than unit gradient boundary condition (Hejazi and Woodbury, 2011). Thus, the total depth of 5 meters is assigned for the soil profile to reach the ground water table. A-19-layer soil profile is considered for the simulations with a thickness of 10 cm for the first three layers, 15 cm thickness for the layers 4 to 9, and 30 and 50 cm thickness for the rest of layers (Figure 5-3). Note that SABAE-HWS can divide the profile into 30 or more layers with the thicknesses specified by the user. Number and thickness of layers as-

signed for the Carberry simulations are based on the depths of each layer reported for the observed data.

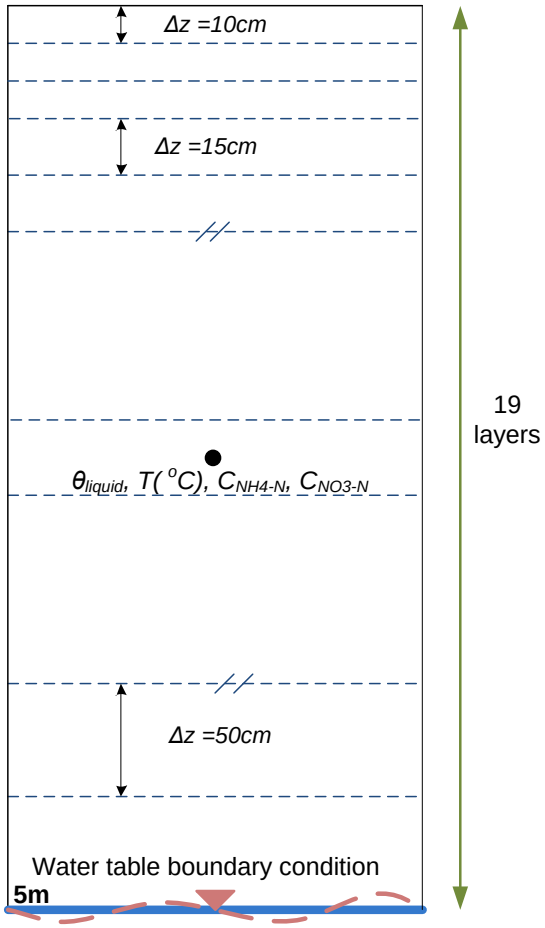

Figure 5-3: Overview of the soil profile applied for SABAE-HWS simulations at Carberry site

The soil parameters and soil water characteristic data used in simulating the hydrologic processes of the site were based on the direct measurements in the field and default code values. Default code parameters are soil texture parameter, pore volume fraction, and saturated soil water suction. It is noticed that the code includes a soil hydraulic char-

acteristic database which can be changed by the user. Soil dispersive parameters were also found in the literature (Table 5-4).

Table 5-4: A summary of soil hydraulic, vegetation inputs and dispersive parameters of Carberry site

Parameters	Value
Saturated hydraulic conductivity (m/s)	$16.6\ e^{-6}$
Leaf area index (m^2/m^2)	5.0
Visible albedo	0.024
Near-infrared albedo	0.140
Root depth (m)	1.5
Molecular diffusion (m^2/day)	$4.0e^{-4}$
Soil dispersivity (m)	0.07
Mineralization rate (1/day)	$3.0\ e^{-3}$
Nitrification rate (1/day)	$3.0\ e^{-2}$
Q_{10}	2
Base temperature (^oC)	10

Model results for all different rates of manure application were analyzed by the value of the correlation coefficient. The correlation coefficient indicates whether the simulated values follow the same linear patterns as the observed data. However, the evaluation of the accuracy of the model based only on correlation values can be misleading. Therefore, additional statistical criteria such as goodness of fit and residual error analysis are also used to evaluate the performance of solute transport models (Mulla and Addiscott, 1999).

The methods include Maximum Error (ME), Root Mean Square Error (RMSE), Coefficient of Determination (CD), Coefficient of Residual Mass (CRM), and Modeling Efficiency (EF). Although these statistical parameters are appropriate for moderate or large data sets, RMSE and CRM are used to evaluate the agreement between experimental measurements and model predictions. RMSE accounts for the variation between data sets while CRM indicates if the observed data are overestimated or underestimated by the simulations. Coefficient of residual mass is defined by Eq. 5-1. Root mean square error and correlation coefficient have been well defined in Chapter 3 by Eq. 3-11 and 3-12.

$$CRM = \frac{\sum_{i=1}^{n} O_i - \sum_{i=1}^{n} P_i}{\sum_{i=1}^{n} O_i} \qquad 5\text{-}1$$

In addition, graphical comparisons including the observed versus simulated values at different depths and the predicted values versus observed median values with error bars for the interquartile range at different times were considered to verify the performance of the SABAE-HWS.

5.4 Summary

The evaluation of SABAE-HWS was undertaken using measured soil moisture, soil temperature, soil ammonium, and soil nitrate data from Carberry site. Carberry is located within the Assiniboine Delta Aquifer (ADA). The combination of an unconfined aquifer (ADA) underlying coarse textured soil increases the potential for aquifer contamination. All comparisons between simulated and actual measurements are presented in the next Chapter. Three rates of manure application (2500, 5000, and 7500 gal/acre) were applied on the Carberry site. The impacts of different rates of manure application in minimizing the risk of nitrate leaching are also discussed in Chapter 6. To verify the performance of

the SABAE-HWS, the results of simulated soil ammonium-N and nitrate-N are also compared with the results of the SHAW model. It should be noted that SHAW is a climate-groundwater-solute transport model simulating all kinds of solute and not specifically nitrogen transport. Moreover, SHAW was developed to simulate soil freezing and thawing. However, SHAW is not able to simulate nitrogen dynamics in the soil layers.

Chapter 6

Results and Discussions

The results of the SABAE-HWS model including the comparisons between measured data (Carberry site) and SHAW simulations are discussed in this Chapter. First, simulated soil moisture and soil temperature results were evaluated as they have direct impacts on nutrient transport. The effects of different rates of manure application on nutrient movement within the soil profile are investigated in section 6.5. In addition, model application which is mainly manure application following the Best Management Practice (BMPs) is described in detail. Soil nitrate distributions over a 10 year climate record from OJP site with 2500 and 7500 gal/acre manure application are also presented in section 6.6.

6.1 Soil Moisture

The simulations of soil moisture at Carberry site during the three growing seasons are shown in Figure 6-1. As expected, the results indicate that SABAE-HWS performed reasonably well in predicting soil moisture at various depths, especially for the top soil layers. The field capacity of the soil changes as clay content changes with depth (Table 5-1). Field capacity first decreased to about a minimum of 23% in the 30-60 cm depth and then

it increased to 34% in the 90-120cm depth due to the high rate of clay content at this depth. Soil moisture plots have the same trend as the field capacity. The top 60 cm had soil moisture values of approximately 25% and it increased to about 35% below this depth. Soil moisture plots clearly show that the maximum amount of water content was in the spring due to snow melt recharge. Therefore, regardless of the manure rate, the risk of nitrate leaching in this period is more than the other seasons. In summer, soil moisture values decreased due to evaporation and crop uptake of water.

A set of statistical parameters calculated for all layers is also shown in Table 6-1. A relatively small positive CRM indicates that simulations tended to underestimate the observations in the upper layers while the soil moistures are overestimated for the rest of layers (CRM<0). The poor simulation of soil water content was at the depth 60-75cm where the RMSE (0.08) was the highest and the CRM (-0.68) was less than the other layers. Since it has been observed that soil hydraulic characteristic is not consistent in terms of sand and clay index at this depth, the model was not able to simulate soil moisture properly. In fact, soil heterogeneity at this depth was the main reason that the model could not simulate correctly the soil hydraulic parameters. It is noted again that field capacity of the soil begins to increase at this depth.

The variation of soil moisture in the 90-105 and 105-120 cm layers was less than the upper layers. However, the relatively small value of the correlation coefficient indicates that the simulations did not fit perfectly to the observations. This might affect the nutrient simulations, especially at the growing season 2003 where it was found a correlation value of 0.37 for the lower layers.

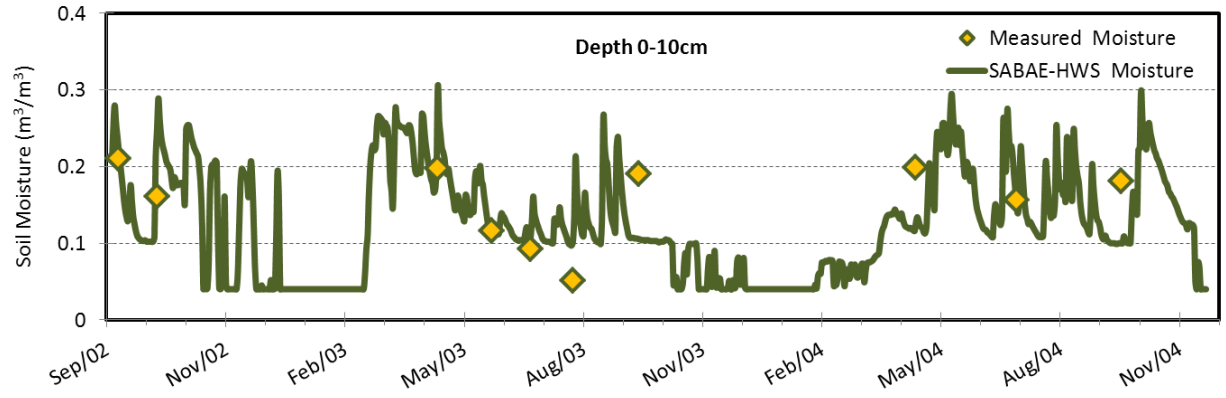
Depth 0-10cm
Measured Moisture
SABAE-HWS Moisture
Soil Moisture (m³/m³)
0.4
0.3
0.2
0.1
0
Sep/02
Nov/02
Feb/03
May/03
Aug/03
Nov/03
Feb/04
May/04
Aug/04
Nov/04

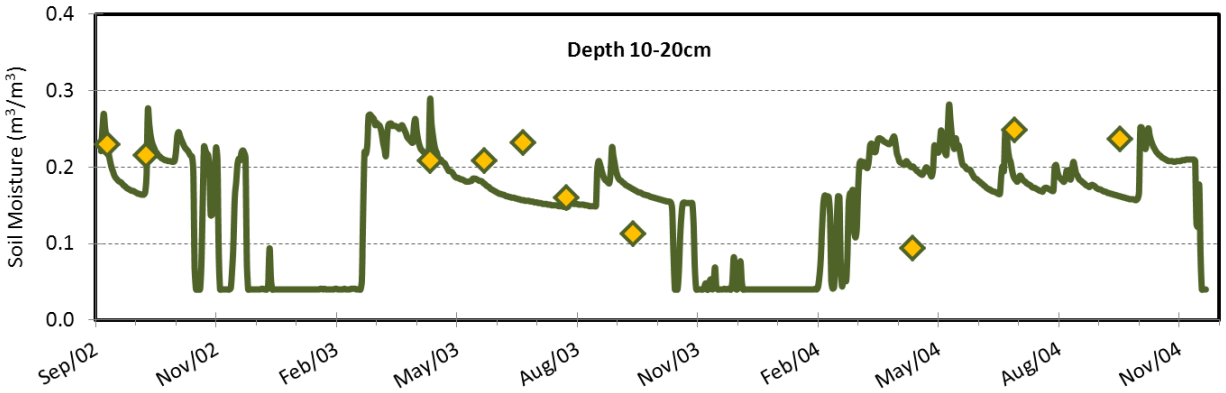
Depth 10-20cm
Soil Moisture (m³/m³)
0.4
0.3
0.2
0.1
0.0
Sep/02
Nov/02
Feb/03
May/03
Aug/03
Nov/03
Feb/04
May/04
Aug/04
Nov/04

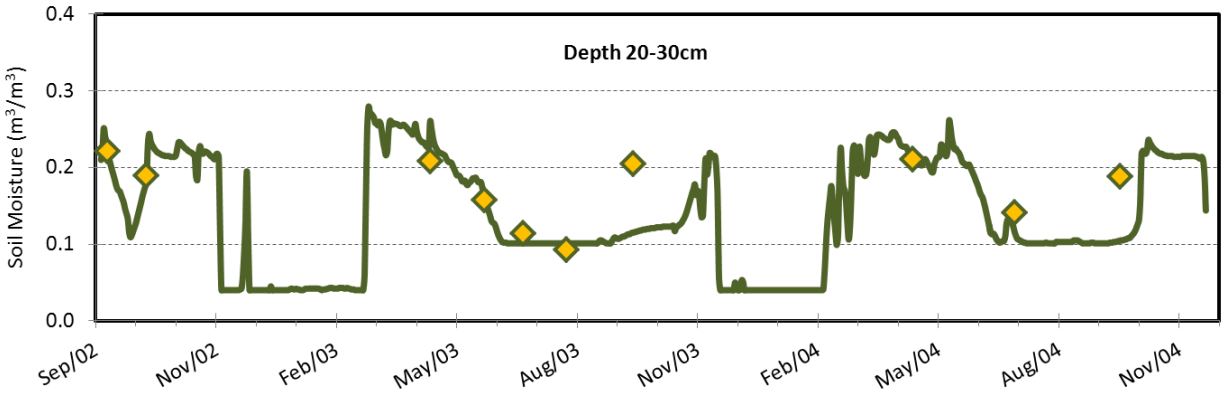
Depth 20-30cm
Soil Moisture (m³/m³)
0.4
0.3
0.2
0.1
0.0
Sep/02
Nov/02
Feb/03
May/03
Aug/03
Nov/03
Feb/04
May/04
Aug/04
Nov/04

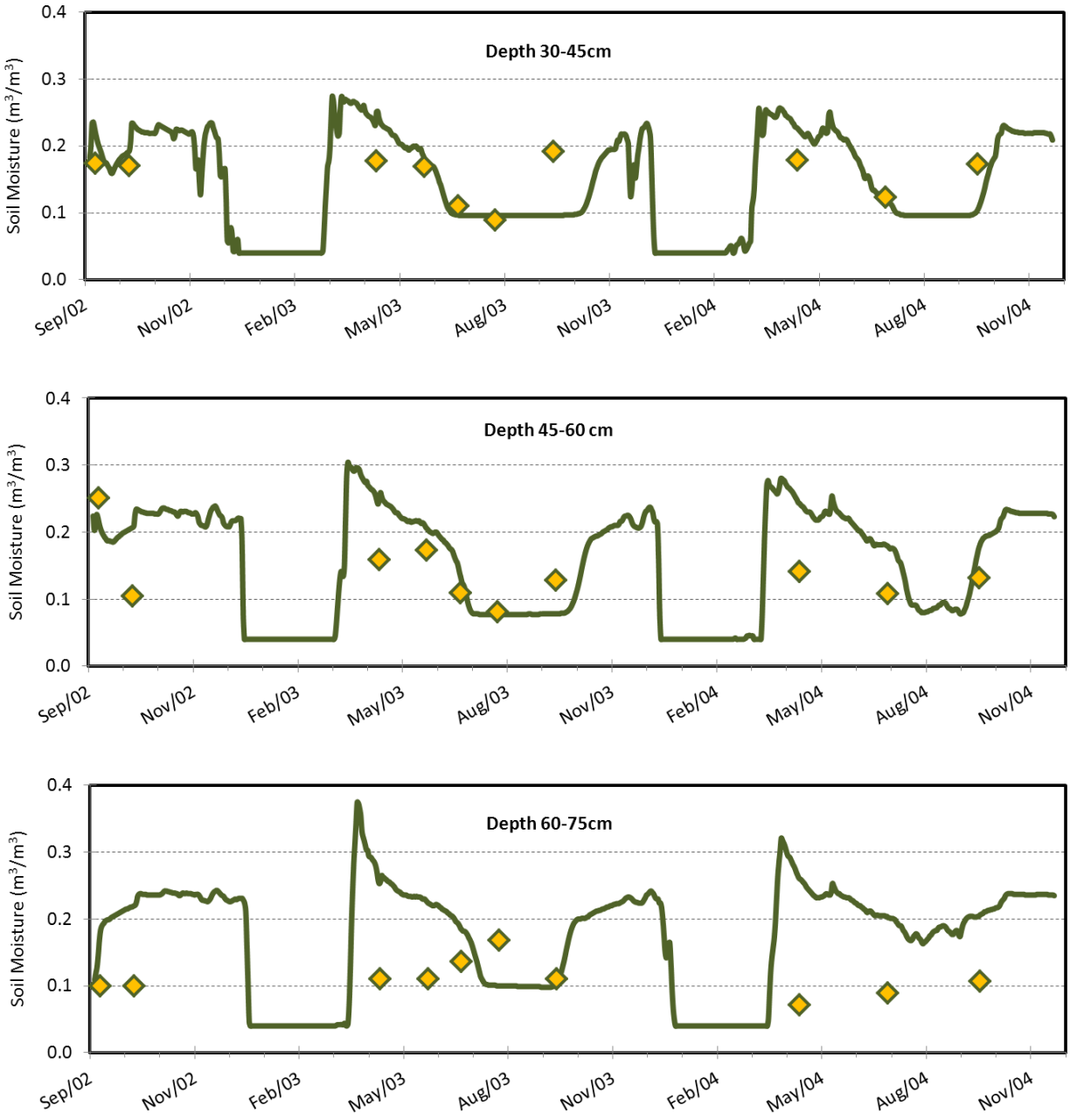
Depth 30-45cm
Depth 45-60 cm
Depth 60-75cm
Soil Moisture (m³/m³)
0.4
0.3
0.2
0.1
0.0
Sep/02
Nov/02
Feb/03
May/03
Aug/03
Nov/03
Feb/04
May/04
Aug/04
Nov/04

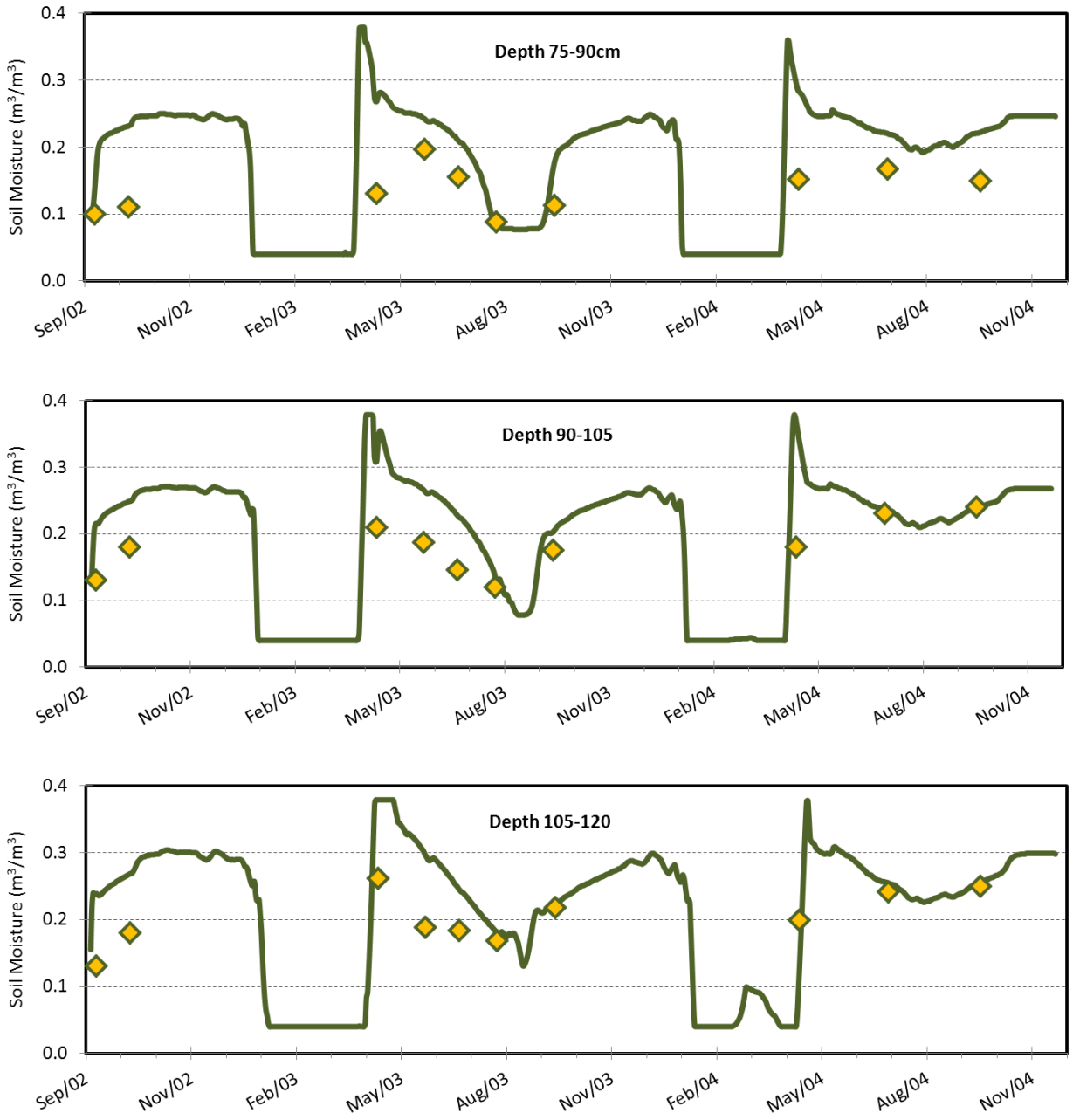

Figure 6-1: Observed and simulated soil water content by SABAE-HWS model during 2002-2004 at different depths

Table 6-1: Statistical evaluation of SABAE-HWS model for simulating soil moisture at different depths

Depth(cm)	R	RMSE	CRM
0-10	0.64	0.04	0.01
10-20	0.75	0.04	0.02
20-30	0.72	0.04	0.10
30-45	0.53	0.05	-0.001
45-60	0.49	0.06	-0.20
60-75	0.69	0.08	-0.68
75-90	0.63	0.08	-0.44
90-105	0.35	0.08	-0.31
105-120	0.37	0.07	-0.21

In summary, soil hydraulic properties as well as soil water content play a major role in controlling ammonium and nitrate transport in the soil profile. Therefore, the good prediction of soil water content was the first priority of this study. In addition, soil moisture affects the abiotic functions in order to simulate the nitrogen dynamics. Based on the simulated results, the model adequately simulated soil moisture.

6.2 Soil Temperature

The result of simulated and observed soil temperature over three years of study at Carberry site is presented in Figure 6-2. The actual average temperatures were used as a boundary condition at the top of soil profile. A range of 0.9 to 0.96 of correlation coefficients in-

dicates that there is a good agreement between predicted and observed soil temperature for all layers (Table 6-2). The negative values of CRM show that soil temperature is overestimated by the SABAE-HWS model for all layers. The main reason of this discrepancy might be the higher values of simulated soil temperatures than observed data during winter time. The average RMSE value was 4.6 (0.046 m^3/m^3) which means the soil temperature is reasonably simulated and compared with the observations. Note that, comparing to the top layers, the simulations are more accurate at the lower layers as the values of RMSE and CRM decreased.

Table 6-2: Statistical evaluation of SABAE-HWS model for simulating soil temperature at different depths

Depth(cm)	R	RMSE	CRM
0-10	0.95	4.85	-0.59
10-20	0.95	4.24	-0.48
20-30	0.96	4.06	-0.55
30-60	0.95	3.67	-0.47
60-90	0.90	3.98	-0.2
90-120	0.90	3.25	-0.1

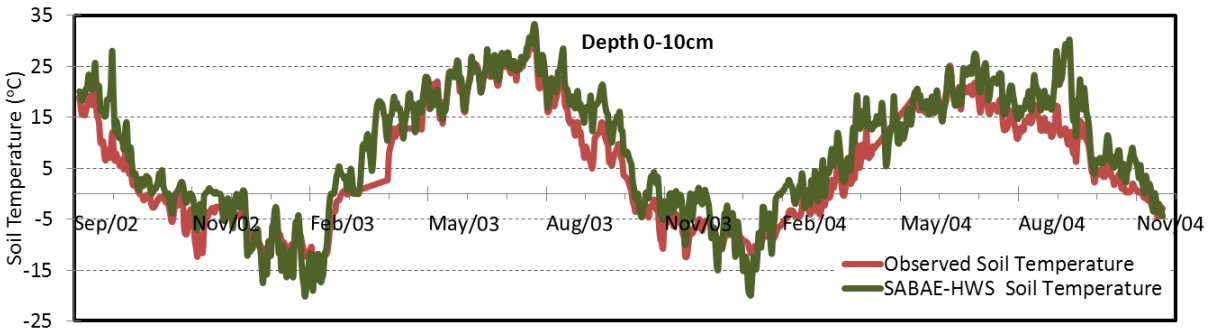
Depth 0-10cm
Soil Temperature (°C)
35
25
15
5
-5
-15
-25
Sep/02
Nov/02
Feb/03
May/03
Aug/03
Nov/03
Feb/04
May/04
Aug/04
Nov/04
Observed Soil Temperature
SABAE-HWS Soil Temperature

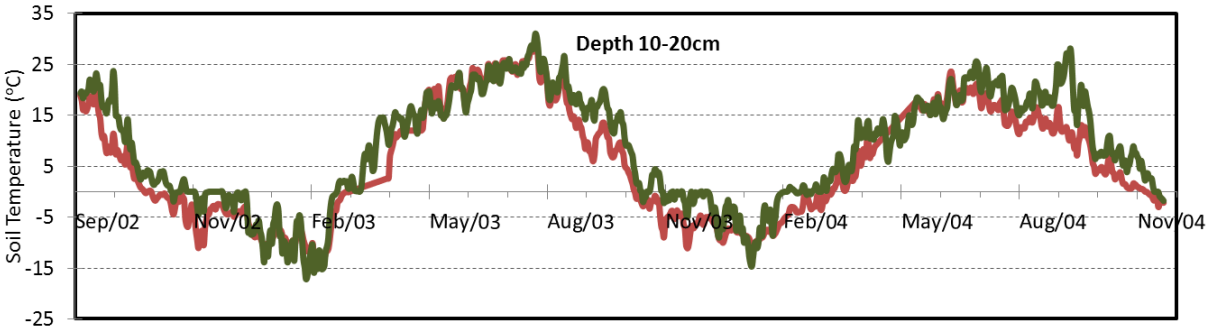
Depth 10-20cm
Soil Temperature (°C)
35
25
15
5
-5
-15
-25
Sep/02
Nov/02
Feb/03
May/03
Aug/03
Nov/03
Feb/04
May/04
Aug/04
Nov/04

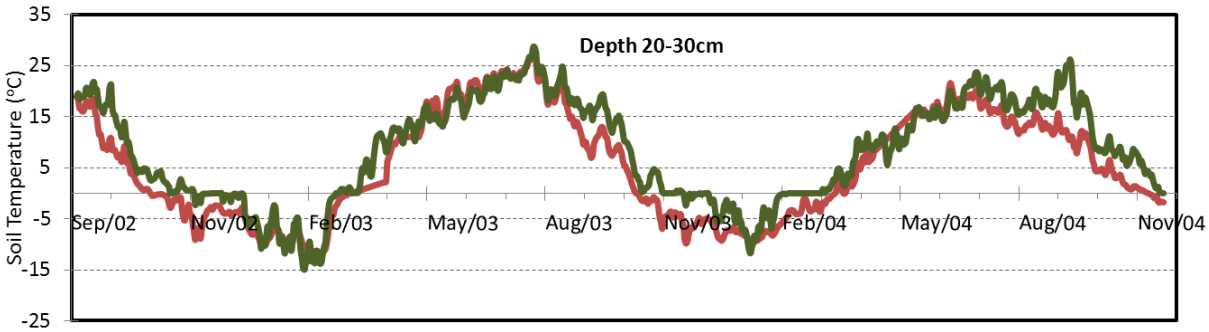
Depth 20-30cm
Soil Temperature (°C)
35
25
15
5
-5
-15
-25
Sep/02
Nov/02
Feb/03
May/03
Aug/03
Nov/03
Feb/04
May/04
Aug/04
Nov/04

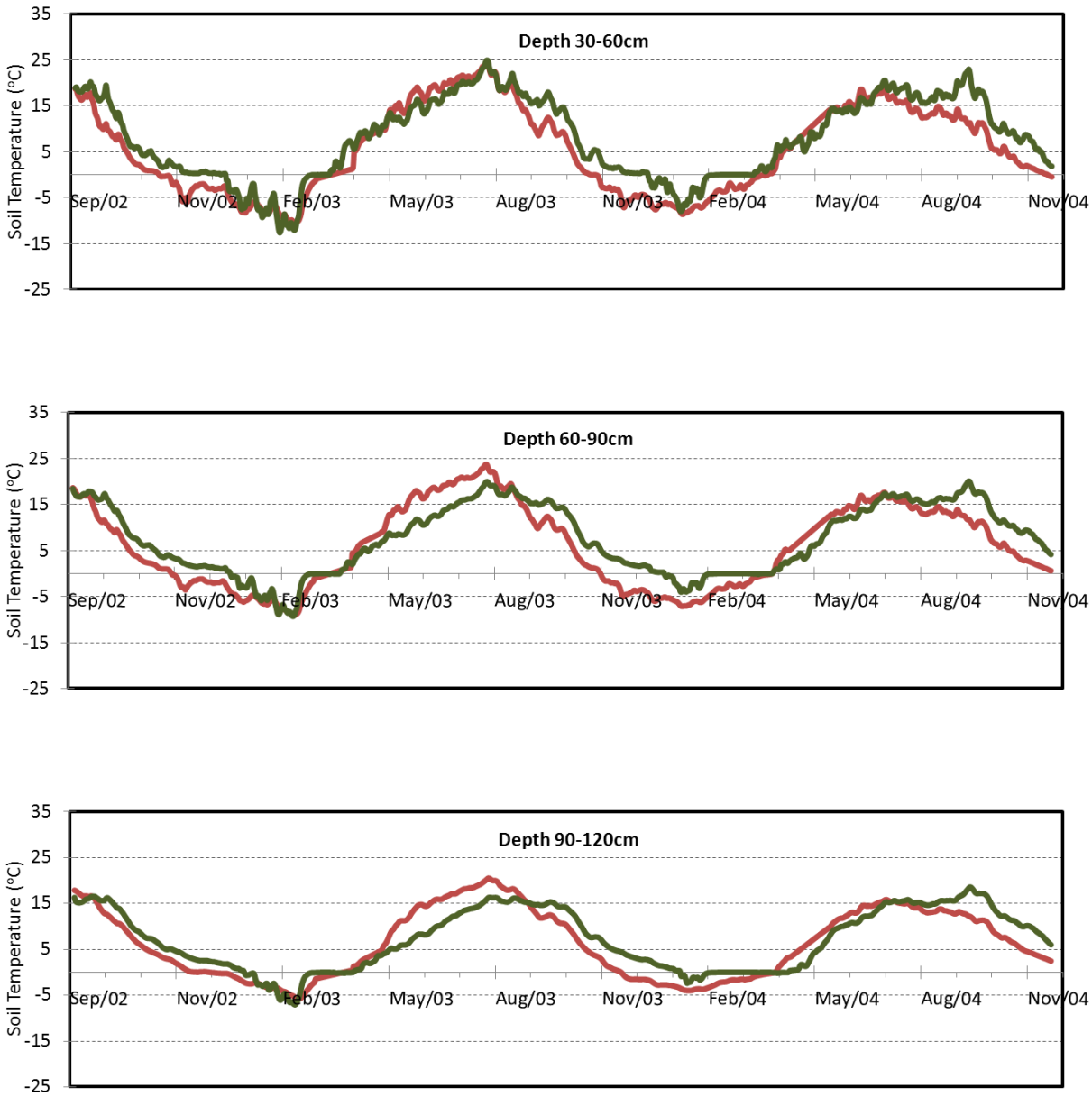

Figure 6-2: Observed and simulated soil temperature by SABAE-HWS model during 2002-2004 at different depths

The amount of soil ammonium and soil nitrate is primarily related to changes in soil temperature and water content. After validating the results of soil moisture, it was necessary to predict soil temperature correctly as it affects ammonium and nitrate production. The results proved the high accuracy of the land surface scheme SABAE-HWS in simulating soil temperature at various depths of Carberry site.

6.3 Soil Ammonium-Nitrogen

Since there were little differences in the soil ammonium–nitrogen distribution among the three rates of manure applications, the main attention is paid to the results obtained for the 2500 gal/acre hog manure application. It should be noted that it was found the same results for the manure applications of 5000 and 7500 gal/acre but with the different peak points. Figure 6-3 shows a comparison between measured and simulated NH_4^+-N at the different depths with the manure application rate of 2500 gal/acre. Application of manure in the field experiment at spring 2003 and 2004 corresponded to a concentration of approximately 54.7 and 83.8 kg/ha NH_4^+, respectively. The ammonium peaks at the top soil, 0-10cm, are due to applications of hog manure on 18 May 2003 and 27 May 2004. As apparent from the results, the simulations of the NH_4^+-N followed the same pattern as the measured data. However, there is a small difference (less than 10 mg/kg) between modeled and observed data. Note that NH_4^+-N analysis at the experimental site had been performed on the dry soils. Since there was a hog barn close to the location of ammonium measurements, dried soil samples adsorbed the amount of available volatilized ammonium by hog manure in the air. Thus, ammonium measurements did not show exactly the amount of soil ammonium nitrogen. In fact, the amount of reported soil ammonium ni-

trogen is a little more than what expected. However, in general, both observed and predicted NH_4^+-N tended to decrease after the manure applications. NH_4^+-N was quickly adsorbed to the soil or taken up by ammonium nitrogen uptake almost one month after applications. Consequently, N mineralization after soil frost did not change significantly due to the lack of NH_4^+-N in the soil. In addition, a rapid nitrification of NH_4^+-N also accelerated the disappearing of NH_4^+-N at the greater depths. The results also showed the higher NH_4^+-N concentrations for top layers at the dry year (2003) when compared to the wet year (2004). A large amount of precipitation in 2004 increased NH_4^+-N loss and transport NH_4^+-N out of the top soils.

Since the SHAW model is able to simulate solute transport with only one application at each time period, both models set to run for the year 2003. The SABAE-HWS performance in simulating NH_4^+-N was compared with the results of the SHAW model and observed data at two months of year 2003 for three different rates of manure applications: one at the growing season (July) and another after harvesting time (October) (Figure 6-4). Both models presented the similar patterns at the deep layers. However, discrepancies between the SABAE-HWS and SHAW models mainly occurred at the top soils. SABAE-HWS showed the higher NH_4^+-N concentrations at the top soils (0-40cm), especially at the growing season. These variations can be explained by the weakness of SHAW model in correctly simulating nitrogen dynamics at the root zone. Also nitrification of NH_4^+-N is not taken into account by the SHAW model. However, these variations disappeared at the end of growing season mainly because there is no root in the soil profile to uptake nitrogen. Note that the concentration of NH_4^+-N decreased at deeper layers for both models mainly because of the soil adsorption.

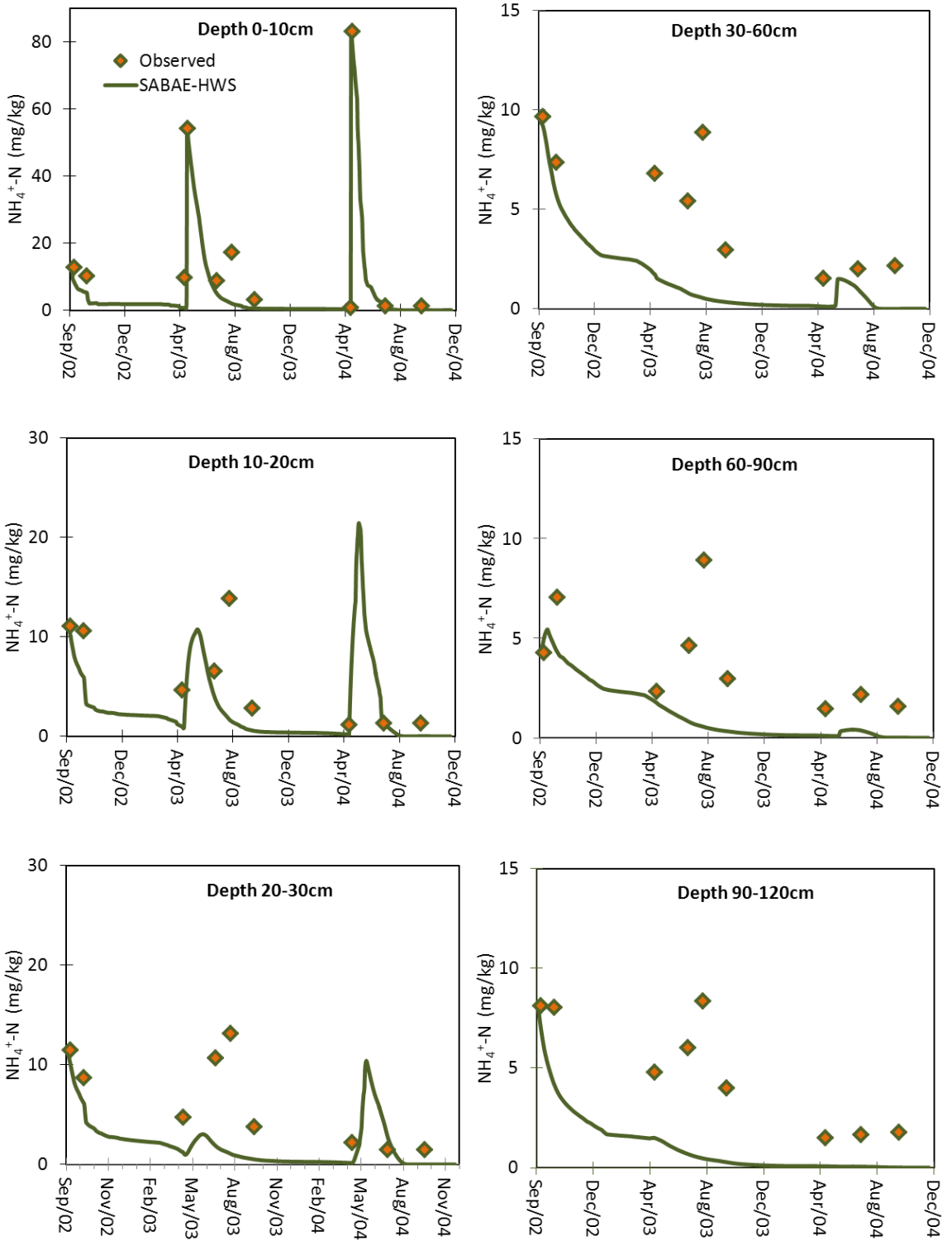

Figure 6-3: Observed and simulated soil ammonium nitrogen by SABAE-HWS model during 2002-2004 at different depths

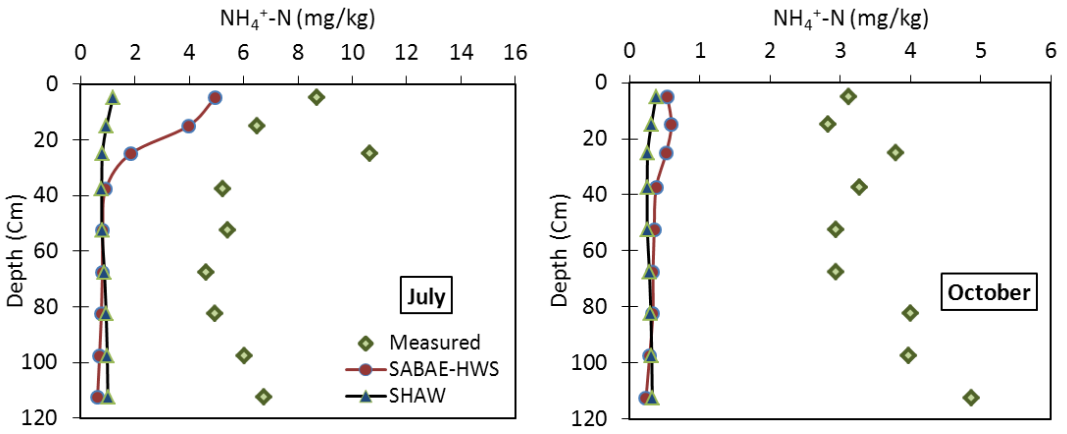

a) 2500 gal/acre manure application

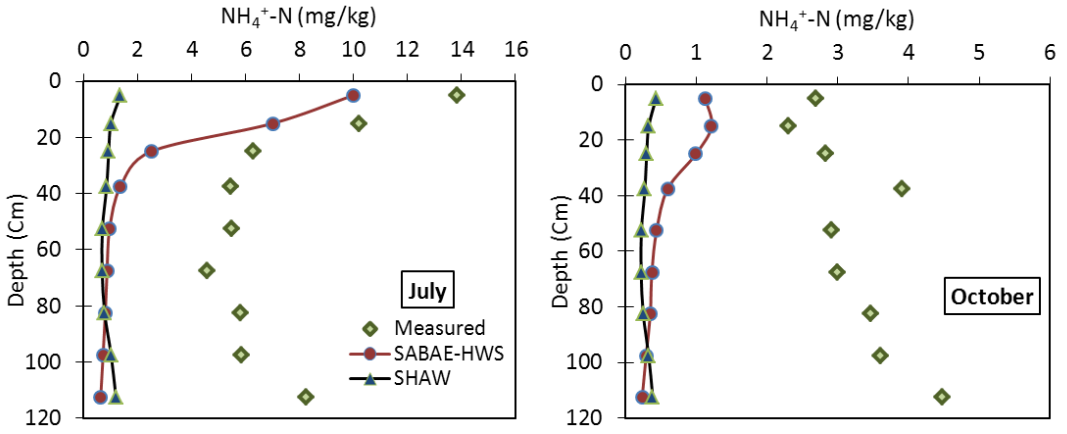

b) 5000 gal/acre manure application

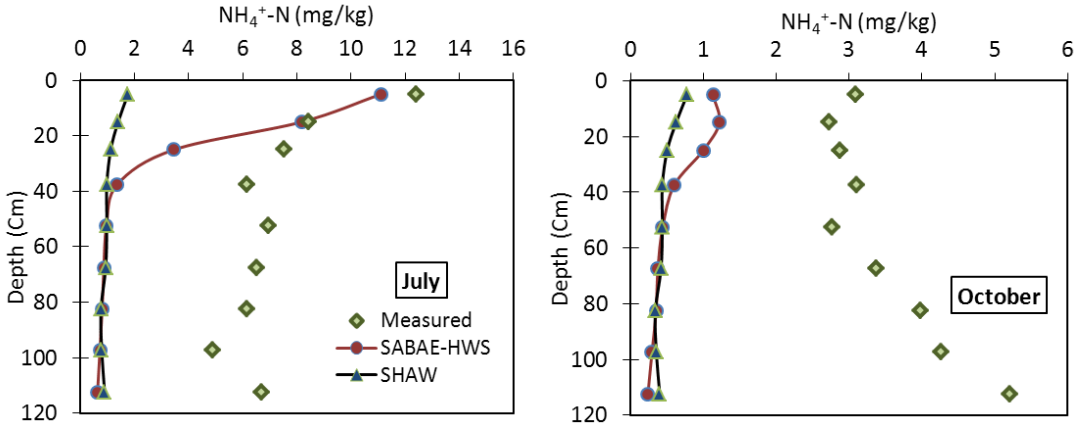

c) 7500 gal/acre manure application

Figure 6-4: Simulated soil ammonium nitrogen by SABAE-HWS and SHAW model in 0-120 cm depth with three rates of manure application at the mid-season (July) and the end of growing season (October) of 2003

6.4 Soil Nitrate-Nitrogen

Measured and simulated soil nitrate-nitrogen against time are shown for different rates of manure application in Figure 6-5 to Figure 6-7. Since the results of 4 replicates were available for 2002 and 2003, uncertainties will be added by adding error bars in the data point. Each observed value is the average of four replicates and error bars are the standard error distributed around the average. In spite of significant differences in the observed values between replicates, simulations are close to observed values for all plots, especially for the 2500 and 5000 gal/acre manure applications. In general, the highest NO_3^--N concentration were found at the soil surface (0-10 and 10-20cm) shortly after the manure applications due to mineralization and nitrification of ammonium. NO_3^--N concentrations decreased during the periods of N uptake by the crops. At the maturity date of the crop, zero concentrations were found at the wet year (2004) for the top layers. This can be explained by the large precipitation and then the downward movement of nitrate in this year. Small rates of organic nitrogen and lack of nitrates due to nitrogen uptake by plant roots are also the main reasons for the disappearing of nitrate concentrations at top soils (0-60cm). This also led to increase in rate of nitrate concentration at depth. It is noted that crops slowly stop taking up nitrogen at the maturity date. Both simulated and observed NO_3^--N concentrations tended to increase after this time (August). However, the observed data increased approximately four times more than simulations. Comparing to the observed data, the simulated NO_3^--N concentrations are considerably small at the end of growing season. Although no clear explanation has been found for these deviations, it is reported that a wet late summer caused the nitrate to increase at the soil profile (Akinremi, 2005). Comparing Figure 6-5 and Figure 6-6 with Figure 6-7 shows that there

was a similar trend between measured and simulated NO_3^--N concentrations at all soil depths for all manure application rates. The rates of nitrate concentration changed according to the different rates of manure applications. Nevertheless, the main disagreement was observed below the root zone (105-120cm) where the measured nitrate-N continued to increase especially at the 7500 gal/acre. However, the simulated nitrate-N did not change significantly. In fact, observed data indicated that there was a risk of nitrate leaching at the end of growing season of 2004 due to the cumulative effect of 3 years of manure application. Note that, nitrate leaching is the amount of nitrate in soluble water which is usually 10 to 20 percent more than soil nitrate concentrations at the bottom of the soil profile during the wet years. It is believed that when nitrate concentrations exceed 10 mg/kg, nitrate leaching occurs. Because of atmosphere data limitations, the model was run from September 2002 and the first application in May 2002 was ignored in the simulations. Since it was considered only two years of manure application (May 2003 and 2004) in this study, SABAE-HWS did not show any significant changes in soil nitrate concentrations at the deeper layers. In addition to manure application, water application also affects the nitrate leaching (Al-Darby and Abdel-Nasser, 2006). Although more water application was added at the time of manure application, no nitrate leaching was simulated for the soil profile. This clearly shows that the residual NO_3^- in the soil profile at the lower layers was not sufficient for nitrate to move to the bottom of the soil profile at the end of the simulations.

Figure 6-5 to Figure 6-7 also confirmed the results of field experiment by Mitchell et al. (1996) and Hentschel et al. (2009). Both observed and simulated results clearly indicated that net nitrification and NO_3^- concentrations tend to increase after freeze and thaw

period, especially in the top soils. The nitrate concentration ranged from 5 to 10 mg/kg at the freezing time (January and February 2004) while it increased to 10-50 mg/kg after thawing period (April and May 2004). It was not found any difference between the simulated nitrate concentration at deeper layers in winter and spring 2004. In fact, the rate of nitrification did not change after thawing period at higher depths.

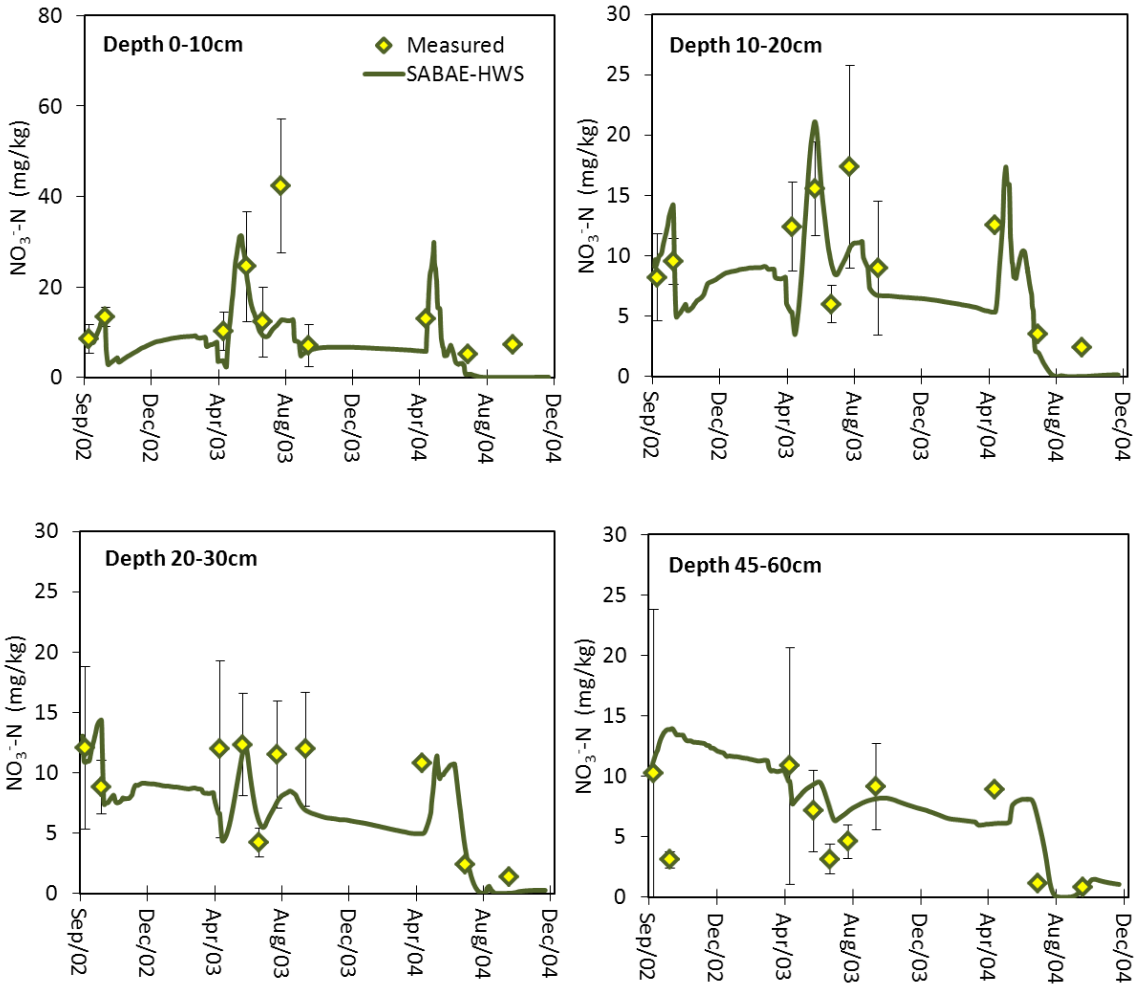
Depth 0-10cm
Measured
SABAE-HWS
Depth 10-20cm
Depth 20-30cm
Depth 45-60cm
NO3-N (mg/kg)
Sep/02
Dec/02
Apr/03
Aug/03
Dec/03
Apr/04
Aug/04
Dec/04

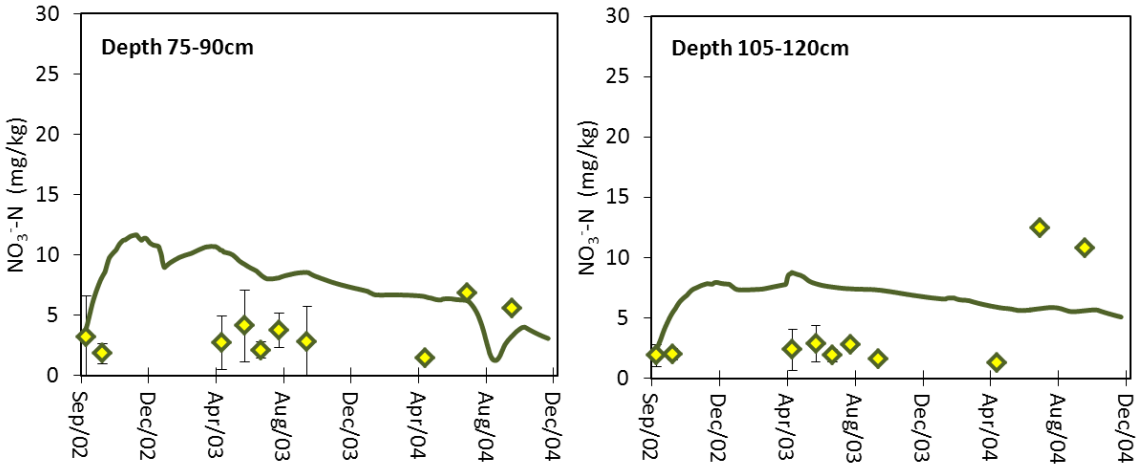

Figure 6-5: Average observed and simulated soil nitrate nitrogen by SABAE-HWS during 2002-2004 with manure application of 2500 gal/acre

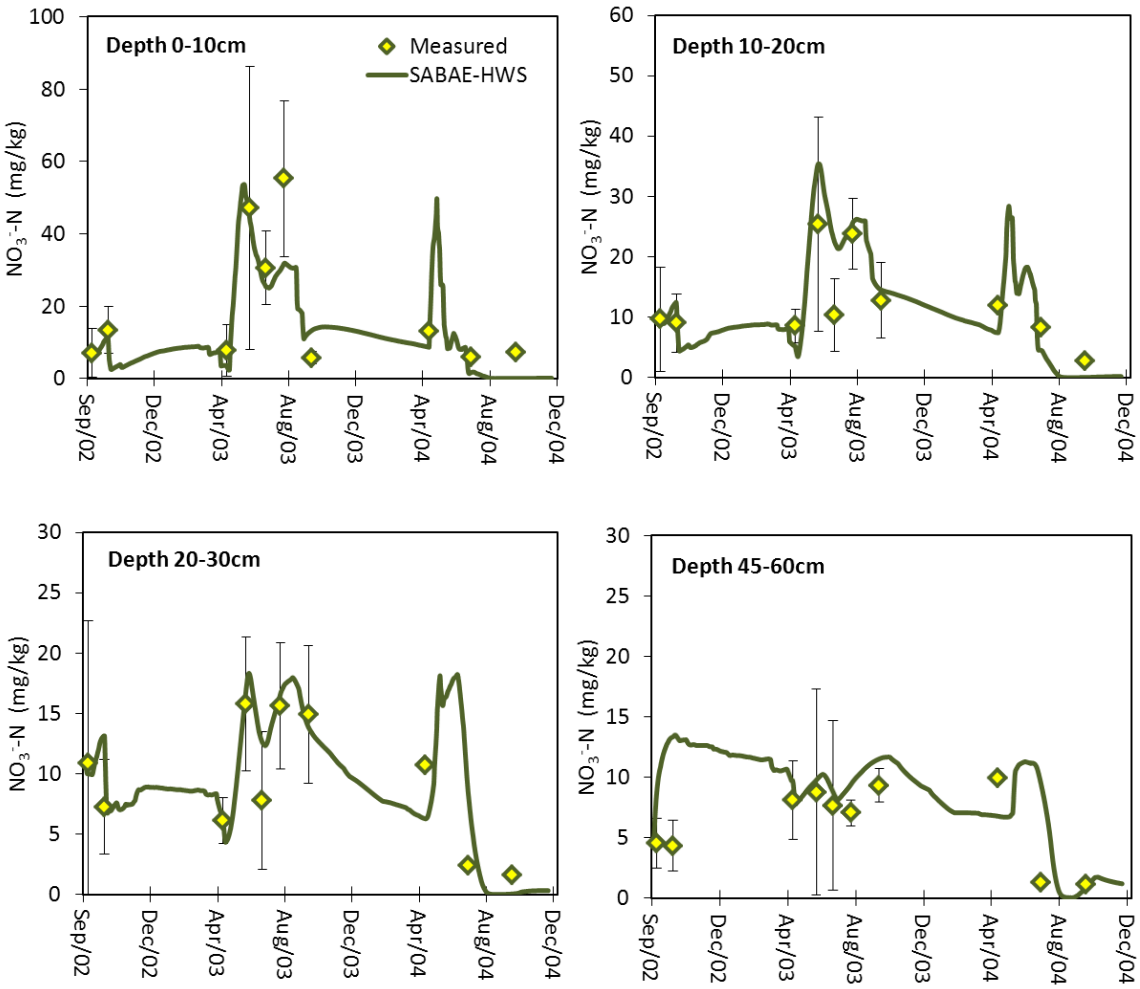

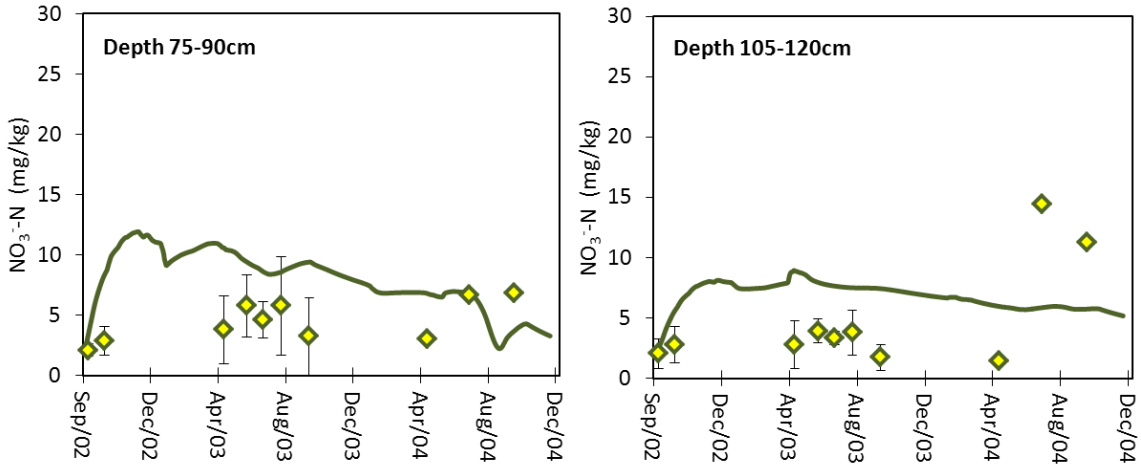

Figure 6-6: Average observed and simulated soil nitrate nitrogen by SABAE-HWS during 2002-2004 with manure application of 5000 gal/acre

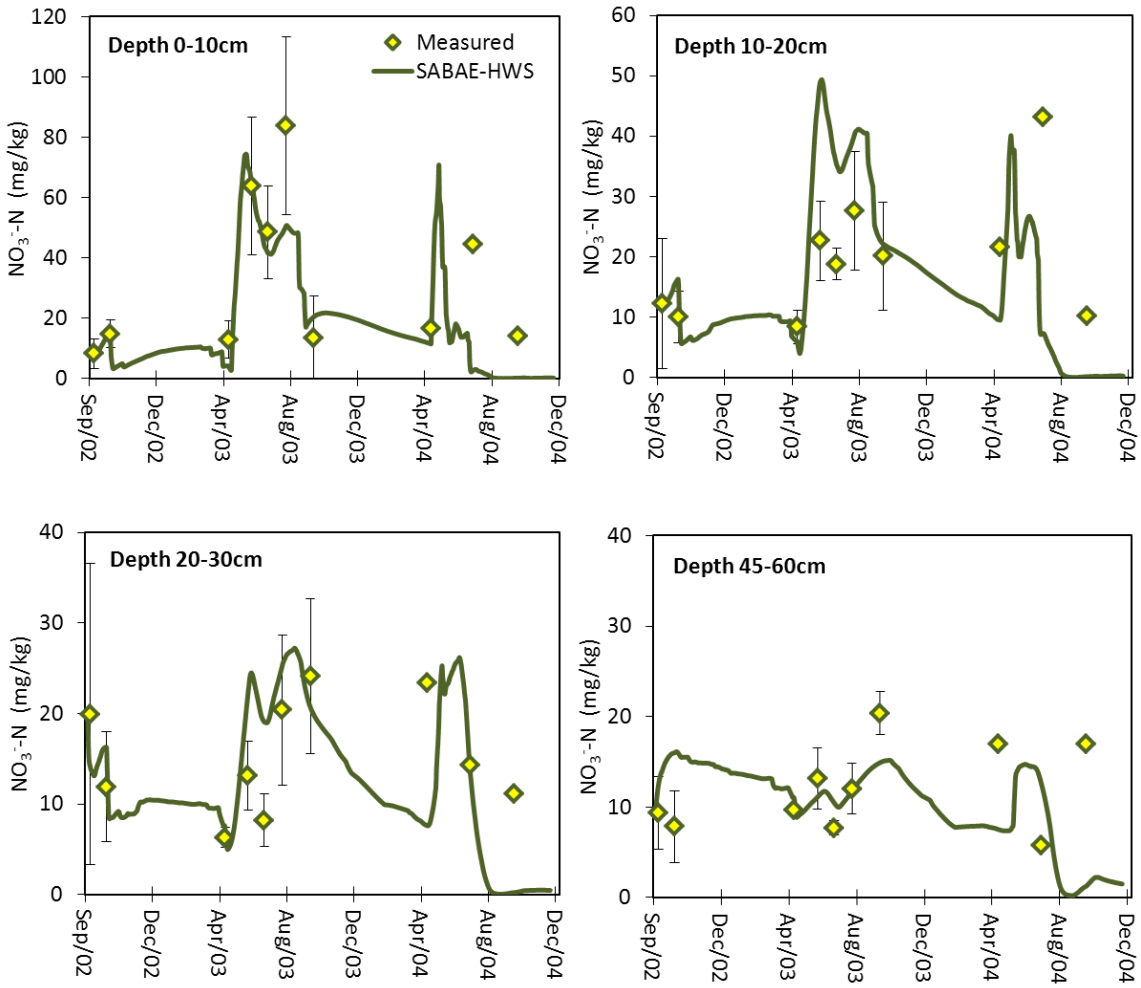

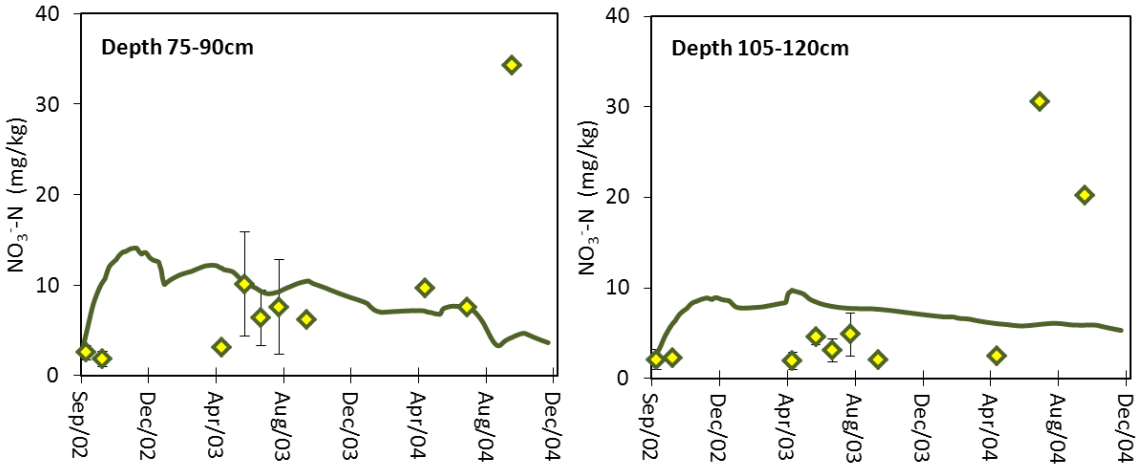

Figure 6-7: Average observed and simulated soil nitrate nitrogen by SABAE-HWS during 2002-2004 with manure application of 7500 gal/acre

Figure 6-8 to Figure 6-10 show a comparison between the observed and simulated NO_3^--N concentration for each soil layer on all sampling dates for the application rate of 2500, 5000 and 7500 gal/acre, respectively. Although the total number of field nitrate observations is too small, scatter plots and statistical measures indicate a reasonable agreement between model and observations (Table 6-3). Except the high RMSE values obtained for the first layers due to relatively high observed nitrate concentration at the end of growing season, the rest of RMSE values had a range of 3 to 5. In contrast to RMSE values, a reasonable correlation between simulated and observed NO_3^--N was found at the first layers. However, the simulated results did not fit properly to the observed data for the 30-90 cm depth. Reasonable correlation (approximately 40%) was found for the greater depths (90-120 cm). In general, simulated nitrate concentrations tended to overestimate the observations in most of the layers due to the negative value of CRM. However, simulated NO_3^--N concentrations were underestimated at the top soil (up to 30cm) for the manure application of 2500 gal/acre.

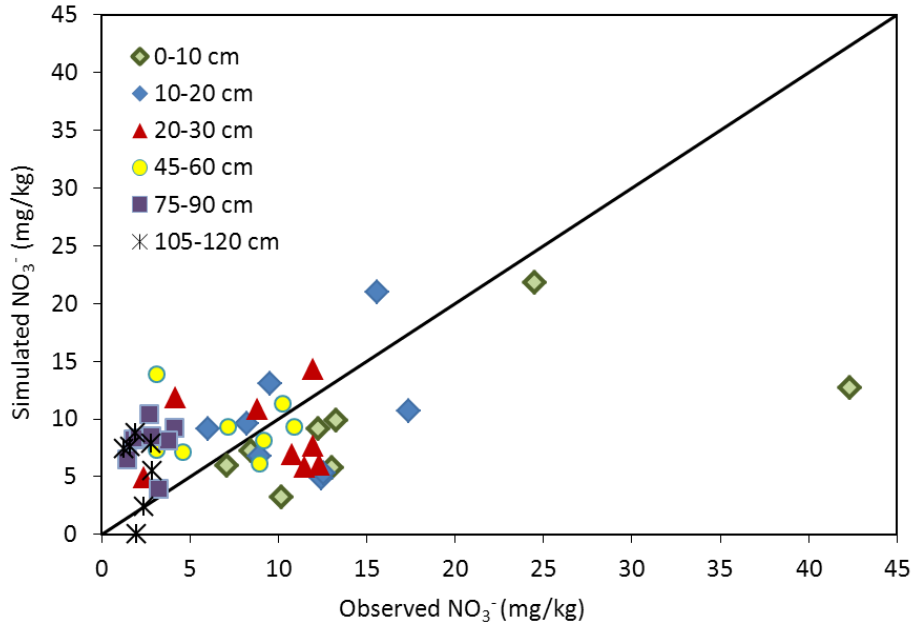

Figure 6-8: Scatter plot of observed versus simulated NO_3^- -N at different depths with 2500 gal/acre manure application

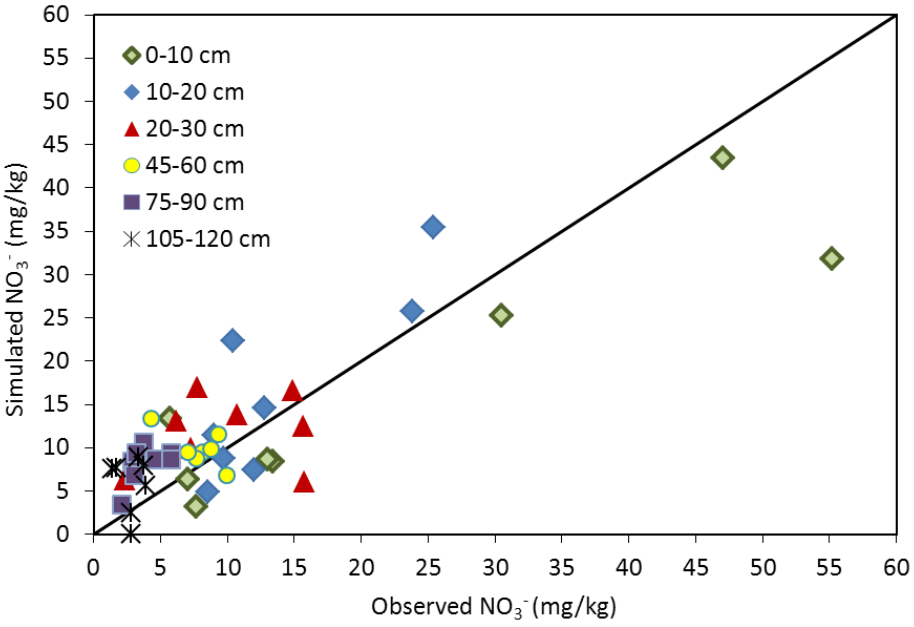

Figure 6-9: Scatter plot of observed versus simulated NO_3^- -N at different depths with 5000 gal/acre manure application

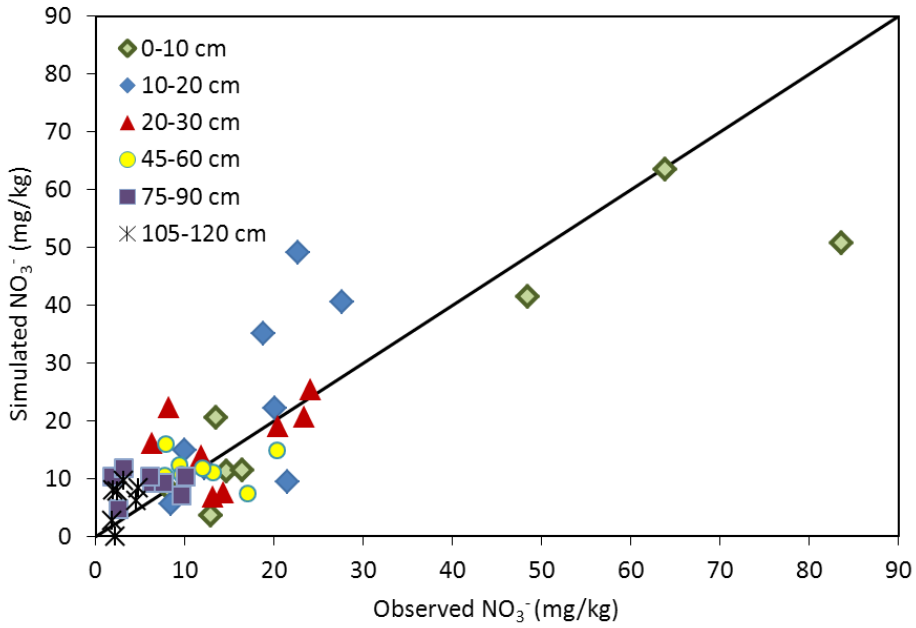

Figure 6-10: Scatter plot of observed versus simulated NO_3^- -N at different depths with 7500 gal/acre manure application

Table 6-3: Statistical evaluation of SABAE-HWS model for simulating NO_3^- -N at different depths with three rates of manure application

Depth(cm)	M2500			M5000			M7500		
	R	RMSE	CRM	R	RMSE	CRM	R	RMSE	CRM
0-10	0.47	10.88	0.29	0.89	8.87	0.13	0.92	12.06	0.14
10-20	0.24	5.16	0.03	0.78	6.87	-0.24	0.67	13.67	-0.41
20-30	0.01	4.12	0.11	0.56	3.62	-0.12	0.16	8.31	-0.13
45-60	-0.21	4.60	-0.20	-0.02	3.74	-0.27	-0.09	5.12	0.02
75-90	0.05	6.14	-1.87	0.57	4.70	-1.06	0.13	5.18	-0.51
105-120	0.38	4.66	-2.07	0.48	4.14	-1.39	0.42	4.27	-1.33

The results of SABAE-HWS nitrate-nitrogen were also compared with the results of SHAW and observed nitrate-nitrogen for the growing season of 2003. Figure 6-11 to Figure 6-13 show the distribution of simulated and observed NO_3^- -N within the soil profile at the 2500, 5000, and 7500 gal/acre manure application, respectively.

The results clearly demonstrated that there is a strong agreement between simulated SABAE-HWS and observed NO_3^- -N in July and August at the presence of nitrogen uptake by roots. It is noted that the largest uptake of nitrogen, observed in Carberry site, occurs in July (mid–season) and then it decreased by time. However, the result of SHAW is not satisfactory. The results were also confirmed by a statistic evaluation between measured and simulated NO_3^- -N (Table 6-4). Although high correlation was obtained for SHAW, the large RMSE values show that the accuracy of the model in simulating nitrate-nitrogen was poor. The negative values of CRM also indicated that observed nitrate are overestimated by SHAW simulations. It seems the major drawback of the SHAW model is that no crop growth model can be simulated for N uptake by roots. Therefore, the model is not able to simulate accurately nitrate during the growing seasons. At the end of the season when there is not root in the soil profile, SHAW simulations are improved significantly as RMSE decreased by half for all manure applications. Although it was not found a good correlation (-0.4) for SABAE-HWS simulations in October 2003 at 2500 gal/acre, the better match between simulated and observed NO_3^- -N was found in October 2003 at 5000 and 7500 gal/acre manure application. Correlation value of 0.9 and RMSE value of 4.6 confirmed the better performance of SABAE-HWS for simulating NO_3^- -N at the end of season. By May 2004, SHAW nitrate concentrations have considerably declined through the soil profile. Graphical and statistical comparisons show that the

SHAW model performed better than SABAE-HWS in simulating nitrate nitrogen at depth of 90-120cm. In general, the better correlation (0.8) was found for SHAW simulations comparing to SABAE-HWS (0.4) in May 2004.

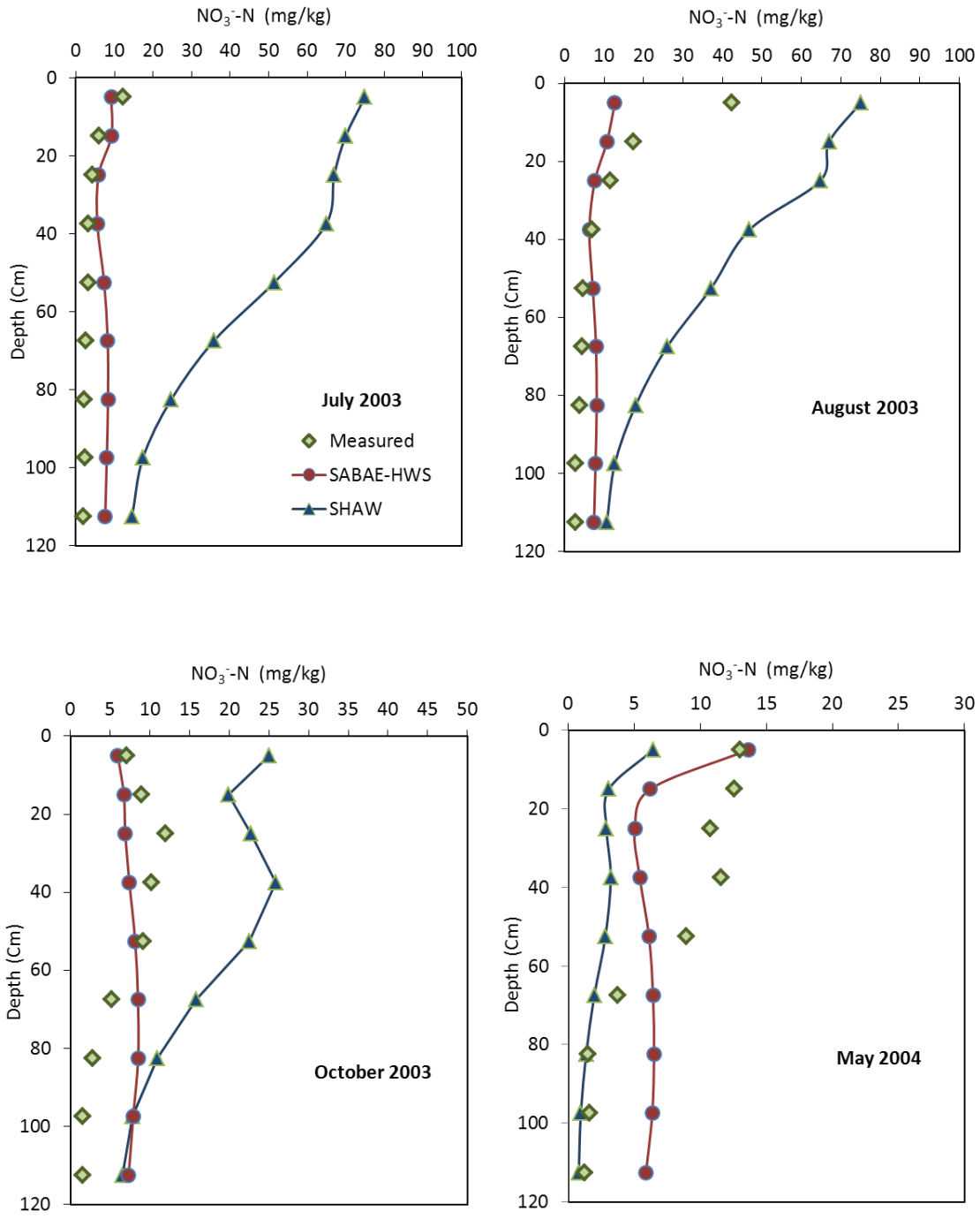

Figure 6-11: Observed and simulated soil ammonium nitrogen by SABAE-HWS and SHAW model in 0-120 cm depth at the 2500 gal/acre manure application during the growing season (July and August) and the end of growing season (October and May) of 2003

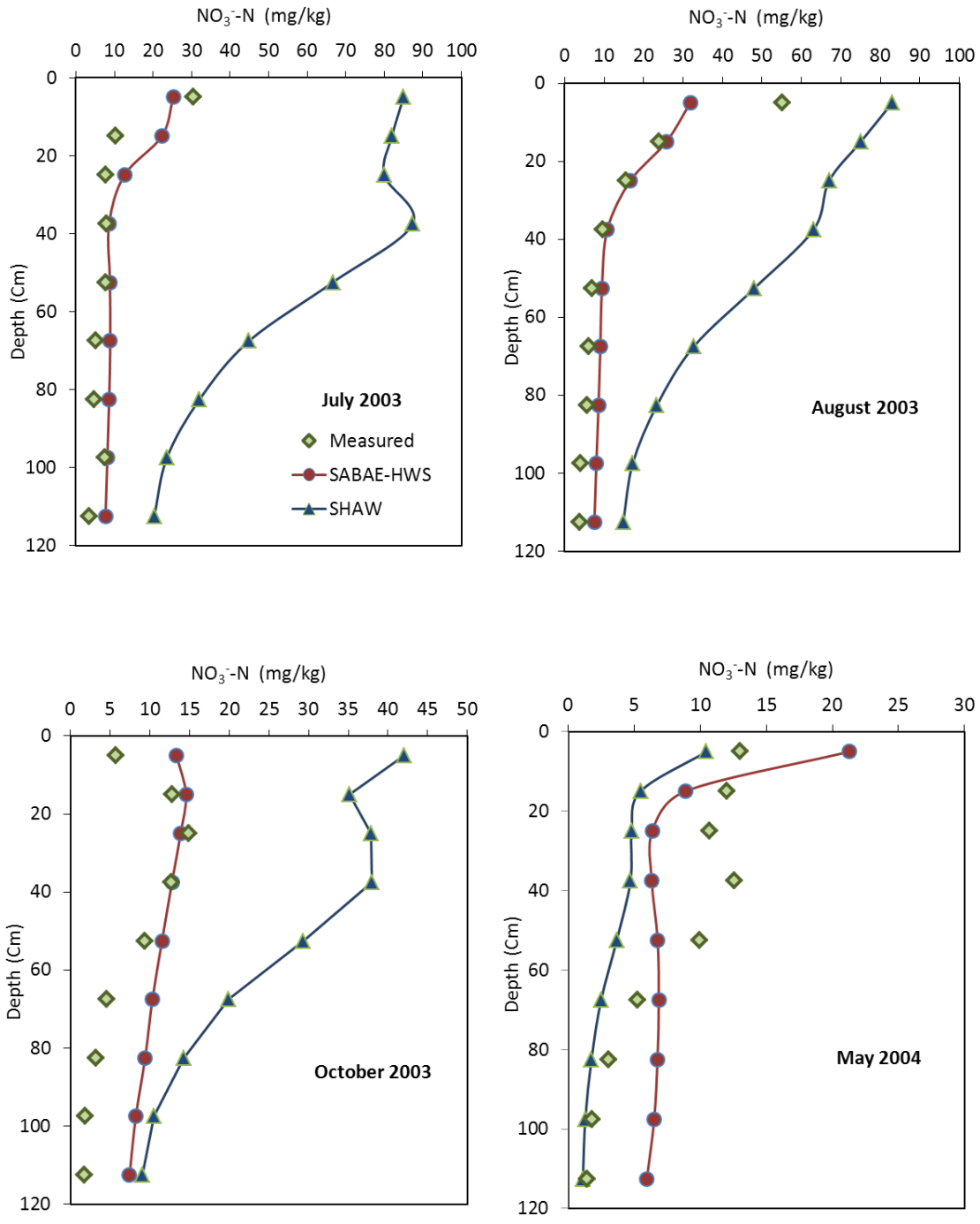

Figure 6-12: Observed and simulated soil ammonium nitrogen by SABAE-HWS and SHAW model in 0-120 cm depth at the 5000 gal/acre manure application during the growing season (July and August) and the end of growing season (October and May) of 2003

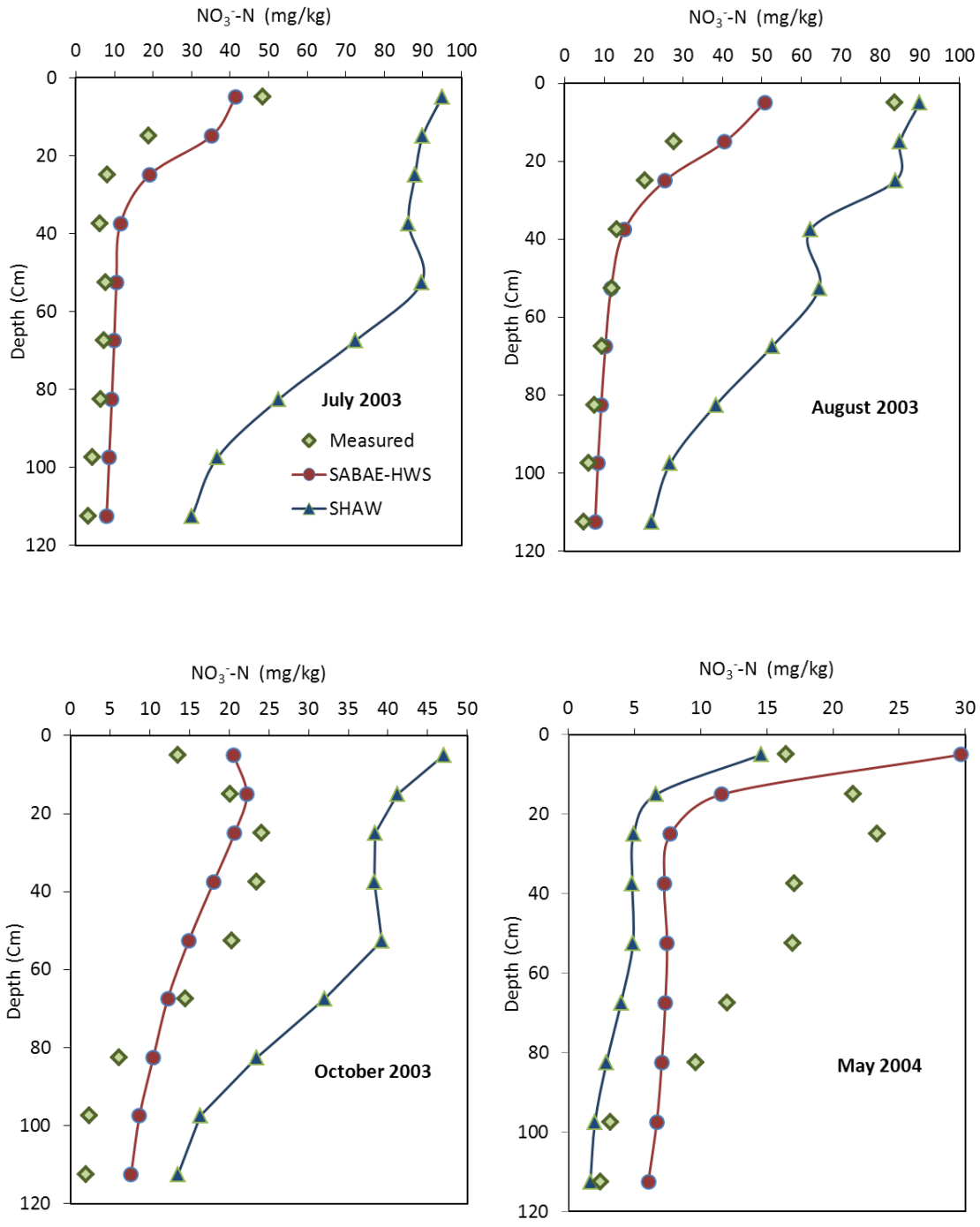

Figure 6-13: Observed and simulated soil ammonium nitrogen by SABAE-HWS and SHAW model in 0-120 cm depth at the 7500 gal/acre manure application during the growing season (July and August) and the end of growing season (October and May) of 2003

Table 6-4: Statistical evaluation of SABAE-HWS and SHAW model for simulating NO_3^--N in 120 cm depth with three rates of manure application during the growing season (July and August) and the end of growing season (October and May) of 2003

Time	Manure Application	SABAE-HWS			SHAW		
		R	RMSE	CRM	R	RMSE	CRM
July 03	M2500	0.42	4.45	0.82	0.69	47.27	-10.11
August 03		0.89	10.66	0.21	0.78	33.06	-2.45
October 03		-0.40	4.19	-0.15	0.91	11.65	-3.95
May 04		0.31	4.66	0.05	0.83	5.8	-0.84
July 03	M5000	0.82	5.21	-0.30	0.53	53.74	-5.15
August 03		0.94	8.20	0.02	0.76	36.34	-3.67
October 03		0.92	4.69	-0.52	0.81	20.74	-7.09
May 04		0.46	4.04	0.04	0.83	4.65	-1.77
July 03	M7500	0.89	7.67	-0.39	0.52	62.30	-4.81
August 03		0.89	12.00	0.03	0.68	42.22	-4.96
October 03		0.83	4.93	-0.06	0.84	19.09	-8.22
May 04		0.38	8.31	0.38	0.51	10.39	-2.8

6.5 Model Application

Manure is one of the most commonly available sources of nutrients that improves the physical condition and the organic matter content of soil. Soil physical properties such as infiltration, aggregation, and bulk density may be influenced by manure application. It is generally accepted that manure application affects runoff and soil erosion and soil loss (Eghball and Power, 1994). In addition, the amount of applied manure has a strong effect on the measured soil ammonium and soil nitrate. Some regression relationships were developed to predict the long term reduction in runoff and soil loss caused by various manure application rates. These relationships are only applicable to a specified studied area (Gilley and Risse, 2000). Note that the rate of nitrate and nitrogen added by manure into the soil is the main concern of environmental investigators. Beckwith et al. (1998) found that one of the main causes of nitrate leaching is the over-fertilization of crops with N by manure. Nitrogen originated from manure is in a readily mineralizable form. It was also observed that the crop cover had an important role in winter to reduce the N leaching loss.

Spring runoff depends on snow melt and rain fall. Therefore, since there is a high risk of N losses by applying liquid manure under these conditions, winter manure spreading is avoided by majority of farmers. It is believed that manure should only be applied in winter if there is lack of storage capacity or inflexibility in spreading manure due to limited storage. Although regulators do not recommend winter manure application, winter manure spreading is widely practiced for economical and practical reasons such as limited manure storage structures, availability of time for manure spreading, and reduced soil

compaction (Srinivasan et al., 2006). The timing and rate of manure spreading play a key role to optimize manure application in agriculture fields. Lewis and Makarewicz (2009) reported that ground slope, application of manure over snow and during the snow fall, warm air, and soil temperatures have significant effects on the loss of nitrogen. It was also observed that winter manure application caused large losses of nitrogen in runoff. Note that the focus of this thesis is on spring manure. Two factors should be taken into account when manure is applied on the soil; hydrological process and nutrient transport from previously applied manure application. The hydrological process depends on infiltration and runoff. Since freeze and thaw activities disrupt soil aggregates, infiltration decreases. The infiltration rate in frozen soil is very slow. Therefore, any amount of solute moves slowly to the root zone. When frozen soil leads to runoff of snow melt, unfrozen soil allows infiltration depending on soil moisture conditions. Most studies show the excessive nutrient losses when manure is applied during thaw periods. In addition, death and lysis of organisms helps to release nitrogen during the thawing process. Consequently, inorganic N is carried by snowmelt and runoff to surface water. Increasing rate of infiltration may also leach excess nitrogen to groundwater. However, mineral N losses by leaching were completely different among manure treatments. Compared to fall manure application, winter manure application had a minor effect on mineral leaching (Kongoli and Bland, 2002).

The effects of different rates of spring hog manure applications on the distribution of soil ammonium and nitrate are illustrated in Figure 6-14 to Figure 6-17. In general, applying a higher rate of manure resulted in an increase in nitrate concentration in the soil profile in both wet and dry seasons. As apparent from Figure 6-14, the total amount of simulated NO_3^--N within the soil (0-120cm) was higher than the observed data in a dry grow-

ing season such as 2003. However, this discrepancy almost disappeared by October 2003 and can be mainly described by the absence of dentrification process in this study. Although denitrification in spring caused a loss of nitrate-nitrogen at the field site, it was ignored in this study because of its minor effects on the overall nitrogen budget.

The results were considerably different in the wet season of 2004. Figure 6-16 shows that there is no difference between simulated and observed cumulative nitrate concentration at 2500 and 5000 gal/acre within the soil profile. However, nitrate leaching occurred at 7500 gal/acre and it caused an increase in observed soil nitrate concentration. Similar results were found in October 2004 (Figure 6-17). Although the observed data clearly confirms that the amount of nitrate leaching is influenced by the rate of manure application, the simulations did not show any changes in soil nitrate concentrations at 7500 gal/acre. Residual nitrate from previous applications and downward movement of nitrate-nitrogen are the main reasons for nitrate leaching at the Carberry site. A reasonable agreement found between the observed and simulated soil moisture confirms that movement of nitrate-N by water flux was considered properly in the simulations. In addition, compared to 2003 (dry season), the wet growing season of 2004 showed greater water flux in the simulations. This also confirms that inadequate representation of hydrological processes is not the reason for the absence of soil NO_3^--N in the simulations. Since the first manure application (May 2002) had not been taken into account for the simulations; the residual nitrate is not enough to simulate nitrate concentrations through the soil profile. It should be noted that manure applied in 2002 remained at the top soils and slowly moved to the depth because of very low rate of water flux. To make sure that manure treatments have a critical role in increasing the soil nitrate concentrations, the rate of ini-

tial nitrate concentration was increased at the beginning of simulations. Not surprisingly, a considerable amount of soil nitrate was found at the bottom of the soil profile. Also, increasing the rate of manure application in 2003 resulted in the higher concentrations of nitrate at the end of growing season 2004.

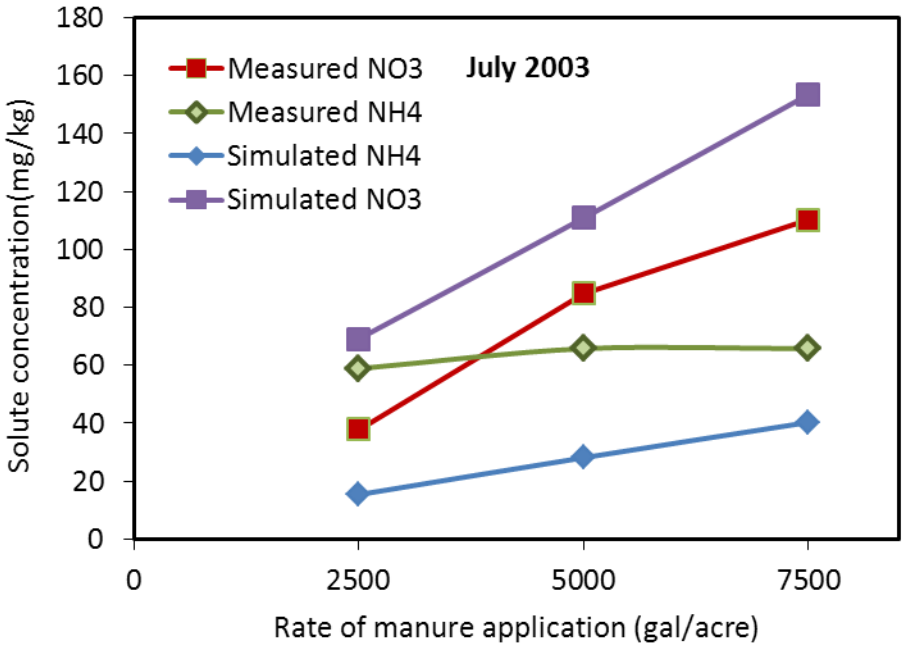

Figure 6-14: Cumulative soil ammonium and nitrate nitrogen in 120 cm depth during the dry growing season of 2003 (July)

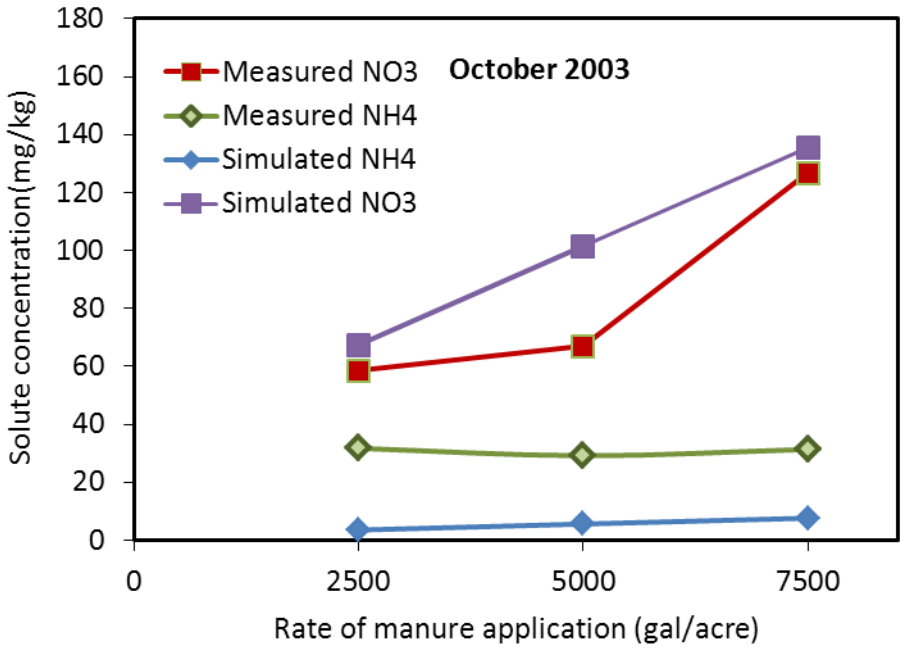

Figure 6-15: Cumulative soil ammonium and nitrate nitrogen in 120 cm depth at the end of dry growing season of 2003 (October)

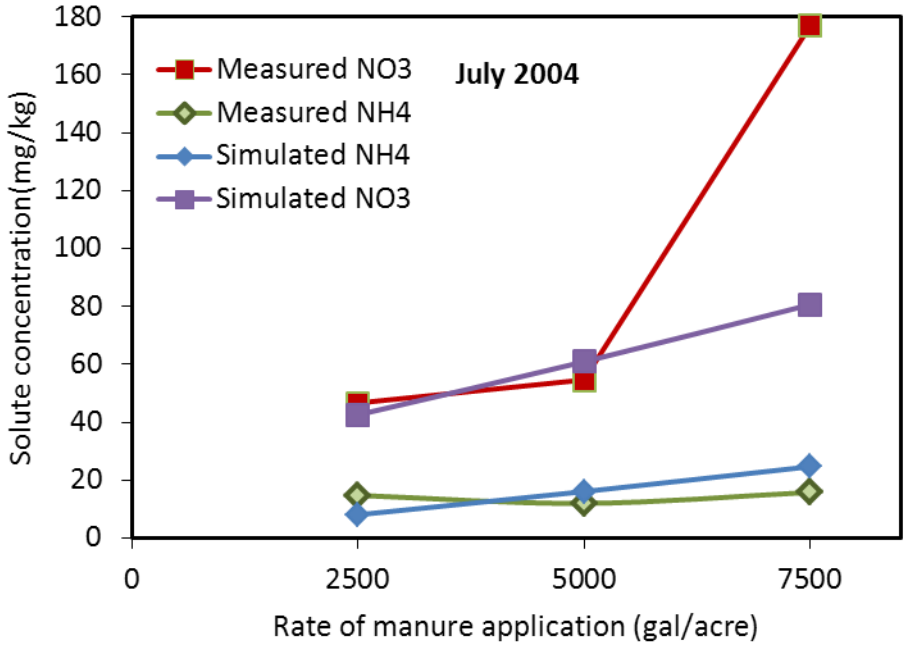

Figure 6-16: Cumulative soil ammonium and nitrate nitrogen in 120 cm depth during the wet growing season of 2004 (July)

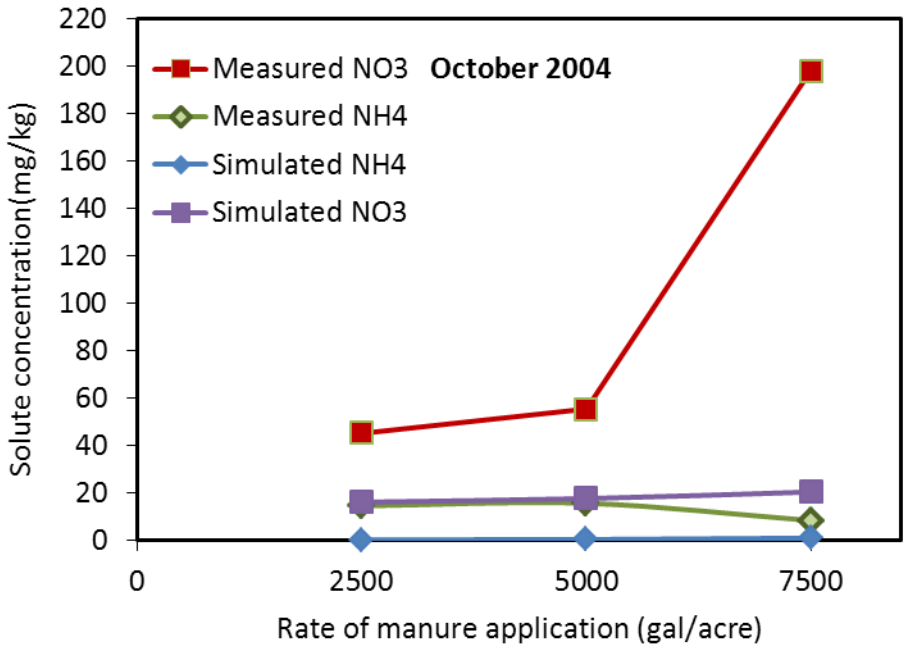

Figure 6-17: Cumulative soil ammonium and nitrate nitrogen in 120 cm depth at the end of wet growing season of 2004 (October)

6.6 Long Term Climate Record

Since the weather conditions of two cities (Saskatoon and Carberry) are approximately similar, the 10 year atmospheric data file from OJP site (Saskatchewan) was applied to the Carberry site (Manitoba). The objective here was carry out generic simulations over a long climate record to investigate the effects of 2500 and 7500 (gal/acre) liquid hog manure on nitrate leaching through the soil profile. To my knowledge this is one of the longest simulations of manure application over an agricultural area. It will be shown that climatic records and prediction of nitrogen leaching are necessary for analysis of BMPs. Studying the precipitation records over the 10 years study period indicated that year 2004, 2005 and 2006 are considered as the wet years compared to the first 6 years of study (Figure 6-18). The annual precipitations in the wet years are 737, 633, and 626 mm, respectively, which are approximately 200 mm higher than the other years of study. It is assumed that manure is applied on the soil on May 15th of each year. Seeding and harvesting dates are June 1st and September 15th of each year, respectively. Soil hydraulic characteristics and soil dispersive parameters remained the same as what obtained from the Carberry simulations (Section 5.3).

Figure 6-19 presents the distribution of soil nitrate-nitrogen at three depths of 20, 60, and 100 cm with manure application of 2500 gal/acre. The results clearly showed that no nitrate leaching occurred with manure application rate of 2500 gal/acre. The peak points (10 mg/kg) at top soils (depth 20 cm) are due to application of manure. At a depth of 100 cm, although the results showed that soil NO_3^--N concentrations were a little higher than the other years (less than 5 mg/kg) during the wet years; soil nitrate did not exceed 5 mg/kg. The high nitrate concentration at the soil surface was subsequently taken up by

crop root and no excessive nitrate was found within the soil profile. This reduces the risk of nitrate leaching. In fact, there was no significant difference between nitrate concentrations during the study period at the depth 100 cm.

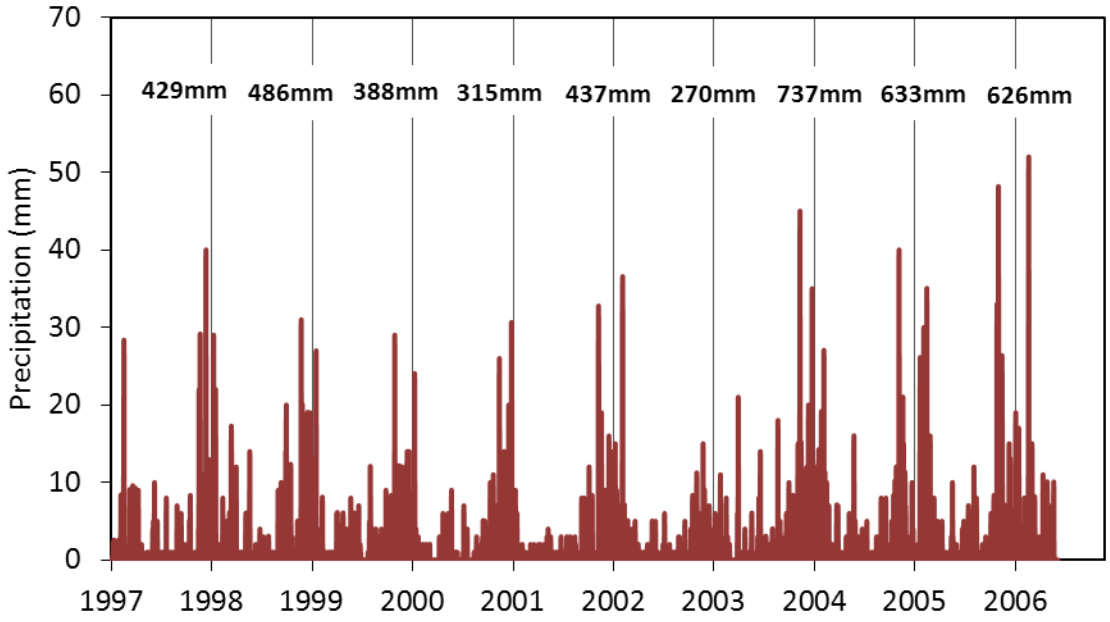

Figure 6-18: Daily precipitation and annual precipitation (top values) in 10 years of study period at Old Jack Pine (OJP), Saskatchewan

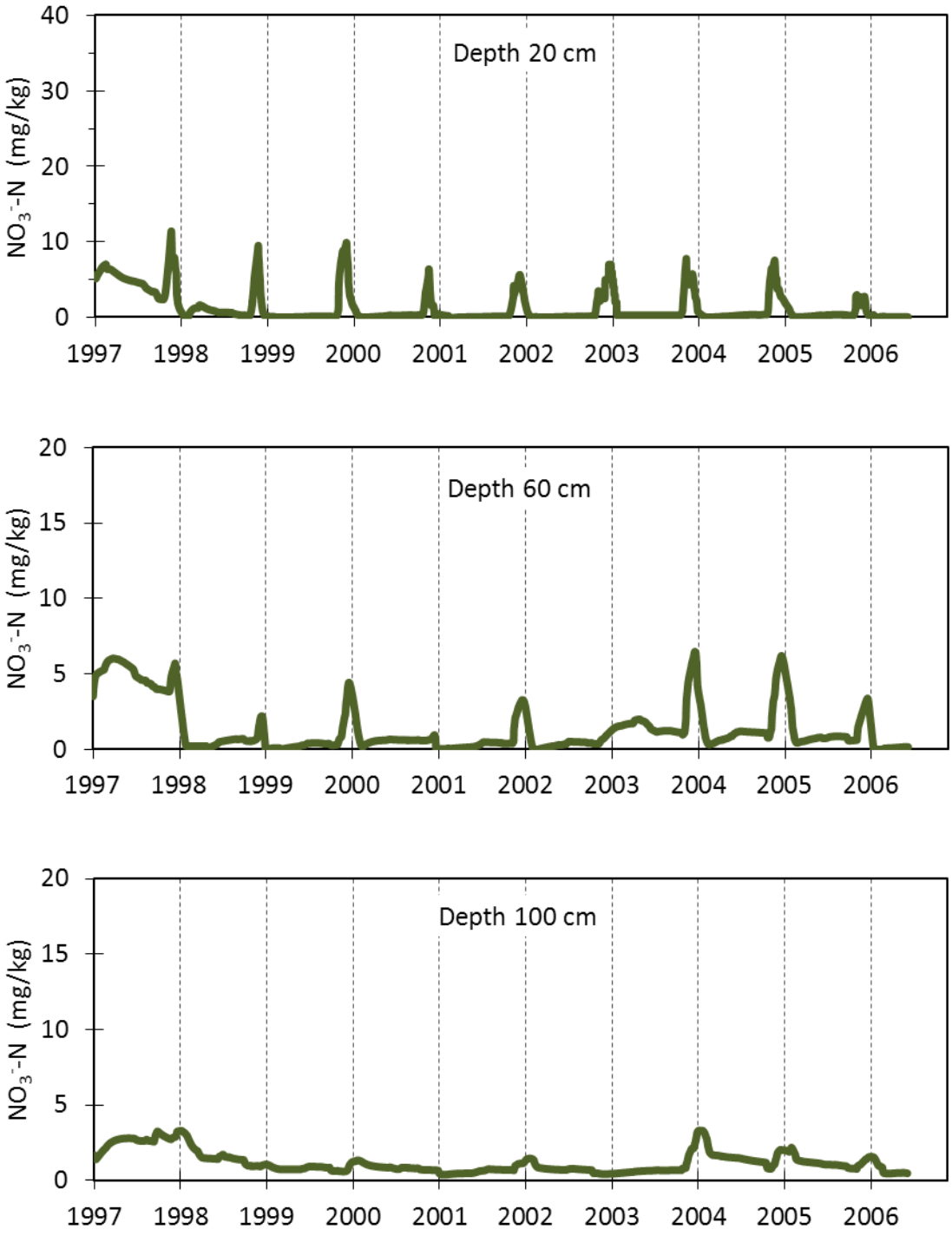

Figure 6-19: Soil nitrate-nitrogen distribution over a 10 year climate record at the depths of 20, 60, and 100cm with 2500 gal/acre manure application

The distribution of soil NO_3^--N concentrations at the depths of 20, 60, and 100 cm with manure application 7500 gal/acre are shown in Figure 6-20. Compared to the results of 2500 gal/acre, the peak points are considerably higher due to the three times higher rate of manure application at the soil surface. It is clear that the high surface nitrate-nitrogen concentration declined with depth. Most of the nitrate concentration was taken up by crop root and the downward movement of nitrate (depth 60cm). However, applying additional manure leads to the accumulation of nitrate in the soil profile. The residual NO_3^--N can be further moved to the deeper layers by downward movement of water flux as a result of high precipitation. The deepest penetration of nitrate occurred at 100 cm depth with the 7500 gal/acre, especially during wet growing seasons. The peak points represent the movement of accumulated nitrate from the previous manure applications due to the high amount of precipitation in the wet years. It is also observed that the greatest potential for nitrate leaching was in the spring when the snow had been melted. Surprisingly, less than 10 mg/kg soil nitrate concentration was found during the driest years of study period (year 2001, 2002, and 2003).

The results of long term climate records confirmed the results obtained from the different rates of manure application at the Carberry site (section 6.5). Comparing ure 6-19 and Figure 6-20 clearly demonstrated that the amount of soil nitrate concentration at the root zone depth was strongly influenced by the rate of manure application, number of applications, and atmospheric conditions. As shown, there is no risk of nitrate contamination in the soil profile with 2500 gal/acre manure application even during the wet growing seasons. However, the higher rate of manure application (7500 gal/acre) led

to increase the rate of soil nitrate at the deeper layers in the wet seasons such as 2004, 2005, and 2006.

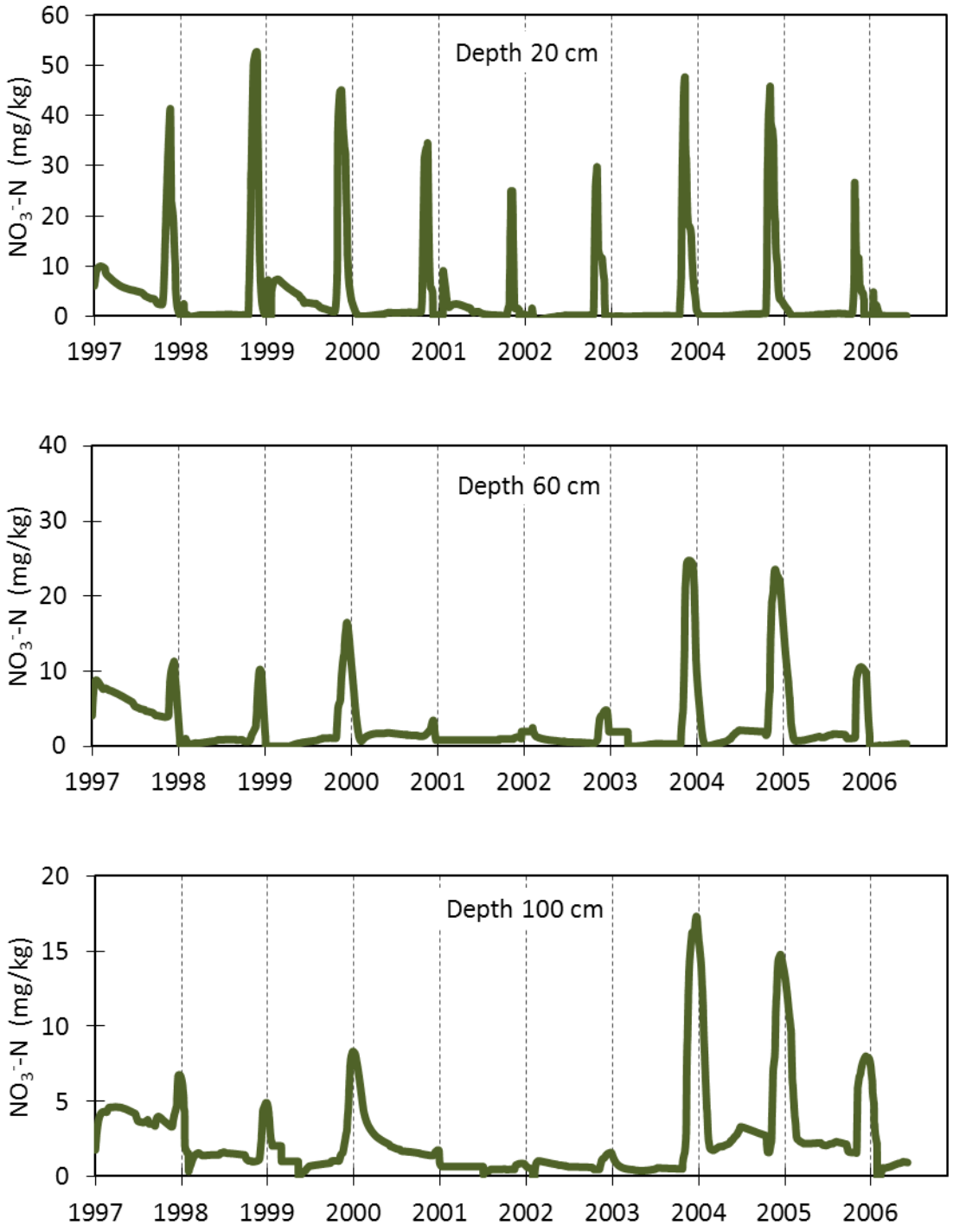

Figure 6-20: Soil nitrate-nitrogen distribution in a 10year climate record at the depths of 20, 60, and 100cm with 7500 gal/acre manure application

Over the last several years, manure application to farm fields and adapting Best Management Practices (BMPs) for manure application have been studied by investigators.

Note that manure is a good source of nitrogen, if applied in the right amount correctly. Therefore, in following best management practices (BMPs), farmers should always exert extreme caution in applying manure. Protecting water quality and environment should be top priority of any manure application. With the increase in cultivation associated with cropping, there has always been an increase in the release of nitrogen from soil organic nitrogen. Carberry is widely used for irrigated potato production. Thus, care must be taken to select the proper rate of manure application depending on the weather conditions, in order to minimize the risk of nitrate movement to the underlying groundwater. The results of this study demonstrated that the proper rate of manure application (2500 gal/acre) could reduce nitrate leaching at the Carbbery while applying additional manure (7500 gal/acre) increased the risk of nitrate leaching, especially during the wet growing seasons.

6.7 Summary

Effective manure management requires applying the correct rate of manure in each season. It is important to investigate the processes that convert manure to nitrate. Nitrogen in manure is converted to nitrate through mineralization and nitrification processes. Nitrate leaching generally occurs if manure is applied at excessive rates. Appropriate rate of manure application is usually determined based on the crop nitrogen demand. Since it is highly recommended to apply manure close to the time of crop demand, spring is the best time to apply manure in Manitoba (Burton and Ryan, 2000). Results of this study clearly

showed that the decision to apply manure should be based on the manure application rate, the number of applications, and weather conditions. Basically, applying manure at higher rates than crop uptake (over-application) can lead to transport of nutrients into the groundwater through nitrate leaching. However, this may not always be the case as illustrated in section 6.5. For example, although 7500 gal/acre manure had been applied for the observations and simulations in 2004, observations only showed nitrate leaching at the end of study period (as a result of three consecutive years of M7500 manure application). It is noticed that if manure is applied to the same field each year, the rate of nitrogen mineralization will exceed the plants available nitrogen. This process resulted in the accumulation of nitrate in the soil. Ignoring the first application in 2002 did not lead to increase soil nitrate concentrations in the simulations unless the rate of manure application or available soil nitrate and ammonium nitrogen is increased in 2003 and 2004. In conclusion, the risk of nitrate contamination of the field as a consequence of excessive rate of manure application is increased due to the residual nitrate remaining in the soil. Thus, identifying the accumulated nitrate in the soil from the earlier applications is important to evaluate the proper rate of manure application to farm fields each year. These results were also confirmed by the long term climate record simulations. The results strongly indicated that it is necessary to consider the rate of application, number of applications, and the atmospheric condition in adopting manure beneficial management practice.

Chapter 7

Conclusions and Future Directions

7.1 Conclusions

The usefulness of the land surface scheme SABAE-HWS in simulating soil moisture, soil temperature, snow depth, soil ammonium nitrogen, and soil nitrate nitrogen was investigated at two sites located in the Canadian Prairies.

SABAE–HW first was field tested using 10 years of data from Old Jack Pine site at the BOREAS/BERMS field station in central Saskatchewan, Canada. The field site consists primarily of sand with a high value of saturated hydraulic conductivity. The model was verified against measured data and compared with another well-known code, SHAW. Snow depth, soil temperature, and soil moisture were simulated and verified in this study with respect to two boundary conditions at the bottom of soil profile: a water table boundary condition and unit gradient boundary condition. Comparing the results of

simulations and observed data showed a satisfactory agreement in terms of snow depth and soil temperature. However, there were some discrepancies in terms of soil temperature in winter due to the insulating effects of snow and residue cover on soil surface temperature. A general agreement was not obtained in terms of unfrozen soil moisture results especially in lower depths mainly because of the underestimation of liquid water in the soil in winter. However, there were similarities in observed and simulated soil moisture trends, especially in winter. Although a unit gradient boundary condition does not influence soil moisture, the plots showed that unit gradient boundary resulted in increased bias towards an overestimation of the soil temperature. Both SABAE-HW and SHAW showed larger errors in measuring RMSE and AE values with respect to the unit gradient boundary condition at the bottom of soil profile. However, the coefficients of correlation did not change for either SHAW or SABAE-HW. Thus, it is believed that a safer and more accurate approach is to adopt a first type boundary (i.e. water table) condition at the bottom of the flow domain. This has implications for climate and weather modeling in general. The result of this field testing demonstrated the potential of SABAE-HW as a Canadian land surface scheme for simulating snow depth, snow temperature, and soil moisture with high accuracy. Further field testing of the model should be conducted later to further validate its application to simulate total and unfrozen soil moisture.

Moreover, SABAE-HW considers the effects of soil freezing and thawing on soil water dynamics. An accurate simulation of solute transport requires the accurate definition of soil water content and soil temperature. Since it was found a good agreement between simulated (snow depths, soil temperatures and soil moistures) and observed data in winter time, the idea of coupling SABAE-HW with nitrogen transport model was implemented,

in order to simulate nitrate and ammonium concentration in the presence of freezing and thawing. To evaluate the performance of the numerical approach (finite volume), solute transport code was compared to the analytical solution in uniform flow. A strong agreement was found between numerical and analytical solutions.

SABAE-HWS is the coupled solute transport and nitrogen transformation model with enhanced water balance Land Surface Scheme (LSS). The model was calibrated and verified using three years data (2002-2004) from Carberry site located in central Canada, Manitoba. The three rates of hog manure application, 2500, 5000, and 7500 gal/acre, were applied to the field site to study the distribution of soil ammonium and soil nitrate within the 120 cm of soil profile. A high portion of hog manure is ammonium nitrogen which is the inorganic form of nitrogen. NH_4^+-N is then converted into NO_3^--N through the nitrification of ammonium. It was found that the amount of soil ammonium decreased rapidly after manure application as ammonium was quickly adsorbed to the soil or taken up by the crop root. Comparisons between simulated and observed soil ammonium indicated that there is a reasonable agreement between simulations and observations for different rates of manure application. Since nitrogen transformation processes were modeled using a single pool soil organic matter, nitrogen mineralization did not change during the study period due to the lack of soil ammonium nitrogen in the soil profile.

In general, the agreement between simulated and observed soil NO_3^--N was quite satisfactory, especially for the dry growing season of 2003. However, the largest differences occurred in the wet growing season of 2004 with 7500 gal/acre manure application. Observed data showed that the combination of the residual NO_3^--N remaining in the soil and 7500 gal/acre manure application increased the risk of soil nitrate concentration at the

end of study period. However, soil nitrate concentration did not exceed 5 mg/kg by SABAE-HWS in deeper soil layers during the simulation period due to the lack of soil nitrate. Also, comparing the results of soil nitrate before and after freezing and thawing clearly showed that the rate of nitrification and soil NO_3^- -N increased significantly during snow melting period.

In addition, the results of long term climate records strongly indicated that there are several parameters that should be taken into account in the Best Management Practices (BMPs). The rate of manure application, the number of applications, and atmospheric conditions should be all investigated to minimize the risk of soil nitrate concentration and also nitrate leaching into groundwater.

A proper crop growth model, discussed in Chapter 4, is also important to accurately simulate the amount of soil NH_4^+-N and NO_3^- -N. It has been found that SHAW model predictions are not reasonable comparable with the observations and SABAE-HWS model because of missing the crop growth model.

7.2 Suggestions and Future Work

This thesis focuses on the soil NH_4^+-N and NO_3^- -N originating from manure. SABAE-HWS can be used to investigate the effects of the other fertilizer application on soil layers in future.

A single pool nitrogen transformation was considered by the SABAE-HWS model. Adding more pools of organic nitrogen with different kinetic rate coefficients helps regulate the transformation and storage of nutrients in the soil. In addition, it makes the model more applicable to evaluate the rate of mineralization and nitrification at the presence of

freezing and thawing. Running the code with various experiment conditions improves the results and makes the model more reliable to apply to a broad range of soil and atmospheric conditions.

The model can be further used to investigate the effects of winter manure application on nitrate leaching. However, this needs to collect more experimental data sets including soil ammonium and nitrate in winter. Soil sites with low permeability and high moisture play an important role to evaluate the denitrification process. Thus, applying the model to fine grained soil site is necessary to consider the denitrification and identify the denitrification coefficient as well. SABAE-HWS is also useful to understand the interaction between the transformation and the nitrogen transport in the field. It may use to identify the proper values of mineralization and nitrification coefficients and provide a significant guidance for laboratory and field experiments.

Bibiliography

Ackerer, Ph., Younes, A., and Mose, R. "Modeling variable density flow and solute transport in porous medium: 1. Numerical model and verification." *Transport in Porous Media* 35, no. 3 (1999): 345-373.

Ahuja, L.R., Rojas, K.W., Hanson, J.D. , Shaffer, M.J., and Ma, L. *Root Zone Water Quality Model: Modeling management effects on water quality and crop production.* Water Resources Publications, Highlands Ranch, CO, 2000.

Akinremi, O. O. "Measurement and simulation of nitrate, phosphorus and carbon leaching from manure and fertilizer." Department of soil scienece, Faculty of agricultural and food sciences, University of Manitoba, Winnipeg, Manitoba, Canada, 2005.

Al-Darby, A., and Abdel-Nasser, G. "Nitrate leaching through unsaturated soil columns: Comparison between numerical and analytical solutions." *Journal of Applied Sciences* 6, no. 4 (2006): 735-743.

Alvarez-Benedi, J., and Munoz-Carpena, R. *Soil-Water-Solute Progress Characterization: An Integrated Approach.* Florida, USA: CRC Press, 2005.

Baca, R.G., Chung, J.N., and Mulla, D.J. "Mixed transform finite element method for solving the non-linear equation for flow in variably saturated porous media." *International Journal for Numerical Methods in Fluids* 24 (1997): 441-455.

Balland, V., Bhatti, J., Errington, R., Castonguay, M., and Arp, P. A. "Modeling snowpack and soil temperature and moisture conditions in a jack pine, black spruce and aspen forest stand in central Saskatchewan." *Canadian Journal of soil Science* 86, no. 2 (2006): 203-217.

Bartlett, P. A., MacKay, M. D., and Verseghy, D. L. "Modified snow algorithms in the Canadian land surface scheme: Model runs and sensitivity analysis at three boreal forest stands." *Atmosphere-Ocean* 44 (2006): 207–222.

Beckwith, C. P., Cooper, J., Smith, K. A., and Shepherd, M. A. "Nitrate leaching loss following application of organic manures to sandy soils in arable cropping. I. Effects of application time, manure type, over winter crop cover and nitrification inhibition." *Soil Use and Management* 14 (1998): 123-130.

Berghuijs-vanDijk, J. T., P. E. Riitema, and C. W. J. Roest. *ANIMO Agricultural Nitrogen Model.* Wageningen, The Netherlands: Institue for Land and Water Management Reserach, 1985.

Bernier, P.Y., Bartlett, P., Black, T.A., Barr, A., Kljun, N., and McCaughey, J.H. "Drough constraints on transpiration and canopy condunce in mature aspen and jack pine stands." *Agricultural and Forest Meteorology* 140 (2006): 64-78.

Boutin, R., and Robitaille, G. "Increased soil nitrate losses under mature sugar maple trees affected by experimentally induced deep frost." *Canadian Journal of Forest Research* 25 (1995): 588–602.

Brooks, P. D., Williams, M. W., and Schmidt, S. K. "Inorganic nitrogen and microbial biomass dynamics before and during spring snowmelt." *Biogeochemistry* 43 (1998): 1-15.

Bruijn, A. M. G., Butterbach-bahl, K., Blagodatsky, S., and Grote, R. "Model evaluation of different mechanisms driving freeze-thaw N2O emissions." *Agriculture, Ecosystems and Environment* 133, no. 3 (2009): 196-207.

Burton, D. L., and Ryan, M. C. *Environmental fate of nitrate in the Assiniboine Delta Aquifer.* Manitoba Horticulture Productivity Enhancement Centre Inc., 2000.

Buss, S.R., Herbert, A. W., Thornton, S. F., and Smith, J. W. N. "A review of ammonium attenuation in soil and groundwater." *Quarterly Journal of Engineering Geology & Hydrogeology* 37, no. 4 (2004): 347-359.

Carlier, E. "Analytical solutions of the advection-dispersion equation for transient groundwater flow." *Hydrological Processes* 22, no. 17 (2008): 3500-3506.

Chowdary, V.M., Rao, N.H., and Sarma, P.B.S. "A coupled soil water and nitrogen balance model for flooded rice fields in India. Agriculture." *Ecosystems and Environment* 103, no. 3 (2004): 425-441.

Clapp, R. B., and Hornberger, G. M. "Empirical equations for some soil hydraulic properties." *Water Resources Research* 14, no. 4 (1978): 601-604.

Darban, A.K., Yong, R.N., and Ravaj, S. "Coupled chemical speciation-solute transport model for prediction of solute transport in clay buffers." *Applied Clay Science*, 2008: 1-6.

Deelstra, J., et al. "Runoff and nutrient losses during winter periods in cold climates—requirements to nutrient simulation models." *Journal of Environmental Monitoring*, 2009: 602-609.

Diersch, H. J., and Kolditz, O. "Coupled groundwater flow and transport: 2. Thermoline and 3D convection systems." *Advance Water Resource* 21 (1998): 401-425.

Djurhuus, J., Hansen, S., Schelde, K., and Jacobsen, O. H. "Modelling mean nitrate leaching from spatially variable fields using effective hydraulic parameters." *Geoderma* 87, no. 3-4 (1999): 261-279.

Eghball, B., and Power, J. F. "Beef cattle feedlot manure management." *Journal of Soil and Water Conservation* 49, no. 2 (1994): 113-122.

Enn, J. M. *The effect of liquid hog manure and commercial fertilzer on nutrient movement in a sandy soil.* University of Manitoba: MSc. dissertation, Winnipeg, Manitoba, Canada, 2004.

Fang, C., and Moncrieff, J. "A model for soil CO2 production and transport 1: Model development." *Agricultural and forest meteorology* 95 (1999): 236– 255.

Fang, C., and Moncrieff, J. "A model for soil CO2 production and transport 1: Model development." *Agricultural and forest meteorology* 49, no. 2 (1999): 236-255.

Feng, X., Kirchner, J.W., Renshaw, C.E., Osterhuber, R.S., Klaue, B., and Taylor, S. "A study of solute transport mechanisms using rare earth element tracers and artificial rainstorms on snow." *Water Resources Research* 37, no. 5 (2001): 1425–1435.

Fitzhugh, R. D., Driscoll, C. T, Groffman, P. M., Tierney, G. L., Fahey, T. J., and Hardy J. P. "Effects of soil freezing disturbance on soil solution nitrogen, phosphorus, and carbon chemistry in a northern hardwood ecosystem." *Biogeochemistry* 56 (2001): 215-238.

Flerchinger, G. N. *The simultaneous Heat and Water (SHAW) Model: Technical Documentation.* Boise, Idaho: USDA Agricultural Research Service, 2000.

Flerchinger, G. N., Aiken, R. M. , Rojas, K. W. , and Ahuja, L. R. "Development of the Root Zone Water Quality Model (RZWQM) for over-winter conditions." *Trans. ASAE* 43 (2000): 59-68.

Flerchinger, G. N., and Saxton, K. E. "Simultaneous heat and water model of a freezing snow-residue-soil system I. Theory and development." *Transactions of the ASAE* 32, no. 2 (1989): 565-571.

Flerchinger, G. N., Baker, J. M., and Spaans, E. J. A. "A test of the radiative energy balance of the SHAWmodel for snowcover." *Hydrol. Proc.* 10, no. 10 (1996): 1359-1367.

Flerchinger, G.N. "Sensitivity of soil freezing simulated by the SHAW model." *Transactions of the American Society of Agricultural Engineers* 34, no. 6 (1991): 2381-2389.

Forrest, G. H., and Knapp, E. D. *Technical report series on the Boreal Ecosystem-Atmosphere 394 Study (BOREAS). BOREAS HYD-3 snow Measurements.* National Aeronautics and Space Adminstration., 2000.

Freppaz, M., Williams, B.L., Edwards, A.C., Scalenghe, R., and Zanini, E. "Simulating soil freeze/thaw cycles typical of winter alpine conditions: implications for N and P availability." *Applied Soil Ecology* 35, no. 1 (2007): 247-255.

Garnier, P., Neel, C., Mary, B., and Lafolie, F. "Evaluation of a nitrogen transport and transformation model in a bare soil." *European Journal of Soil Science* 52, no. 2 (2001): 253-268.

Gilley, J., and Risse, L. M. "Runoff and soil loss as affected by the application of manure." *Transactions of the ASAE* 43, no. 6 (2000): 1583-1588.

Groffman, P.M., Hardy, J.P., Driscoll, C.T., and Fahey, T.J. "Snow depth, soil freezing, and fluxes of carbon dioxide, nitrous oxide and methane in a northern hardwood forest." *Global Change Biology* 12 (2006): 1748–1760.

Gupta, S., Munyankusi, E., Moncrief, J., Zvomuya, F., and Hanewall, M. "Tillage and manure application effects on mineral nitrogen leaching from seasonally frozen soils." *Journal of Environmental Quality* 33, no. 4 (2004): 1238-1246.

Hansen, S., Jensen, H. E., Nielsen, N. E., and Svendsen, H. "Simulation of nitrogen dynamics and biomass production in winter wheat using Danish simulation model DAISY." *fertilizer research* 27 (1991): 245-259.

Harrington, R., and Bales, R.C. "Modeling ionic solute transport in melting snow." *Water Resources Research* 34, no. 7 (1998): 1727–1736.

Heinen, M. "Simplified denitrification models: overview and properties." *Geoderma* 133 (2006): 444–463.

Hejazi, A., and Woodbury, A. D. "Evaluation of Land Surface Scheme SABAE-HW in Simulating Snow Depth, Soil Temperature and Soil Moisture within the BOREAS Site, Saskatchewan." *Atmosphere-Ocean* 49, no. 4 (2011): 408-420.

Heng, H.H., and Nikolaidis, N. P. "Modeling of nonpoint source pollution of nitrogen at the watershed scale." *Journal of the American Water Resources Association* 34, no. 2 (1998): 359–374.

Henry, H. A. L. "Soil freeze-thaw cycle experiments: trends methodological weaknesses and suggested improvements." *Soil Biology & Biochemistry* 39 (2007): 977–986.

Hentschel, K., Borken, W., Zuber, T. , Bognerw, C., Huwew, B. , and Matzner, E. "Effects of soil frost on nitrogen net mineralization, soil solution chemistry and seepage losses in a temperate forest soil." *Global Change Biology* 15 (2009): 825–836.

Hentschel, K., Borken, W., and Matzner, E. "Leaching losses of nitrogen and dissolved organic matter following repeated frost/ thaw events in a forest soil." *Journal of Plant Nutrition and Soil Science* 171 (2008): 699–706.

Herrmann, A., and Witter, E. "Sources of C and N contributing to the flush in mineralization upon freeze-thaw cycles in soils." *Soil Biology & Biochemistry* 34 (2002): 1495–1505.

Hinman, W. C. "Effects of freezing and thawing on some chemical properties of three soils." *Canadian Journal of Soil Science* 50 (1970): 179-182.

Hutson, J. L. "LEACHM: model description and user's guide." School of chemistry, physics, and earth Sciences, The Flinders University of South Australia, Adelaide, South Australia, 2000.

Jaiswal, D. K., Kumar, A., Kumar, N., and Yadav, R. R. "Analytical solutions for temporally and spatially dependent solute dispersion of pulse type input concentration inone dimensional semi-infinite media." *Journal of Hydro-environment Research* 2 (2009): 254-263.

Jansson, P. E., and Karlberg, L. "Coupled Heat and Mass Transfer Model for Soil-Plant-Atmosphere Systems." Department of Civil and Environmental Engineering, Royal Institute of Technology, Stockholm, 2001.

Jansson, P-E., and Karlberg, L. *Coupled heat and mass transfer model for soil-plant-atmosphere systems.* Dep. of Land and Water Resources Engineering, Stockholm, Sweden: Royal Institute of Technology, 2004, 427.

Johnsson, H., Bergström, L., and Jansson, P. "Simulated nitrogen dynamics and losses in a layered agricultural soil." *Agriculture, Ecosystems and Environment* 18 (1987): 333–356.

Johnsson, H., Bergstrom, L., Jansson, P. E., and Paustian, K. "Simulated nitrogen dynamics and losses in alayered agriculture soil." *Agriculture, Ecosystems, and Environment* 18 (1987): 333-356.

Ju, S.H., and Kung, K.J.S. "Mass types, Element orders and Solution schemes for." *Computers & Geosciences* 23, no. 2 (1997): 175-187.

Jyrkama, M. I., Sykes, J. F., and Normani, S. D. "Recharge Estimation for Transient Ground 406 Water Modeling." *Ground Water* 40 (2002): 638-648.

Kartha, S., and Srivastava, R. "Effect of immobile water content on contaminant transport in unsaturated zone." *Journal of Hydro-environmnet Research* 1, no. 3-4 (2008): 206-215.

Keshta, N., Elshorbagy, A., and Barbour, L. "Comparative probabilistic assessment of the hydrological performance of reconstructed and natural watersheds." *Hydrological Processes* 24 (2010): 1333-1342.

Kongoli, C.E., and Bland, W.L. "Influence of manure application on surface energy and snow cover: Model development and sensitivities." *Journal of Environmental Quality* 31, no. 4 (2002): 1174-1183.

Kroes, J., and Roelsma, J. "Simulation of water and nitrogen flows on field scale: application." In *Modelling Water and Nutrient*, by K. Ch. Kersebaum, 111-128. Springer, 2007.

Kuchment, L. S., Demidov, V. N., and Startseva, Z. P. "Coupled modeling of the hydrological 413 and carbon cycles in the soil-vegetation-atmosphere system." *Journal of Hydrology* 323 (2006a): 4-21.

Kuchment, L. S., Demidov, V. N., and Startseva, Z. P. "Modeling of vertical heat and moisture transfer and carbon exchange in the soil-vegetation-atmosphere system." *Atmospheric and Oceanic Physics* 42, no. 4 (2006b): 539-553.

Kumar, A., Jaiswal, D.K., and Kumar, N. "Analytical solutions of one-dimensional advection- diffusion equation with variable coefficients in a finite domain." *Journal of Earth System Science* 118, no. 5 (2009): 539-549.

Lafolie, F. "Modelling water flow, nitrogen transport and root uptake including physical non-equilibrium and optimization of the root water potential." *Fertilizer Research* 27 (1991): 215–231.

Lafolie, F., Bruckler, L., and Cockborne, A. M. "Modeling the water transport and nitrogen dynamics in irrigated salad crops." *Irrigation Science* 17 (1997): 95-104.

Lan, C.W., and Chen, F.C. "A finite volume method for solute segregation in directional solidification and comparison with a finite element method." *Computer Methods in Applied Mechanics and Engineering* 131, no. 1-2 (1996): 191-207.

Larsen, K.S., Jonasson, S., and Michelsen, A. "Repeated freezethaw cycles and their effects on biological processes in two arctic ecosystem types." *Applied Soil Ecology* 21 (2002): 187–195.

Lee, J., Nez, V. E., Feng, X., Kirchner, J. W., Osterhuber, R., and Renshaw, C. E. "A study of solute redistribution and transport in seasonal snowpack using natural and artificial tracers." *Journal of Hydrology* 357 (2008): 243– 254.

Lee, J., Feng, X., Posmentier, E. S., Faiia, A. M., Osterhuber, R., and Kirchner, J. W. "Modeling of solute transport in snow using conservative tracers and artificial rain-on-snow experiments." *Water Resources Reserach* 44 (2008): 1-12.

Lee, M.S., Lee, K. K., Hyun, Y., Clement, T.P., and Hamilton, D. "Nitrogen transformation and transport modeling in groundwater aquifers." *Ecological Modelling* 192, no. 1-2 (2006): 143-159.

Leonard, R. A., Knisel, W. G., and Still, D.S. "GLEAMS: Groundwater Loading Effects of Agricultural Management Systems." *Trans. ASAE* 30 (1987): 1403-1418.

Levine, E.R., and Knox, R.G. "Modeling soil temperature and snow dynamics in northern forests." *Journal of Geophysical Research* 102, no. 24 (1997): 29407-29416.

Lewis, T. W., and Makarewicz, J. C. "Winter application of manure on an agricultural watershed and its impact on downstream nutrient fluxes." *Journal of great lakes research* 35 (2009): 43-49.

Link, T.E., Flerchinger, G.N., Unsworth, M.H., and Marks, D. "Simulation of water and energy fluxes in an old growth seasonal temperate rainforest using the Simultaneous Heat and Water (SHAW) Model." *Journal of Hydrometeorology* 5, no. 3 (2004): 443-457.

Loukili, Y., Woodbury, A. D., and Snelgrove, K. R. "SABAE-HW: An enhanced water balance prediction in the canadian land surface scheme compared with existing models." *Vadose Zone Journal* 7 (2008): 865–877.

Ma, L., Ascough, J. C., Ahuja, L. R., Shaffer, M. J., Hanson, J. D., and Rojas, K. W. "Root zone water quality model sensitivity analysis using Monte Carlo simulation." *American Society of Agricultural Engineers* 43, no. 4 (2000): 883-895.

Ma, L., et al. "Integrating system modeling with field research in agriculture: applications of the root zone water quality model (RZWQM)." *Advances in Agronomy* 71 (2001): 233-292.

Maggi, F., et al. "A mechanistic treatment of the dominant soil nitrogen cycling processes: Model development, Testing, and Application." *Journal of Geophysical Reserach* 113 (2008): 1-13.

Marinov, D., Querner, E., and Roelsma, J. "Simulation of water flow and nitrogen transport for a Bulgarian experimental plot using SWAP and ANIMO models." *Journal of Contaminant Hydrology* 77 (2005): 145-164.

Matzner, E., and Borken, W. "Do freeze-thaw events enhance C and N losses from soils of different ecosystems? A review." *European Journal of Soil Science* 59 (2008): 274–284.

Mazzia, A., and Putti, M. "Mixed-finite element and finite volume discretization for heavy brine simulations in groundwater." *Journal of Computational and Applied Mathematics* 147, no. 1 (2002): 191-213.

McHale, M. R., McDonnell, J. J., Mitchell, M. J., and Cirmo, C. P. "A field based study of soil- and groundwater nitrate release in an Adirondack forested watershed." *Water Resources Research* 38 (2002): 1029–1038.

Mehran, M., Noorishad, J., and Tanji, K.K. "A numerical technique for simulation of the effect of soil nitrogen transport and transformations on groundwater contamination." *Environmental Geology* 5, no. 4 (1984): 213-218.

Miller, A. E., Schimel, J. P., Sickman, J. O., Meixner, T., Doyle, A. P., and Melack, J. M. "Mineralization responses at near zero temperatures in three alpine soils." *Biogeochemistry* 84 (2007): 233–245.

Mirbagheri, S. A. "Modeling contaminant transport in soil column and groundwater pollution control." *International journal of environmental science and technology* 1, no. 2 (2004): 141-150.

Mitchell, M. J., Driscoll, C. T., Kahl, J. S., Likens, G. E., Murdoch, P. S., and Pardo, L. H. "Climatic control of nitrate loss from forested watersheds in the northeast United States." *Environmental Science and Technology* 30 (1996): 2609–2612.

Moreels, E., De Neve, S., Hofman, G., and Van Meirvenne, M. "Simulating nitrate leaching in bare fallow soils: a model comparison." *Nutrient Cycling in Agroecosystems* 67 (2003): 137–144.

Mulla, D. J., and Addiscott, T. M. "Validation approches for field-, basin-, and regional-scale water quality models." In *Non-point source pollution in the vadose zone*, by

D. L. Corwin, K. Loague and T. R. Ellsworth, 63-78. Washington, USA: American Geophysical Union, 1999.

Nassar, I. N., and Horton, R. "Salinity and compaction effects on soil water evaporation and water and solute distributions." *Soil Science Society of America* 63, no. 4 (1999): 752-758.

Nassar, I. N., Horton, R., and Flerchinger, G. N. "Simultaneous heat and mass transfer in soil columns exposed to freezing/thawing conditions." *Soil Science* 165, no. 3 (2000): 208-216.

Neilsen, C.B., Groffman, P.M., Hamburg, S.P., Dricsoll, C.T., Fahey, T.J., and Hardy, J.P. "Freezing effects on carbon and nitrogen cycling in northern hardwood forest soils." *Soil Science Society of America Journal* 65 (2001): 1723–1730.

Neumann, L.N., Cook, F., Western, A.W., and Verburg, K. "A one dimensional solute transport model for hydrological response units." *18th world IMACS/MODSIM Congress.* Cairrns, Australia, 2009.

Neumann, N. N., Deksen, C., and Goodison, B. "Characterizing local scale snow cover using point measurements during the winter season." *Atmosphere-Ocean* 44, no. 3 (2006): 257-269.

Noorishad, J., and Mehran, M. "An upstream finite element method for solution of transient transport equation in fractured porous media." *Water Resources Research* 18, no. 3 (1982): 588-596.

Oehler, F., Mitchell, M.J., Silva, S.R., and Kendall, C. "Sources of nitrate in snowmelt discharge: Evidence from water chemistry and stable isotopes of nitrate." *Water, Air, and Soil Pollution* 165, no. 1-4 (2005): 13-35.

Parton, W. J., and Rasmussen, P. E. "Long term effects of crop management in wheat fallow. II. CENTURY model simulations." *Soil Science Society of America Journal* 58, no. 2 (1994): 530-536.

Piatek, K. B., Mitchell, M. J., Silva, S. R., and Kendall, C. "Sources of Nitrate in Snowmelt Discharge: Evidence From Water Chemistry and Stable Isotopes of Nitrate." *Water Air and Soil Pollution* 165, no. 1-4 (2005): 13-35.

Priesack, E., Gayler, S., and Hartmann, P. "The impact of crop growth sub-model choice on simulated water." *Nutrient Cycling in Agroecosystems* 75 (2006): 1-13.

Pruess, K. *TOUGH2 - Ageneral purpose numerical simulator for multiphase fluid and heat flow*. Berkeley, California: Lawrence Laboratory Report, 1991.

Putti, M., Yeh, W. W. G., and Mulder, W. A. "A triangular finite volume approach with high resolution upwind terms for the solution of ground water transport equations." *Water Resources Research* 26, no. 12 (1990): 2865–2880.

Rahnama, M. B., and Barani, G. A. "Prediction of contaminant transport in pasangan groundwater aquifer, using control volume model." *Journal of applied science* 4, no. 3 (2004): 369-373.

Reeves, M., Ward, D. S., Johns, N. D., and Cranwell, R. M. *Theory and implementation of SWIFT II, the Sandia waste isolationflow and transport model for fractured media.* Albuquerque: Sandia National Lab, 1986.

Ross, D. S., Lawrence, G. B., and Fredriksen, G. "Mineralization and nitrification patterns at eight northeastern." *Forest Ecology and Management* 188 (2004): 317-335.

Saâdi, Z., and Maslouhi, A. "Modeling nitrogen dynamics in unsaturated soils for evaluating nitrate contamination of the Mnasra groundwater." *dvances in Environmental Research* 7 (2003): 803-823.

Schleppi, P., Hagedorn, F., and Providoli I. "Nitrate leaching from a mountain forest ecosystem with Gleysols subjected to experimentally increased N deposition." *Water, Air, Soil Pollution* 4, no. 2-3 (2003): 453–467.

Scott, M. E. A. *Grand river watershed analysis of nitrate transport as a result of agricultural inputs using a geographic information system.* Master of Applied Science Thesis, Department of Civil Engineering, University of Waterloo, University of Waterloo: MSc. dissertation,Waterloo, Ontario, Canada, 2006.

Shaffer, M. J., and Hansen, Ma, L. *Modeling carbon and nitrogen dynamics for soil management.* Boca Raton, FL: Lewizs Publishers, 2001.

Shan, C., and Javandel, I. "Analytical Solutions for Solute Transport in a Vertical Aquifer Section." *Journal of Contaminant Hydrology* 27, no. 1-2 (1997): 63-82.

Sierra, J. "Nitrogen mineralization and nitrification in a tropical soil:effects of fluctuating temperature conditions." *Soil Biology & Biochemistry* 34 (2002): 1219-1226.

Šimunek, J., and Van Genuchten, M.Th. "Modeling nonequilibrium flow and transport processes using HYDRUS." *Vadose Zone Journal* 7, no. 2 (2008): 782-797.

Šimunek, J., M., Šejna, M., and van Genuchten, M.Th. "The HYDRUS-1D software package for simulating the one-dimensional movement of water, heat, and multiple solutes in variably- saturated media." Colorado School of Mines, International Ground Water Modeling Center, Colorado, 1998.

Soraganvi, V.S., and Kumar, M.S.M. "Modeling of flow and advection dominant solute transport in variably saturated porous media." *Journal of Hydrologic Engineering* 14, no. 1 (2009): 1-14.

Srinivasan, M. S., Bryant, M. P., and Weld, J. L. "Manure management and nutrient loss under winter conditions: A literature review." *Journal of soil and water conservation* 61 (2006): 200-209.

Taheri, S., and Ataie, B. "Comparison of Finite Difference Schemes for Water Flow in Unsaturated Soils." *Proceedings of world academy of science, Engineering and technology* 30 (2008): 21-25.

Tang, X.L., et al. "Dependence 439 of soil respiration on soil temperature and soil moisture in successional forests in Southern China." *Journal of Integrative Plant Biology* 48, no. 6 (2006): 654-663.

Ullah, S., and Moore, T. R. "Soil drainage and vegetation controls of nitrogen transformation rates in forest soils, southern Quebec." *Journal of Geophysical Research* 114 (2009): 1-13.

Vanclooster, M., Viaene, P., Diels, J., and Feyen, J. "A deterministic evaluation analysis applied to an integrated soil-crop model." *Ecological Modelling* 81, no. 1-3 (1995): 183-195.

Vanderborght, J., Kasteel, R., and Vereecken, H. "Stochastic Continuum Transport Equations for Field-Scale Solute Transport: Overview of Theoretical and Experimental Results." *Vadose Zone Journal* 5, no. 1 (2006): 184-203.

Verseghy, D. L., McFarlane N. A., and Lazare. M. "CLASS – A Canadian land surface scheme for GCMS. II. Vegetation model and coupled runs." *International Journal of 447 Climatology* 13 (1993): 347-370.

Verseghy, D.L. "CLASS – A Canadian land surface scheme for GCMS. I. Soil model." *International Journal of Climatology* 11 (1991): 111-133.

Xiao, W., Yu, Q., Flerchinger, G. N., and Zheng, Y. F. "Evaluation of SHAW model in simulating energy balance, leaf temperature, and microclimate within a maize canopy." *Agronomy Journal* 98, no. 3 (2006a): 722-729.

Xiao, X., Flerchinger, G. N., Yu, Q., and Zheng, Y. F. "Evaluation of the SHAW Model in Simulating the Components of Net All-Wave Radiation." *American society of Agricultural and biological engineers* 49, no. 5 (2006b): 1351-1360.

Yadav, R. R., Jaiswal, D. K., Gulrana, and Yadav, H. K. "Analytical solution of one dimensional temporally dependent advection-dispersion equation in homogenous

porous media." *International Journal of Engineering, Science and Technology* 2, no. 5 (2010): 141-148.

Yang, K., Wu, W., Jing, Q., and Zhu, L. "Aqueous Adsorption of Aniline, Phenol, and their Substitutes by Multi-Walled Carbon Nanotubes." *Environmental Science Technology* 42 (2008): 7931-7936.

Younes, A., Ackerer, PH., and Mose, R. "Modeling Variable Density Flow and Solute Transport in Porous Medium: 2. Re-Evaluation of the Salt Dome Flow Problem." *Transport in Porous Media* 35 (1999): 375-394.

Youssef, M. A., Skaggs, R. W., Chescheir, G. M., and Gilliam, J. W. "Field evaluation of a model for predicting nitrogen losses from drained lands. Journal of Environmental Quality." *Journal of Environmental Quality* 35, no. 6 (2006): 2026-2042.

Appendix A

SABAE-HWS Input Data File

Figure A.1: Atmospheric data file: *sabaeatmo.dot*

```
-------------------------------------------------------------------SABAE-HWS
  Test02

  U.ofManitoba
-------------------------------------------------------------------------

Using Specific humidity --> 'sh' , or relative humidity --> 'rh'
'rh'
               *** Meteorological data provided at each time step ***
                   ---------------------------------------------
K|IncSWR K|IncAtR Precipitation Temperature Wind speed Air pressure Humidity
  W m-2    W m-2     mm s-1           C          m         Pa
 ------   ------    -----------  ----------- ---------- ----------- --------
  0.00    238.97    0.000000        13.36     2.646924   96500.00    0.9660
  0.00    238.97    0.000000        13.36     2.646924   96500.00    0.9660
  0.00    239.83    0.000000        13.52     2.624751   96500.00    0.9770
  0.00    239.83    0.000000        13.52     2.624751   96500.00    0.9770
  0.00    239.40    0.000000        13.44     3.098702   96470.00    0.9800
  0.00    239.40    0.000000        13.44     3.098702   96470.00    0.9800
  0.00    238.22    0.000000        13.22     3.018325   96440.00    0.9820
  0.00    238.22    0.000000        13.22     3.018325   96440.00    0.9820
  0.00    237.68    0.000000        13.12     3.087616   96470.00    0.9780
  0.00    237.68    0.000000        13.12     3.087616   96470.00    0.9780
  0.00    237.41    0.000000        13.07     3.065443   96560.00    0.9810
  0.00    237.41    0.000000        13.07     3.065443   96560.00    0.9810
  0.11    236.02    0.000000        12.81     3.503363   96570.00    0.9870
  0.11    236.02    0.000000        12.81     3.503363   96570.00    0.9870
  9.37    236.29    0.000000        12.86     3.281631   96660.00    0.9890
  9.37    236.29    0.000000        12.86     3.281631   96660.00    0.9890
  49.10   238.11    0.000000        13.20     3.356466   96700.00    0.9820
  49.10   238.11    0.000000        13.20     3.356466   96700.00    0.9820
```

Figure A.2: Soil characteristics data file: *sabaesoil.dot*

```
-------------------------------------------------------------------------SABAE-HWS
  Test02

  U.ofManitoba
-------------------------------------------------------------------------------

Initial storage (mm) :
940

Lower water flow b.c. ( 'wt' for water table , or 'ug' for unit gradient, or
'3d' for SABAE3D ) : 'wt'

Number of soil layers :
17
-------------------------------------------------------------------------------
Sand index = min( (%sand-17)/5 , 15)    Clay index = min ( (%clay+2)/5 , 12 )
-------------------------------------------------------------------------------
Soillayer Thickness Sand index Clay index organic Init temp Init liq Init fro
--------- --------- ---------- ---------- ------- --------- -------- --------
  1        0.10        12.0         5.0      0.0     16.85     0.210   0.000
  2        0.10        9.0          8.0      0.0     18.47     0.230   0.000
  3        0.10        13.0         4.0      0.0     19.17     0.220   0.000
  4        0.15        14.0         4.0      0.0     19.0      0.160   0.000
  5        0.15        14.0         3.0      0.0     19.01     0.250   0.000
-------------------------------------------------------------------------------
       --- Database of soil parameters -- can be modified by the user
-------------------------------------------------------------------------------

Soil texture parameter b following the clay index :
b( 1)  b( 2)  b( 3)  b( 4)  b( 5)  b( 6)  b( 7)  b( 8)  b( 9)  b(10)  b(11)
b(12)  b(13)
3.39   4.18   4.98   5.77  7.203   7.36   8.16   8.95   9.75  10.54  11.34
12.13   6.10

Pore volume fraction p following the sand index :
t( 1) t( 2) t( 3) t( 4) t( 5) t( 6) t( 7) t( 8) t( 9) t(10) t(11) t(12) t(13)
t(14) t(15) t(16) t(17) t(18)
0.461 0.455 0.449 0.442 0.436 0.430 0.423 0.416 0.411 0.405 0.398 0.392 0.386
0.379 0.373 0.000 0.880 1.000

Multiplier m for obtaining effective porosity used for infiltration (follows
the clay index) :
m( 1)  m( 2)  m( 3)  m( 4)  m( 5)  m( 6)  m( 7)  m( 8)  m( 9)  m(10)  m(11)
m(12)  m(13)
0.9315 0.9408 0.9479 0.9534 0.9579 0.9616 0.9647 0.9674 0.9696 0.9716 0.9734
0.9749 1.0000

Saturated soil water suction p following the sand index :
p( 1) p( 2) p( 3) p( 4) p( 5) p( 6) p( 7) p( 8) p( 9) p(10)  p(11)  p(12)
p(13)  p(14)  p(15) p(16) p(17) p(18)
0.391 0.336 0.289 0.248 0.214 0.184 0.158 0.132 0.117 0.101 0.0865 0.0744
0.0639 0.0550 0.0473 1.0e8 0.300 0.000
```

```
Saturated hydraulic conductivity k following the sand index :
k( 1)     k( 2)     k( 3)     k( 4)     k( 5)     k( 6)     k( 7)     k( 8)
k( 9)     k(10)   k(11)   k(12)   k(13)   k(14)   k(15)   k(16)   k(17)
k(18)
2.00e-6   2.39e-6   2.85e-6   3.39e-6   4.05e-6   4.83e-6   5.76e-6 7.1045e-6
8.19e-6   9.76e-6 11.6e-6 13.9e-6 16.6e-6 19.8e-6   23.6e-6    0.00 2.00e-6
0.00

Hydraulic conductivity k~ behind the wetting front ( k~ = k / 2 ) :
k~( 1)    k~( 2)    k~( 3)    k~( 4)    k~( 5)    k~( 6)    k~( 7)    k~( 8)
k~( 9)    k~(10)  k~(11)  k~(12)  k~(13)  k~(14)  k~(15)  k~(16)  k~(17)
k~(18)
1.00e-6   1.19e-6   1.42e-6   1.70e-6   2.02e-6   2.41e-6   2.88e-6 3.5522e-6
4.09e-6   4.88e-6 5.82e-6 6.94e-6 8.28e-6 9.88e-6  11.8e-6    0.00 2.00e-6
0.00
```

Figure A.3: Vegetation data file: *sabaesite.dot*

```
---------------------------------------------------------------------- SABAE-HWS
  Test02

  U.ofManitoba
-------------------------------------------------------------------------------

  Latitude  Longitude  Ref.Height  1 for Inc. LWR   0 without flood routing
                                   2 for Net LWR    1 with flood routing

    49.90     99.35      90.00          2                 0

    Fractional coverages of grid cell          Maximum Leaf Area Indices
Needleaf Broadleaf Crops   Grass   Urban     Needleaf Broadleaf Crops   Grass
   0.000   0.000   1.000   0.000   0.000        2.860   2.860   5.000   1.800

   Maximum heights given as Ln(Hmax/10)        Minimum Leaf Area Indices
Needleaf Broadleaf Crops   Grass   Urban     Needleaf Broadleaf Crops   Grass
   0.405   0.405  -2.302  -4.828  -4.828        2.450   2.450   2.500   1.800

         Visible Albedos                           Canopy mass
Needleaf Broadleaf Crops   Grass   Urban     Needleaf Broadleaf Crops   Grass
   0.024   0.024   0.024   0.150   0.150        5.520   5.520   1.500   1.500

     Near-infrared Albedos                       Vegetation rooting depth
Needleaf Broadleaf Crops   Grass   Urban     Needleaf Broadleaf Crops   Grass
   0.140   0.140   0.140   0.450   0.450      0.349   0.349   2.000   0.150

Trees growth index

     0.000

Soil colour  Drain   No use  No use  No use
    9.0       1.0     0.995   0.995   0.000

Init Canopy Temp   Init snow Temp
      0.00             0.00

Init water/canopy  snow/canopy  snow mass  snow albedo  snow density
      0.0000          0.0000       0.00       0.800       100.0000

Time initialization
      Year       Day      Hour    Minute
      2002        248      00        00

Simulation time in days      Time step in seconds
       827                          1800

Output for this period         Daily output for this period
   from day    to day                 from day    to day
     248         344                    248       344

      of year   of year                of year   of year
       2002      2004                   2002      2004
```

Figure A.4: Soil Nitrogen data file: *sabaenitr.dot*

```
---------------------------------------------------------------------- SABAE-HWS
  Test05

  U.ofManitoba
-------------------------------------------------------------------------------

dispersivity :
0.07
molecular diffusion :
0.0004
response to a 10 C soil temperature change :
2.000
base temperature :
10.000
residual soil water content(thrsw) :
0.040
soil water content at wilting point(thwp) :
0.0130
soil water content at field capacity(thfc) :
0.0700
relative effect at saturation(fsat) :
0.600
adsorption coefficient :
0.0002
nitrification coefficient(knit) (1/day):
0.03
mineralization coefficient(kmin) (1/day):
0.003
denitrification coefficient(kdenit) :
0.000
cumulative max nitrogen mass in the crop(nitmax) (kg/m2):
40
evaporative zone depth(evapzd) :
1
Number of soil layers :
5
-------------------------------------------------------------------------------
Soil layer Thickness soil density  Nsorg   Nmorg  Init ammonium  Init nitrate
               (m)     (gr/cm3)    (kg/ha) (kg/ha)    (mg/kg)       (mg/kg)
---------- --------- ------------  -----   -----  -------------  ------------
     1       0.10        1300       0.20     0.0        9.40         7.30
     2       0.10        1450       0.17     0.0        10.4         9.60
     3       0.10        1420       0.13     0.0        8.30         10.8
     4       0.15        1500       0.07     0.0        18.50        11.9
     5       0.15        1500       0.06     0.0        9.70         4.55
-------------------------------------------------------------------------------
Number of manure applications :
2

Day    Nmorg  surfamoconc  surnitconc   water volume   GrowTime   MatureTime
      (kg/ha)   (mg/kg)      (mg/kg)        (mm/s)      (day)       (day)
-----  -----  -----------  ----------   ------------   --------   ----------
251     27.4      109.4        0          0.00308880      258          329
608     31.2      167.6        0          0.00308880      632          744
```